Development of a Method for Trace Analysis of Dioctyl Sodium Sulfosuccinate by Liquid Chromatography Mass Spectrometry and its Application to Samples from the MV Rena Incident

A thesis submitted in partial fulfilment

of the requirements for the degree

of

Master of Science (Research) in Chemistry

at

The University of Waikato

by

Daniel Richard Bernstein

The University of Waikato

2015

THE UNIVERSITY OF
WAIKATO
Te Whare Wānanga o Waikato

Abstract

The grounding of the MV Rena off the coast of Tauranga, New Zealand in 2011 prompted the application of Corexit® oil spill dispersants in an attempt to mitigate the impact of the spilled oil to coastal ecosystems. A quantitative method was developed employing sonication assisted extraction from beach sand followed by sample clean up by solid phase extraction and analysis by liquid chromatography tandem mass spectrometry for the analysis of Corexit® component dioctyl sodium sulfosuccinate (DOSS) at trace levels. The chromatographic method included the use of a C8 stationary phase with a gradient elution and quantitation by an internal standard approach based on mass spectrometer instrument response. Validation studies gave recoveries of 72 ± 1.7% with an accuracy of 94%. Calibration curves were shown to have a linear range of 0 – 200 $\mu g.L^{-1}$. Application of the method to the available environmental samples showed no presence of DOSS.

An attempt was made to apply the instrumental method to heavy fuel oil (HFO) tar-balls and oiled sand samples. Multiple extraction techniques were trialled including liquid-liquid extraction, sonication assisted extraction and anion exchange chromatography with recovery experiments for each method being carried out. Analysis of the extracts showed that quantitative recovery of DOSS had not been achieved for any of the methods investigated.

The difficulties associated with extracting DOSS from HFO tar-balls and oil sands suggest that the application of DOSS to surface oil slicks results in the preferential partitioning of DOSS into HFO. This has implications with respect to the distribution of DOSS in the environment following application, subsequent environmental monitoring and the degradation of HFO components by microbial communities.

Acknowledgements

Firstly, I would like to thank my supervisor Associate Professor Merilyn Manley-Harris for organizing the project and for the opportunity to undertake this work. Your knowledge and experience has been invaluable and I am grateful for the time you have made for me in reviewing this thesis.

To my co-supervisor, Professor Chris Battershill, I am grateful for the opportunity and appreciate you providing and organizing the project.

Thanks to Rex Fairweather from the Coastal Marine Field Station, for helping to supply sediments and track down the samples for analysis.

At the University of Waikato, I would like to extend my thanks to our great technicians in the chemistry department; Annie Barker, Pat Gread, Jenny Stockdill, John Little and Tom Featonby for all their help and Wendy Jackson for my initial training on the LC-MS. Thanks also to Megan Grainger, John McDonald Wharry and Maria Revell for the useful insights and showing me around when I was starting out.

Thanks to Stephen O'Neill at Z Energy Ltd, for generously providing HFO samples for the method development.

Finally, a big thank you to my Mum and Dad for all their support and especially for their patience. Also, thanks to all of my family and friends who have been supportive throughout this time.

Table of Contents

List of Figures

List of Tables

List of Abbreviations

%CV	Percent coefficient of variation
1-PSA	1-pyrene sulfonic acid sodium salt
ACN	Acetonitrile
AE	Alcohol ethoxylate
AES	Alcohol ethoxysulfate
AEX	Anion exchange
BOP	Bay of Plenty
C18	Octadecylsilane
C8	Octylsilane
C9500	Corexit 9500
C9527	Corexit 9257
CID	Collision induced dissociation
CMC	Critical micelle concentration
CoA	Coenzyme A
DAD	Diode array detector
DCM	Dichloromethane
DI	Deionized
DOSS	Dioctyl sodium sulfosuccinate
DWH	Deep Water Horizon

EC	Emerging contaminant
EC_{50}	Median effective concentration
EHSS	Ethylhexyl sodium sulfosuccinate
EIC	Extracted ion chromatogram
ELSD	Evaporative light scattering detector
EO	Ethylene oxide
EPA	Environmental Protection Agency
GC	Gas chromatography
GC-MS	Gas chromatography mass spectrometry
GOM	Gulf of Mexico
HDPE	High density polyethylene
HFO	Heavy fuel oil
HLB	Hydrophilic-lipophilic balance
HPLC	High performance liquid chromatography
IPA	Isopropanol
IS	Internal standard
IT	Ion trap mas analyzer
IT-MS	Ion trap mass spectrometry
LAS	Linear alkylbenzene sulfate
LAS	Linear alkylbenzene sulfonate

LC	Liquid chromatography
LC_{50}	Median lethal concentration
LC-MS	Liquid chromatography mass spectrometry
LC-MS-MS	Liquid chromatography tandem mass spectrometry
LD_{50}	Median lethal dose
LLE	Liquid-liquid extraction
LLOQ	Lower limit of quantitation
LOD	Limit of detection
MeOH	Methanol
MRM	Multiple reaction monitoring
MS	Mass spectrometry
MS^2	Tandem mass spectrometry
MS-MS	Tandem mass spectrometry
NRC	National Research Council
ODS	Octadecylsilane
PAH	Polyaromatic hydrocarbons
PLE	Pressurized liquid extraction
POE	Polyoxyethylene
PTFE	Polytetrafluoroethylene
PVDF	Polyvinylidene fluoride

QC	Quality control
QqQ	Triple quadrupole mass analyzer
SD	Standard deviation
SDS	Sodium dodecyl sulfate
SIM	Selected ion mode
SIS	Surrogate internal standard
SPE	Solid phase extraction
SRM	Selected reaction monitoring
TIC	Total ion chromatogram
t_r	Retention time
UV-VIS	Ultraviolet-visible wavelength detector
WAF	Water accommodated fraction
WAX	Weak anion exchange
WWTP	Waste water treatment plant

1 Introduction

The continued reliance of humankind on petroleum-based products has established a colossal industry, which, despite dwindling resources, continues to grow. Increased demand has led to the transportation of large volumes of petrochemicals from their point of origin (oil fields etc.) across the world's oceans. Inevitably, accidents which have occurred during mass transport and drilling, have resulted in many large scale oil spills. Coupled with the purposeful discharge of oil and natural oil seepage, the volume of oil released to the environment worldwide is estimated at 1.3M metric tonnes *[1]*. Although many of the sources that contribute to this are of small scale and dealt with by natural processes (Figure **1-1**), large scale, acute events such as the grounding of oil tankers which make up the bulk of accidental spills, pose serious ecological threats.

Crude oil is a naturally occurring mixture of hydrocarbons formed by the breakdown of organic matter under the influence of heat and pressure over geological timescales. The exact composition of crude oil varies significantly with geographic origin, although alkanes, aromatics, napthenes and alkenes are the main constituents (~98%). Hydrocarbon derivatives containing oxygen, sulfur and nitrogen make up a small proportion (~2%) of crude oil as well as trace heavy metal components (<1%) *[2]*.

Crude oil is refined industrially to give products such as kerosene, petrol and heavy fuel oil (HFO) which are used in many aspects of human life worldwide. Many components of crude oil and its refined products are known carcinogens and ecotoxins which can severely impact ecological systems. These include polyaromatic hydrocarbons (PAH's) and trace heavy metals. Hence, a range of oil spill remediation technologies have been introduced over the years to meet the need for effective clean-up of oil spills in order to mitigate their toxic effect. These include mechanical methods such as containment booms and skimmers as well as chemical methods like oil sorbent materials and chemical dispersants *[3]*.

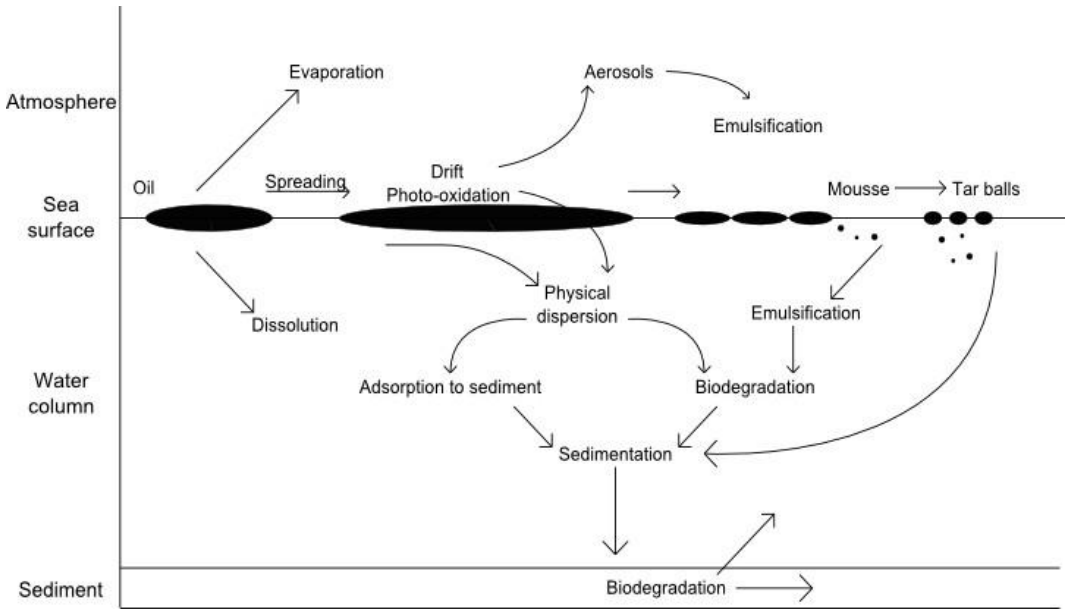

Figure 1-1: Weathering processes involved in the degradation of crude oil (adapted from *[4]*).

The use of chemical oil dispersants came under public scrutiny in 2010 following their extensive use during the Deep Water Horizon (DWH) oil spill in the Gulf of Mexico (GOM). This spill resulted in the release of an estimated 580,000 metric tonnes of oil into the environment and is considered to be the largest accidental marine oil spill in the history of the petroleum industry. Over the course of the clean-up, around 7 million litres of Corexit® oil dispersants were applied *[5]*. This prompted a great deal of subsequent research into the efficacy of chemical dispersants, their potential toxicology and methods for monitoring their fate in the environment. Initial findings by the Environmental Protection Agency (EPA) on the comparative toxicity of the available dispersants at the time showed no activity as endocrine disruptors. It was also shown that Corexit® 9500 (C9500) was no more toxic than the available alternatives and the EPA set an aquatic life benchmark of 40 $\mu g.L^{-1}$ on the major component of C9500, dioctyl sodium sulfosuccinate (DOSS) *[5,6]*. However, these initial tests focused on the toxicity of the dispersant alone, not when present as a dispersed oil aggregates. Further tests of the toxicity of dispersed oil showed that the oil-dispersant mixtures for C9500 were of similar toxicity to the oil alone *[5,6]*. The tests were conducted using mysid shrimp (an aquatic invertebrate), and inland silverside (a small estuarine fish species) which are commonly used in toxicity testing by the EPA.

Contrary to this, more recent studies have demonstrated that chemically dispersed oil is more toxic than oil alone in some cases, and has a species and environment specific effect *[7,8]*. These mixed results illustrate the need for thorough testing of such technologies prior to their use and the need for adequate monitoring following large scale applications. In the years preceding this incident, the National Research Council (NRC) noted research funding on oil spill response was "limited and declining", with only one quarter of $40 M proposed in a 2005 report being granted *[9]*. Recommendations made in 2011 stressed the need for prior funding, studies into the environmental impact of chemical dispersants, their long term fate and the distribution of degradation products *[9]*.

On October 5, 2011, the MV Rena ran aground on the Astrolabe (Otaiti) reef off the coast of Tauranga, Bay of Plenty (BOP), New Zealand (Figure **1-2**). The contents of the ship included 1760 tonnes of HFO and 200 tonnes of marine diesel. Of this, about 1300 tonnes was recovered from the ship with an estimated 400 tonnes being released to the surrounding ocean *[10]*.

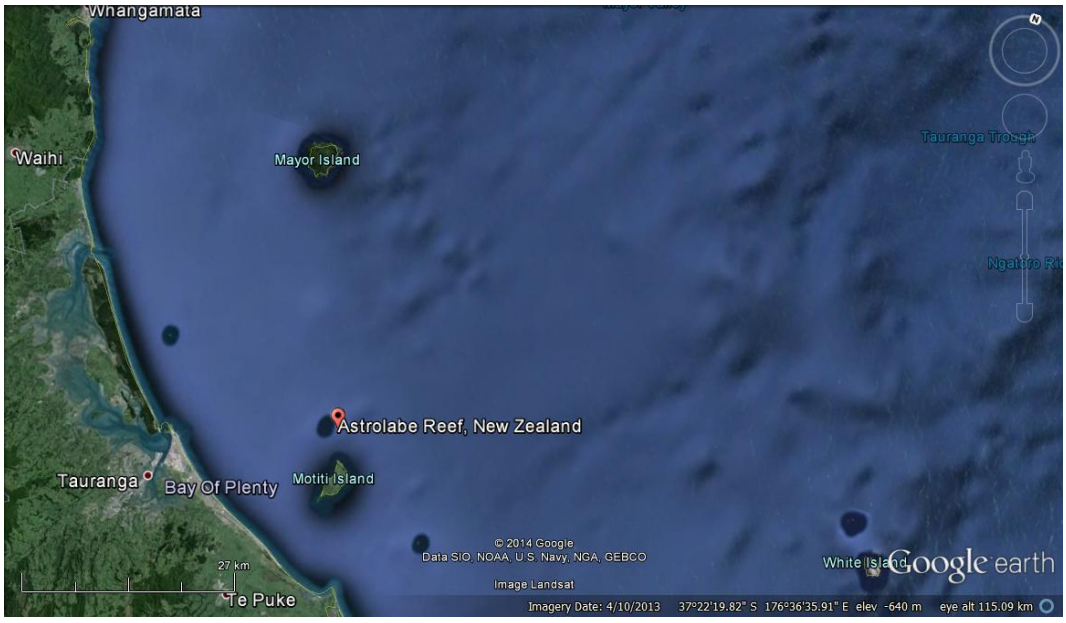

Figure 1-2: Map of the Western Bay of Plenty showing the location of the Astrolabe Reef (Source: "Astrolabe Reef", 32°22'19.82" S 178°36'35.91" E. GOOGLE EARTH. October 4, 2013. November 24, 2014).

The incident prompted Maritime New Zealand to declare a Tier 3 emergency (the highest level response to an oil spill). As part of the initial clean-up response, approximately 3000 L of C9500 was applied and a small amount of Corexit® 9257 (C9527). The use of dispersants was discontinued after three days of use as they were deemed to be ineffective in the prevailing sea conditions and showed little activity against weathered oil *[10,11]*. Following the incident, a long term environmental monitoring programme was implemented and carried out by the Te Māuri Moana research partnership. The research included two studies into the toxicity of oil and dispersant-oil mixtures on local marine organisms. However, these preliminary studies suffered from small sample size and returned ambiguous results. Tentative interpretation of the available data indicated no synergistic toxic effects between HFO and Corexit® on the majority of tested organisms although some toxic effect may exist between C9500 and kingfish larvae *[12,13]*.

1.1 Oil Dispersants

Oil dispersants are a chemical based, oil spill response technology designed to break up surface oil slicks into small droplets and solubilize the oil, allowing it to be dispersed and diluted throughout the water column by wave and wind action. Solubilization of the oil is achieved by the action of the major components of oil dispersants, which are surfactants *[3]*.

The use of chemical dispersants in oil spill remediation is often seen as an environmental trade-off. Essentially, the dispersants that are used are deemed to be less toxic than the oil to which they are applied and in some cases the dispersant/oil mixtures have been shown to be no more toxic than oil alone *[5,6]*. However, some studies have demonstrated that, in fact, some synergistic toxicity may occur with dissolved oil/dispersant aggregates and their use may also increase the concentration of aerosolized oil components, posing a risk to human health due to their carcinogenic nature *[8,14-16]*.

1.1.1 Surfactants

Surfactants (surface active agents) are a class of chemical compounds that contain both lyophilic and lyophobic functionalities as part of their molecular structure. Lyophobic groups are those that have low affinity for the solvent with lyophilic groups having high affinity for the solvent. This is termed an amphipathic structure *[17]*. In the case of a polar solvent (like water) the lyophobic group is said to be hydrophobic and the lyophilic group is referred to as hydrophilic *[18]*. The amphipathic (or amphiphilic) structure of these compounds give rise to their surface-active properties, most notably their ability to lower the interfacial free energy (surface tension) between two immiscible phases when present at low concentration and their tendency to aggregate at surfaces or interfaces *[17,18]*. The unique properties these compounds exhibit make them ideal for use as wetting agents, emulsifiers, cleaning agents and dispersants resulting in widespread use in both industrial and domestic settings.

A key property of surfactants in the context of the dispersion of HFO, is their tendency to aggregate in solution and form micelles. This occurs at the so called critical micelle concentration (CMC). Below the CMC, surfactants exist in solution as free monomers, however when the CMC is exceeded, the hydrophobic groups begin to aggregate. This forms a thermodynamically favorable hydrophobic phase which is surrounded by a hydrophilic shell. The monomeric surfactant molecules and the micellar surfactant aggregates exist in an equilibrium at surfactant concentrations above the CMC. The presence of micelles allows compounds of low aqueous solubility (like HFO components) to partition to the hydrophobic interior of the micelle, increasing the concentration of such compounds above that of their usual limits of solubility in aqueous media. This is termed solubilization *[19]*.

1.1.1.1 Types of surfactants

Surfactants can be grouped into four basic categories based on the nature of the hydrophilic group present (Table **1-1**) *[17,18,20,21]*.

1. Anionic: The hydrophilic group is negatively charged.
2. Cationic: The hydrophilic group is positively charged.
3. Non-ionic: The hydrophilic group is neutral. Hydrophilicity arises from the presence of highly polar groups.
4. Amphoteric: The hydrophilic group contains (or can contain) both positive and negatively charged groups (also termed zwitterionic).

These differences lead to differing chemical behaviours and subsequent use in commercial formulations depending on the required function of the surfactant. For example, polyoxyethylene (POE), or alcohol ethoxylate (AE), based surfactants are highly effective at reducing the interfacial tension of oils *[17]*, making them ideal for use in liquid laundry detergents and oil dispersing agents. Others, like the amphoteric alkylamido betaine based surfactants, have proven to be very mild towards skin and hair and are used extensively in personal care products *[21]*. This widespread use of surfactants in virtually all aspects of human life has led to their ubiquitous presence as environmental contaminants.

Table 1-1: Classes of surfactants

Class		Example
Anionic	Sodium dodecyl sulfate	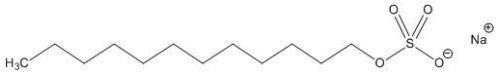
Cationic	Cetrimonium chloride	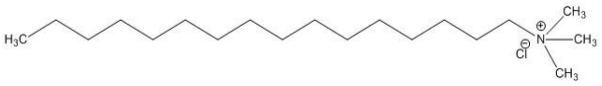
Nonionic	Pentaethylene glycol monododecyl ether	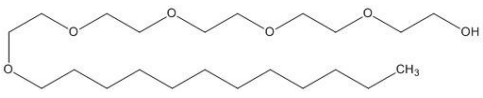
Amphoteric	Cocamidodopropyl betaine	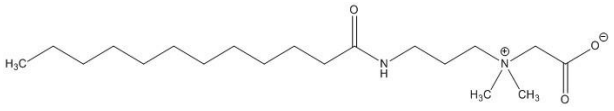

Surfactants can also be classified numerically, by use of the so called hydrophilic-lipophilic balance (HLB) number system. The HLB number of a surfactant is defined by numerical values assigned to particular functional groups that make up surfactant molecules (Table **1-2**) *[22]*. Using these group numbers, the HLB number for a given surfactant can be calculated (Equation **1-1**).

$$HLB = 7 + \Sigma(hydrophilic\ group\ numbers) - \Sigma(lipophilic\ group\ numbers) \quad \textbf{(1-1)}$$

The HLB system is particularly useful when formulating a new emulsifying agent from multiple surfactants for a particular purpose, where the HLB of the mixture can be estimated from the HLB of each surfactant multiplied by its mass fraction *[22]*.

Table 1-2: HLB numbers for various functional groups *[22]*.

Type	Functional group	Group number
Lipophilic	-CH-	0.475
	=CH-	0.475
	$-CH_2-$	0.475
	CH_3-	0.475
Hydrophilic	$-SO_4Na$	38.7
	-COOK	21.1
	$-SO_3Na$	19.1
	=N-	11.0
	Ester (sorbitan)	9.4
	Ester	6.8
	-COOH	2.4
	-OH	2.1
	-O-	1.3
	-OH (sorbitan)	0.5

1.1.2 Components of Corexit® 9500 and Corexit® 9527

C9500 and C9527 are commercially available oil dispersion formulations composed of various surfactants dissolved in a de-aromatized hydrocarbon solvent produced by Nalco *[23]*. Prior to the DWH disaster, the formulations of Nalco's Corexit® products were considered proprietary information, hence,

information regarding the composition of each formulation was limited *[15]*. However, following the use of unprecedented volumes of oil dispersants during this spill, public pressure forced the EPA and Nalco to release the constituents of each Corexit® product used (Figure **1-3**) *[5]*. Using this information, subsequent studies have attempted to quantify the relative proportions of each surfactant in these products, although it is possible that the exact proportions of each surfactant varies between batches (Table **1-3**) *[24,25]*. Additionally, a number of analytical methods have been developed to detect and quantify the surfactant components of these dispersants at trace levels in sea water samples and aquatic environments *[24-33]*.

Table 1-3: Compositional analysis of C9500 and C9527 as determined by Place *et al.* *[25].*

Surfactant	% w/w (C9500)*	%w/w (C9527)*
α-/β - EHSS	0.28	0.17
DOSS	18.00	17.00
Span 80	4.40	2.70
Tween 80	18.00	11.00
Tween 85	4.60	4.30

*%w/w balance of solvent and non-surfactant components.

Table 1-4: Calculated HLB values for individual components of Corexit® formulations.

Compound	Calculated HLB number
DOSS	30.200
Span 80	6.325
Tween 80	17.475
Tween 85	9.775
2-butoxy ethanol	7.550
Butoxypropylene glycol	7.425
Propylene glycol	10.275

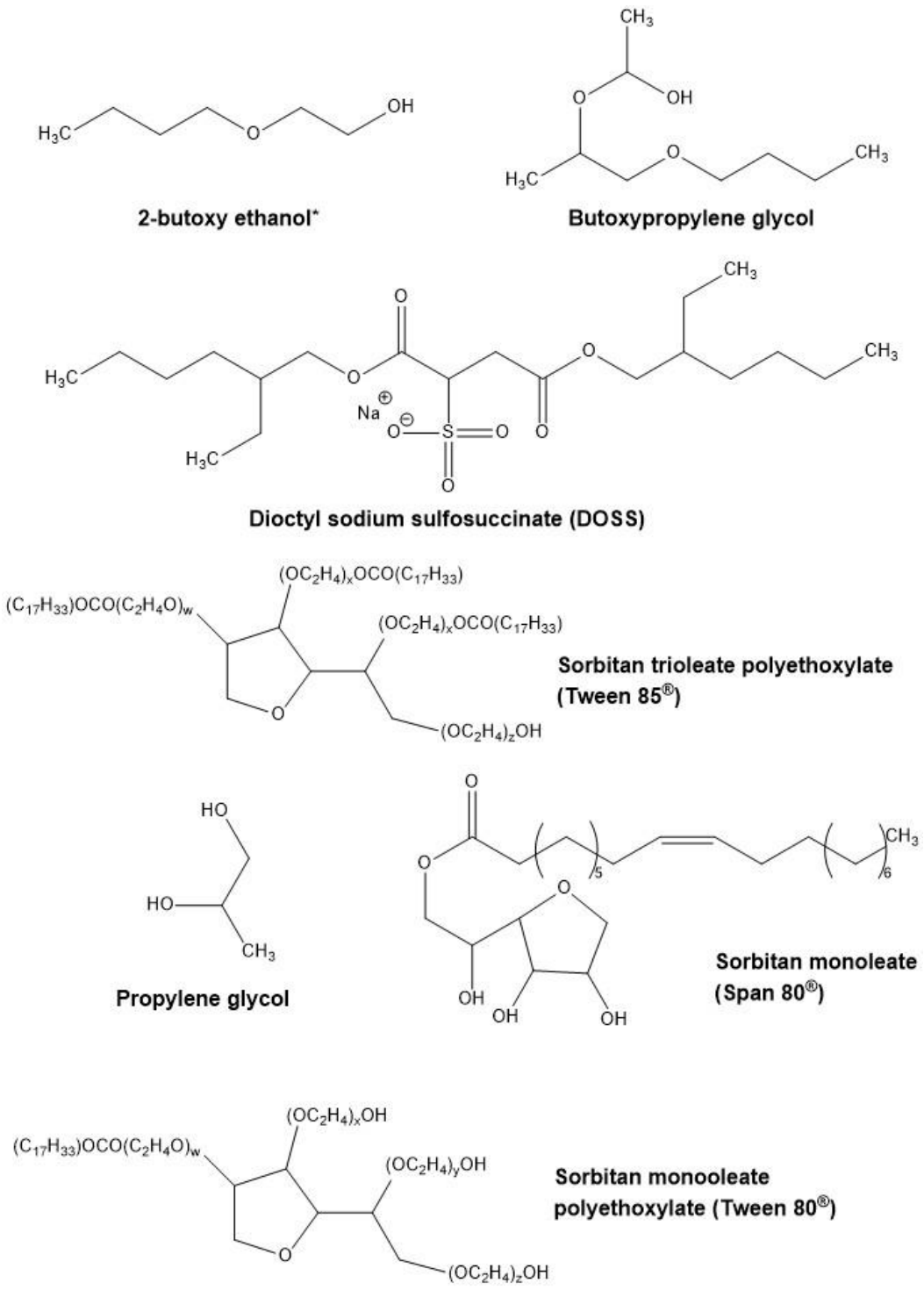

Figure 1-3: Chemical components of Corexit® formulations 9500 and 9527 (Note: * present in Corexit® 9527 only).

1.1.2.1 Anionic components

For both Corexit® formulations, the only anionic surfactant present is bis-(2-ethylhexyl) sulfosuccinate (often referred to as DOSS, dioctyl sodium sulfosuccinate, docusate sodium, Aerosol OT, AOT) and was identified early on in preliminary experiments following the DWH disaster *[34]*. Many of the methods developed since, in the effort to monitor the spread and ultimate fate of Corexit® products in the environment, have focused primarily on DOSS as a marker for the presence of these oil dispersants *[24,27-29,31,32,35]*. This is in part due to its relative ease of analysis (compared to the non-ionic constituents) but also due to its suspected toxicity towards marine life, both as a freely dissolved chemical and also when used as a dispersant and present as solubilized DOSS-oil aggregates *[8,14-16]*. The use of DOSS as an oil dispersant is also thought to inhibit bacterial degradation of dispersed oil, leading to the persistence of DOSS-oil aggregates in the environment *[36]*.

The use of DOSS is widespread in industry, finding applications in medicine, paper and textiles, emulsion polymerization, paints and coatings, agrochemical formulations, and dry cleaning *[37,38]*.

1.1.2.2 Non-ionic components

Both Corexit® formulations consist largely of non-ionic surfactants, all of which are sorbitan oleate ester derivatives which exhibit varying degrees of esterification and ethoxylation marketed under the trade names Span® and Tween® (Figure **1-3**). Production of Span® surfactants involves cyclization of sorbitol (hexitol) by intramolecular dehydration to give 1,4-sorbitan (and isosorbide) which is then esterified with a fatty acid (oleic acid in this case). The production of Tween® type surfactants requires an extra step, where the sorbitan ester is polymerized with ethylene oxide (EO) in the presence of a base catalyst to give the sorbitan oleate polyethoxylate (polysorbate) product (Figure **1-4**) *[33,39]*. Other products of the synthesis include stearic and palmitic acid analogues and their isosorbide equivalents *[40]*.

The nature of the synthetic process means that the final polysorbate products are a mixture of oligomers of varying molecular weights which form a Poisson distribution around the desired molecular weight, which is itself a reflection of the desired degree of polymerization. This randomness and inconsistency also means that the mixtures usually contain unreacted starting materials and show varying physicochemical properties between different batches *[33,41]*. Due to this, the analysis and quantification of polysorbate surfactants in an environmental setting is a challenging task in terms of sample preparation, chromatographic separation, detection and quantification *[33,41-43]*. As such, these surfactants have generally been avoided as a marker for the presence of Corexit® oil dispersants. However, in a recent study, Place *et al.* presented a method which demonstrated the detection and quantification of both anionic and non-ionic components of Corexit® at trace levels *[25]*.

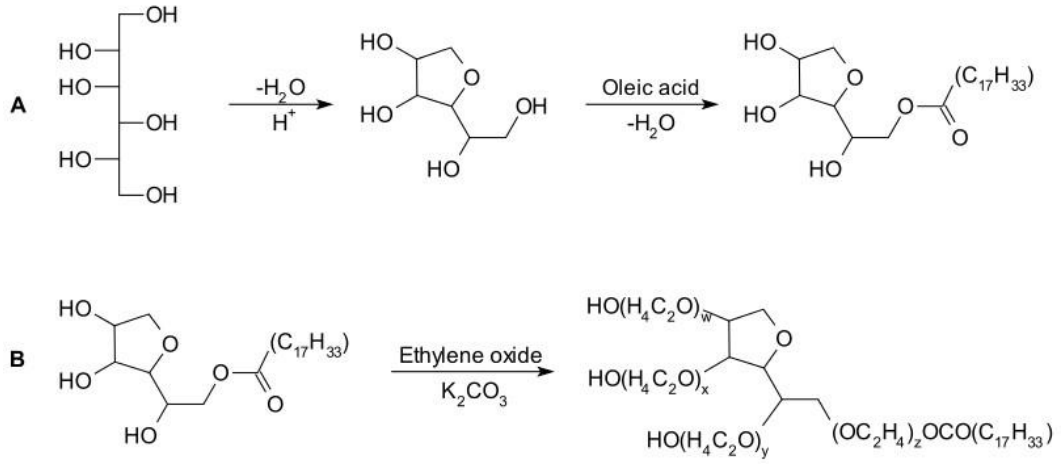

Figure 1-4: Synthetic route for sorbitan ester surfactants; (A) Span surfactants and (B) Tween surfactants.

As with DOSS, sorbitan ester surfactants are used extensively in a wide range of applications. Due to their superior degreasing properties, low foaming characteristics and increased electrolyte compatibility compared with anionic surfactants, they are used widely for industrial and institutional cleaning products. Further applications are found in the cosmetic, agricultural, textile, paper and oil industries *[41]*. The use of sorbitan ester surfactants is so widespread, they are one of the listed surfactants considered to be an emerging contaminant in the environment *[44]*.

1.1.2.3 Toxicity of Corexit® 9500 in the marine environment

The toxicity of C9500 seems to be quite variable and dependent upon species and environmental conditions. Initial toxicity tests conducted by the EPA following the DWH incident showed Corexit® to be relatively non-toxic both as dispersant only and when present as dispersed oil and was less toxic than HFO alone (Table **1-5**) *[5,6]*. This was used as an initial justification for the use of dispersants during the DWH clean-up. However, a more recent study on marine rotifers by Rico-Martinez *et al.* demonstrated that dispersant-oil mixtures were more toxic than HFO and C9500 separately, with toxicity being increased by up to 52-fold (Table **1-5**). A similar effect was observed by Kuhl *et al.* in a study on the fish species *Fundulis grandus [7]*. Additionally, the study showed that toxicity was affected by salinity, which alongside other similar investigations *[45]*, indicates that C9500 (specifically DOSS) affects osmoregulation across gill membranes of fish. Hence, the toxicity of DOSS may be increased by hypo- or hyper-osmotic conditions *[7]*.

Table 1-5: LC_{50} values for various marine organisms exposed to HFO, C9500 and HFO/C9500 mixtures.

Species	LC_{50} (mg.L^{-1})*			Reference
	HFO	C9500	HFO + C9500	
Calanus glacialis	1.1	17-50	22 - 62	*[46]*
Boreogadus saida	3.3	-	55	*[46]*
Myoxocephalus sp.	4.0	-	28	*[46]*
Americamysis bahia	2.5-3.5	5.03**	5.4	*[6]*
Menidia beryllina	3.5-4.05	15.6**	7.6	*[6]*
Brachionus manjavacas (cyst)	11.02	14.25	0.17-0.28	*[8]*
B.manjavacas (parthenogenetic)	5.43	10.39	-	*[8]*
B. plicatilis s.s	2.47	0.447	-	*[8]*
B. rotundiformis	11.02	1.75	-	*[8]*
Brachionus sp.	19.33	4.30	-	*[8]*
Haliotis rufescens	-	12.8-19.7	-	*[16]*
Holmesimysis costata	-	158-248.5	-	*[16]*

*EC_{50} = LC_{50} where effect (E) is defined as death of the organism (lethal effect)

**density of C9500 = 119.8 g.L^{-1} *[47]*

Contrary to this, in a toxicity study on arctic cod, copepod and larval sculpin, Gardiner *et al.* showed that dispersed oil was of similar toxicity to C9500 alone,

with HFO being much more toxic. This study also showed that the age of individual fish in the population was an important factor in determining LC_{50} *[46]*. These varied results reflect the need for toxicity studies on local marine organisms under local conditions in order to assess the potential toxicity of oil dispersants.

1.1.3 Degradation of surfactants in the environment

As free, non-aggregated compounds, the degradation of these surfactants in the environment is fairly well understood. In fact, it is a necessary property of a surfactant to be readily broken down by (bio)chemical processes in order to meet the stipulations of many international regulatory requirements. Such regulations were implemented in the 1960's after widespread use of branched alkyl surfactants led to excessive foaming of natural waterways due to their resistance to breakdown in the environment *[41]*.

The degradation of surfactants in the environment occurs primarily due to biodegradation. Biodegradation (degradation due to biological activity) of surfactants can be divided into two stages: primary and ultimate. Primary degradation is said to have occurred when structural change in the molecule results in a loss of surface activity. Ultimate biodegradation results from the breakdown of the carbon chains of the surfactant and their incorporation into bacterial cell components (mineralization) and the production of carbon dioxide *[48]*.

1.1.3.1 Degradation of dioctylsulfosuccinate

DOSS is a diester of sulfosuccinic acid produced from maleate anhydride reacted with 2-ethylhexanol followed by sulfonation with a sulfonating agent such as sodium metabisulfate (Figure **1-5**) *[41]*.

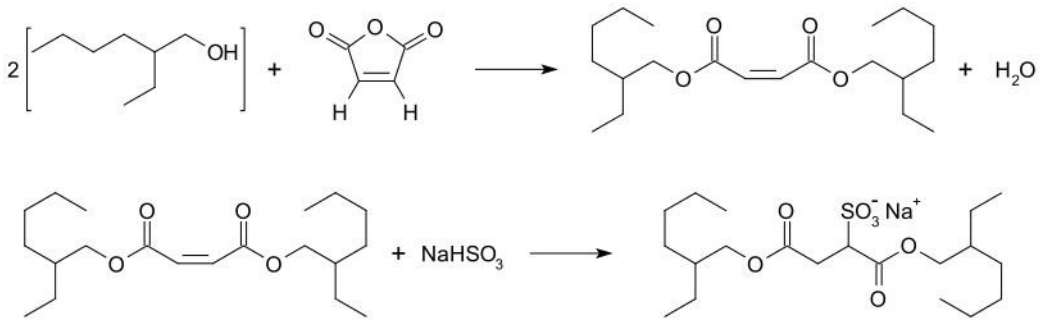

Figure 1-5: Synthetic pathway for the production of sodium dioctylsulfosuccinate.

As such, it can undergo both acid and base hydrolysis as primary degradation processes *[49]*. The primary degradation products, α and β ethylhexyl sulfosuccinate (α/β-EHSS), seem to show differing resistance to further degradation. Of these, the α isomer appears to be more amenable to biodegradation with the β form breaking down more slowly. Ultimate biodegradation of the carbon chains proceeds through ω (oxidation of a terminal carbon to COO^-) and β oxidation (Figure **1-6**) via bacterial processes to yield the final, ultimate degradation product of CO_2 (Figure **1-7**) *[48,50,51]*. The process of β oxidation begins with the activation of a fatty acid ($R\text{-}COO^-$) by its reaction with the thiol group of coenzyme A (CoA) via the acyl-CoA synthetase reaction. The activated complex then undergoes an iterative oxidation cycle which progressively shortens the carbon chain by two carbon units per cycle producing one unit of acetyl-CoA per cycle *[50]*.

Under aerobic conditions, biodegradation of DOSS is around 70% after 25 days. Anaerobic biodegradation is somewhat slower and dependent on surfactant concentration, although around 40% degradation can be expected after a period of 70 days *[14]*. However, this study was conducted in the context of a waste water treatment plant (WWTP) and therefore may not be applicable to the marine environment. A more relevant study by Campo *et al.,* which focused on the biodegradability of C9500 (specifically DOSS) in conjunction with dispersed oil, found that in cooler water temperatures (5°C), the degradation of DOSS and oil was significantly inhibited relative to warm water environments (25°C). This results in DOSS persisting in the environment for at least 42 days in the presence

of HFO in cold water conditions, which was the total timeframe of this experimental study (Table **1-6**) *[36]*.

Table 1-6: DOSS degradation in the absence and presence of HFO at 5°C and 25°C *[36]*

Temperature	DOSS	DOSS + HFO
5°C	98% (42 days)	61% (42 days)
25°C	99% (8 days)	99% (14 days)

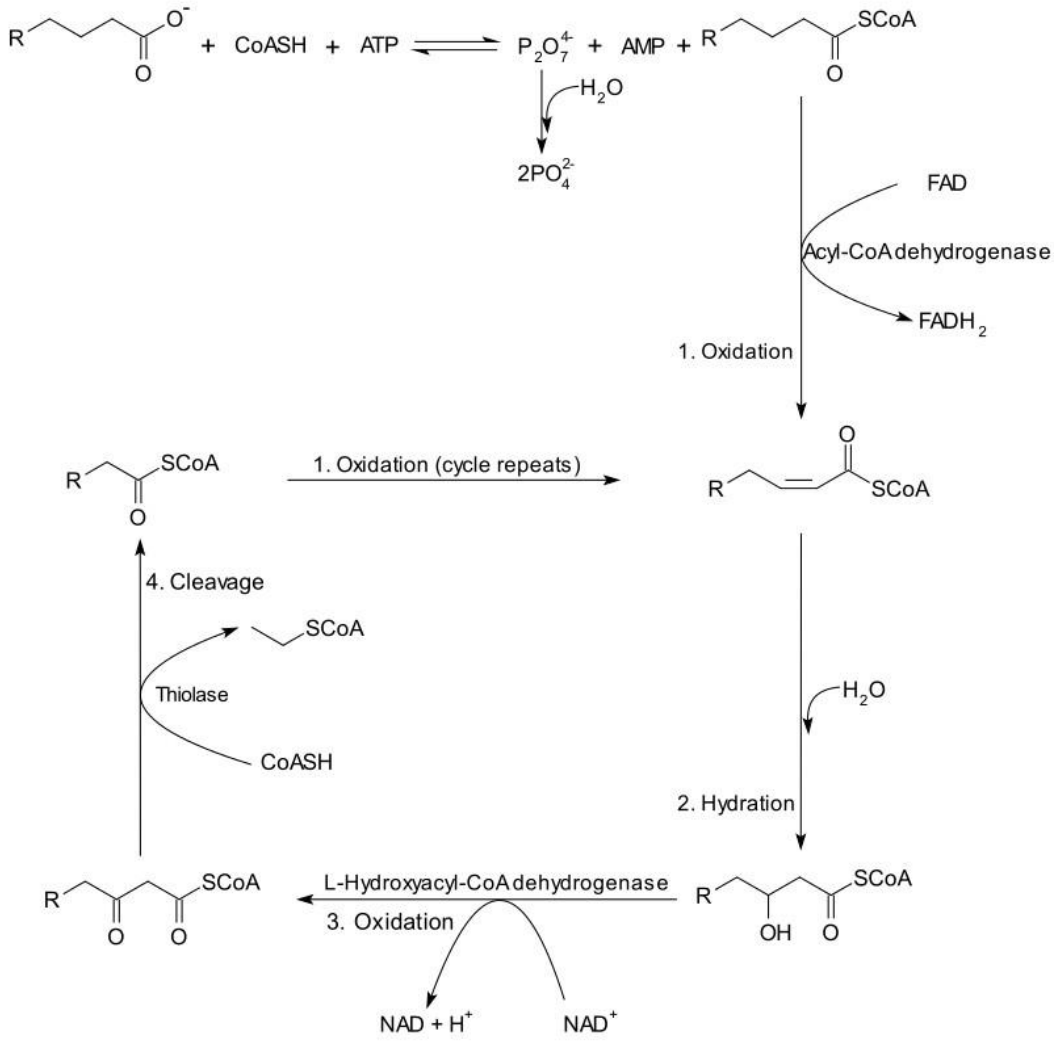

Figure 1-6: Biodegradation of fatty acids via β oxidation (adapted from *[50]*)

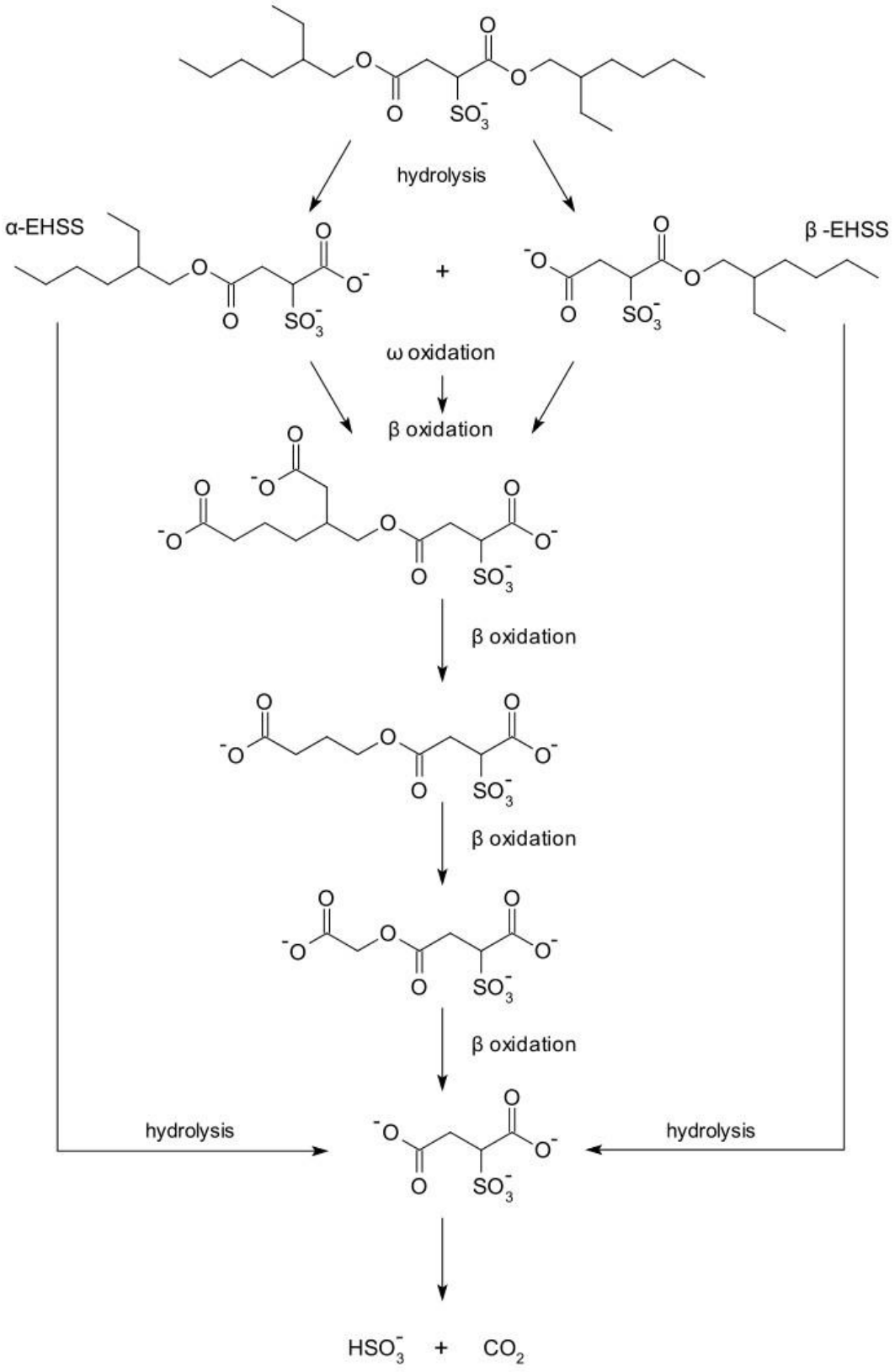

Figure 1-7: Biodegradation scheme for DOSS.

1.1.3.2 Degradation of sorbitan ester surfactants

The degradation of Span 80 begins with the hydrolysis of the ester linkage to give the fatty acid (oleic acid) and sugar components (sorbitol) that make up this surfactant. This results in primary degradation where the surface activity of the molecule is lost. The fatty acid component then undergoes β oxidation (Figure **1-6**) while the sugar component can be broken down via fructolysis (as part of glycolysis) *[50]* after conversion of sorbitol to fructose by sorbitol dehydrogenase *[52,53]*.

While the Tween type surfactants can also be hydrolyzed to liberate oleic acid, the POE groups require additional microbial processes in order to give free sorbitol that is available to undergo enzymatic conversion to fructose. In general, the greater the length of the POE chains, the slower the rate of biodegradation *[51]*. The biodegradation pathway of POE's generally proceeds by initial oxidation of the terminal alcohol group to an aldehyde followed by further oxidation to a carboxylic acid and subsequent cleavage of the ether bond. This results in a POE chain that is shortened by one EO unit. The process is repeated until the chain is depolymerized with the free glyoxylic acid moieties being processed via the oxidative dicarboxylic acid cycle and the glycerate pathway *[54-56]*. The free sorbitan can then be processed.

Short chain POE's, like those present in Tween surfactants, have been shown to be fully biodegraded within 37 days under aerobic conditions in a saltwater environment *[55]*. Additionally, the use of Tween type surfactants to disperse HFO's has been shown to stimulate the effectiveness of some types of bacteria that oxidize and consume hydrocarbons, increasing the rate of HFO degradation *[57,58]*.

1.2 Analysis of surfactants in the environment

Environmental analysis of surfactants poses many technical difficulties which are a direct result of their chemical structure. Historically, analysis of these compounds has suffered from low sensitivity and poor selectivity. Such methods were based on colorimetric principles such as the methylene blue active substance assay or complexometric principles such as the use of bis-(ethylenediamine) copper (II) followed by flame atomic absorption spectroscopy and as such were highly prone to chemical interferences *[41,51,59]*.

With the advent of modern instrumental analysis, issues of selectivity and sensitivity have generally been solved. However, a host of new problems arise with the use of such sensitive instruments. The current method of choice in the detection and quantification of surfactants is liquid chromatography tandem mass spectrometry (LC-MS-MS). Although the method offers excellent selectivity and extremely low limits of detection (highly sensitive), there are a number of problems associated with the technique. These include, amongst others, matrix effects, mobile phase incompatibility and ionization efficiency problems.

1.2.1 Sampling

Adequate sampling is vital to producing a meaningful analytical result. Primarily, it is crucial that the sample is representative. Non-representative sampling will result in an otherwise accurate methodology producing poor results. Hence, sampling methods need to be carefully designed, implemented and controlled *[60]*.

1.2.2 Sample Preparation

Sample preparation in the analysis of surfactants, like all trace analyses, depends on the physical state of sample matrix and the chemical properties of the target analyte. An ideal sample preparation methodology aims to maximize the amount of analyte extracted from the sample matrix and deliver the extract in a form that is as clean as possible, present in an appropriate phase and at a

concentration that is appropriate for the instrument chosen for the analytical measurement. After the samples have been gathered appropriately, sample preparation generally comprises four main steps:

1. Homogenisation
2. Extraction
3. Pre-concentration/dilution
4. Separation

1.2.2.1 Homogenization

Homogenization is required when the sample matrix is heterogeneous or the target analyte is thought or known to be dispersed heterogeneously throughout the sample matrix. In general, this applies to solid sample matrices such as soil and sediment samples. Such matrices invariably are made up of particulates of varying sizes which can affect the efficiency of the extraction method. Also, they are often made up of mixed matrix components which affects the partitioning of analytes due to differing chemical interactions between the various matrix-analyte domains. This can lead to a heterogeneous distribution of target compounds throughout the sample matrix, necessitating homogenization. Issues with partitioning in gaseous and liquid sample matrices can generally be solved by the implementation of an appropriate sampling regime *[44,60-63]*.

1.2.2.2 Extraction methods

After the sample has been homogenized, the analyte needs to be extracted from the raw sample matrix. This can be achieved in many ways, but is largely dictated by the physical state of the sample matrix.

At present, studies that have attempted to detect and quantify Corexit® components in the marine environment have focused on the water accommodated fraction (WAF) of these surfactants. Many of these methods used only a filtered sea water sample directly without any extraction methodology. Others employ a solid phase extraction (SPE) or liquid-liquid extraction (LLE) step as part of the sample preparation process. This

concentrates the analyte, allowing for lower limits of detection for trace analyses.

Gray *et al. [27,28]* presented two methods where the quantification of DOSS was achieved in coastal water samples. Sample preparation for both methodologies consisted of mixing to disperse particulates evenly followed by removal of a sub-sample from the bulk sample and addition of internal standards. The sub-sample was then filtered through a 0.2 µm polytetrafluoroethylene (PTFE) filter from a polypropylene syringe. Each filter was pre-cleaned with sequential flushing of methanol (MeOH), 1mM formic acid, isopropanol (IPA), 50:50 MeOH and MeOH. This filter cleaning procedure helped to reduce contamination problems. The filter was then eluted with 50% MeOH solution and the eluent collected for analysis. In a sense, this procedure is rather similar to an SPE type method, with sorption of the analyte to the polymeric material of the filter frit as opposed to the use of an SPE cartridge. Field blank and laboratory field blank recovery experiments of 5 $\mu g.L^{-1}$ DOSS fortified blanks with $^{13}C_4$-DOSS internal standard gave DOSS recovery values of 89 ± 9.5%.

Kujawinski *et al. [35]*, in a study aimed at determining the fate of DOSS in marine waters after the DWH disaster, compared the efficiency of LLE with an SPE technique. The LLE procedure consisted of 3 extractions of 500 mL of water sample with 100 mL of dichloromethane (DCM). The aqueous layer was then acidified to pH 3 followed by a further 3 extractions with DCM. The DCM fractions were combined and dried with combusted sodium sulfate. The aqueous fraction was extracted by SPE on a modified divinyl benzene polymer (PPL type) to extract any remaining water soluble dispersant and oil components. The SPE only extraction consisted of extraction of a 400 mL water sample on the PPL SPE resin only. Analysis showed that the additional LLE procedure was not necessary. Recoveries were in the range of 70-80%.

A direct injection LC-MS-MS method developed by Mathew *et al. [31]* employed a very simple sample preparation step in the analysis of DOSS in marine waters. Internal standard spiked water samples (20mL) were amended with 1M ammonium formate (NH_4HCO_2) to a give a 5 mM NH_4HCO_2 solution. Acetonitrile

was then added to give a 50% ACN solution. The sample was then filtered through a 0.22 µm polyvinylidene fluoride (PVDF) filter. Recoveries were 60-100% depending on the delay between recovery sample preparation and time of analysis. This has been attributed to the degradation of DOSS in seawater samples over time due to the ability of GOM microbial communities to hydrolyze DOSS *[64]*.

Ramirez *et al.* also developed an LC-MS-MS method for the quantification of DOSS in sea water, however an online SPE approach was taken, coupled to the HPLC system. After sample loading onto an end capped octadecylsilane (C18) SPE cartridge, the retained analytes were eluted with a gradient elution starting at 100% 10 mM NH_4HCO_2 proceeding to 100% ACN. Recoveries were found to be 92 ± 9%.

In a method developed by Place *et al. [25]* that quantified all of the surfactant components of C9500, no sample extraction procedure was implemented. Instead, frozen seawater samples (50 mL) were transferred into high density polyethylene (HDPE) bottles. The original sample containers were then rinsed with IPA to ensure the full transfer of surface adsorbed surfactants. The volume of IPA used to rinse the sample bottles equated to 25% of the total volume. A subsample of 5 mL was taken from the 25% IPA sample and spiked with internal standard before analysis. Recoveries for each component are listed in Table **1-7**.

Table 1-7: Percent recovery values for C9500 components as reported by Place *et al [25].*

Compound	% Recovery (95% CI)
DOSS	88 ± 10
α/β EHSS	91 ± 6
Span 80	91 ± 21
Tween 80	119 ± 13
Tween 85	106 ± 20

Although little information is available on the extraction of Corexit® components from marine sediments or other solid matrices (such as tar-balls or weathered oils), there are studies that deal with the extraction of the main classes of surfactants from various environments. Lara-Martin *et.al* employed the use of Soxhlet extraction and pressurized liquid extraction (PLE) in a method designed to determine multiple surfactants simultaneously in marine and aquatic sediments. This work included methodologies for both anionic and non-ionic surfactant classes *[65-68]*. Of these, Soxhlet extraction with methanol for 5 hours provided the most reliable extraction recovery for anionic surfactants with recoveries of 65%-112% for linear alkylbenzene sulfonate (LAS) based surfactants and 45%-109% for alcohol ethoxysulfate (AES) surfactants (Figure **1-8**). However, the authors recommended the use of PLE extraction when dealing with large numbers of samples due to its low solvent use and time efficiency. PLE was used for the extraction of non-ionics with recoveries of 66%-92% for the optimized PLE protocol.

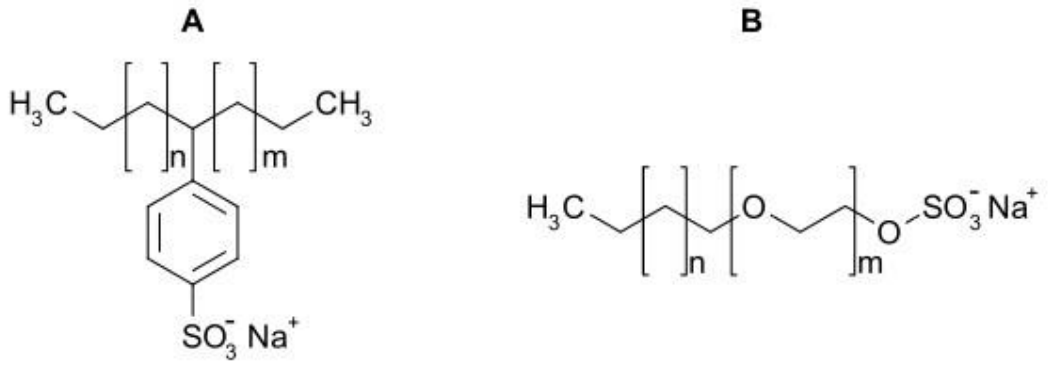

Figure 1-8: General structures for (A) LAS and (B) AES based surfactants.

Yeudakimau *et al.* have described a method for the extraction of DOSS from avian egg tissue by means of a QuEChERS (Quick, Easy, Cheap, Effective, Rugged, and Safe) extraction followed by SPE *[69]*. Although the extraction from egg tissue is not entirely relevant to extractions from marine sediments, the extraction clean up step by SPE illustrates how sample clean up post-extraction affords greater analytical sensitivity by reducing the detection limits of the analytical procedure. This method used a weak anion exchange (WAX) SPE

cartridge, which is ideal for anionic surfactants like DOSS, but is unlikely to be appropriate for non-ionic surfactants.

There are some problems that seem to be commonly encountered with the recovery of DOSS during sample preparation. These stem from the tendency for DOSS to bind to many surfaces, which is typical of a surfactant. Most researchers working with this surfactant report the loss of DOSS concentration to the surfaces of sample containers, syringe filters and storage containers *[24,25,31,35]*. To reduce this, some measures can be taken to reduce the extent of DOSS partitioning at interfaces. The use of an organic solvent (ACN or IPA) in proportions of 25-50% when preparing samples, stock standards and calibration standards has been shown to be effective at eliminating this effect *[24,25,31]*. Choice of syringe filter is also important as DOSS binds to certain polymers used in their manufacture. Aside from the use of PTFE filters as an extraction medium as demonstrated by Gray *et al. [27,28],* the use of PTFE filters is not recommended as it can significantly reduce the recovery of DOSS to as little as 6%. Instead, PVDF syringe filters are recommended, averaging 96% recovery for the same method *[31]*.

A further problem is the stability of DOSS in collected samples. In sea water samples, this is likely due to biodegradation by bacteria present in the collected waters *[31,64]*. This problem has also been reported with respect to the non-ionic constituents of C9500 *[25]*. Because of this, it is recommended that samples be stored at 4^{o}C or frozen until analysis *[24,25,27,28,31,35]*. The addition of sodium azide (NaN_3) or mercury (II) chloride ($HgCl_2$) to samples prone to biodegradation has been shown to be an effective method in preserving samples *[66,70]*.

1.2.3 Chromatographic Separation

Chromatographic separation of mixtures of compounds is based on the relative affinity of differing chemicals for a specific stationary phase (chromatography column) and mobile phase (eluent). Modern chromatographic methods employ either the use of Gas Chromatography (GC) or a Liquid Chromatography (LC).

In the analysis of surfactants, the use of liquid chromatography is prevalent, due to the high polarity, high molecular weight and consequent low volatility of many surfactants that precludes the use of GC despite its superior resolution *[41,71]*. This can be overcome by the use of a suitable derivatizing agent in order to impart the required volatility to the target compounds. Commonly used derivatizing agents in surfactant analysis include trifluoroethanol, diazomethane and N,O-bis(trimethylsilyl)trifluoro acetamide (BSTFA) *[41,71]*.

The use of GC has been employed in the detection of DOSS as a dispersed oil mixture, however the method was not quantitative and was focused on samples containing relatively high concentrations of DOSS (as C9500 and C9527) and is therefore unlikely to be an effective method for trace detection *[15]*.

A wide range of LC methods have been developed for the analysis of all major classes of surfactants. In the detection and quantification of DOSS and polysorbates (i.e. the surfactant components of C9500 and C9527), it is the most commonly used chromatographic technique (Table **1-8**).

Typically, the environmental analysis of C9500 has focused on DOSS as the primary marker for the presence of these dispersants, particularly for quantitative methodologies. The separation of DOSS by HPLC generally employs the use of a gradient elution of H_2O and ACN or MeOH through an octadecylsilane (ODS, C18) column with mass spectrometric (MS) detection *[24,27,28,31,35,69]*. Methods for polysorbate surfactants have generally been qualitative in nature, focusing on detection only. This is largely due to the lack of sufficiently pure, commercially available analytical standards *[33,42,72]*. A recent study *[25]* by Place *et al.* reported a method that quantified all surfactant components of C9500, including α/β-EHSS. The chromatographic conditions are

fairly standard, as the solvent selection and organic modifiers are somewhat restricted by the use of MS detection *[63]*. Separation of the components required gradient elution and the use of a flow rate ramp over the course of 36.5 min from 19.5 min to the end of the chromatographic run. The method also employed the use of a divert valve to prevent the accumulation of dissolved, non-volatile salts (raw sea water samples) on the MS source *[25]*. The separation of the non-ionic components shows poor resolution and very broad peak shape, which is somewhat expected with the distribution of oligomers present in these mixtures. The broad peak shape reflects the sequential elution of higher molecular weight oligomers where the individual peak response of each overlap, forming one broad peak. The use of MS-MS detection still allows for quantitation of the overlapping peaks as they are detected on a mass to charge ratio (m/z) basis, so co-elution is not as problematic as it would be for UV-VIS and ELSD based detection, provided ionization suppression or enhancement is accounted for.

Table 1-8: HPLC conditions for surfactant analysis relevant to C9500.

Surfactant	Column	Temperature (°C)	Flow rate ($mL.min^{-1}$)	Eluent A	Eluent B	Eluent regime	Detection*	Reference
Span 80	5µm C18	Ambient	1.0	H_2O	IPA	10:90 Isocratic	UV-VIS	*[42]*
DOSS	1.8µm C18	Ambient	0.65	H_2O 1mM NH_4HCO_2	MeOH 1mM NH_4HCO_2	Gradient	MRM-MS-MS QqQ-MS	*[28]*
DOSS	3µm C18 end capped	35	0.3	95% H_2O 4mM NH_4HCO_2	95% ACN 4mM NH_4HCO_2	Gradient	IT-MS	*[35]*
Span 80	5µm C4	60	0.2	H_2O 1% HCOOH	ACN 1% HCOOH	Gradient	ELSD IT-MS	*[72]*
DOSS	3µm C18	35	0.3	95% H_2O 5mM NH_4HCO_2	95% ACN 5mM NH_4HCO_2	Gradient	MRM-MS-MS QqQ-MS	*[31]*
Span/Tween	3.5µm C18	20	1.0	50% ACN or 50% ACN 0.1% HCOOH	THF	Gradient	ELSD IT-MS	*[33]*
DOSS	3µm C18	Ambient	0.325	H_2O 10mM NH_4HCO_2	ACN	Gradient	MRM-MS-MS QqQ-MS	*[24]*
DOSS	1.8µm C18	Ambient	0.65	H_2O 1mM NH_4HCO_2	MeOH 1mM NH_4HCO_2	Gradient	MRM-MS-MS QqQ-MS	*[27]*
DOSS/Span/ Tween α/β-EHSS	5µm C18	Ambient	0.5-0.75	H_2O 0.5mM NH_4HCO_2	ACN 0.5mM NH_4HCO_2	Gradient	MRM-MS-MS QqQ-MS	*[25]*
DOSS	1.7µm C18	50	0.5	H_2O 0.1% HCOOH	ACN 0.1% HCOOH	Gradient	UV-MRM-MS-MS QqQ-MS	*[69]*

* UV-VIS = Ultra violet – Visible wavelength detector; MRM-MS-MS = Multiple reaction monitoring tandem mass spectrometry; QqQ-MS = Triple quadrupole mass spectrometry; ELSD = Evaporative light scattering detector; IT-MS = Ion trap mass spectrometry.

1.2.4 Mass Spectrometric Detection

Based on the current literature, the most suitable detection method in the analysis of Corexit® formulations is MS. MS detection allows for unequivocal identification of analytes based upon the molecular weight of the parent molecular ion and, when tandem mass spectrometry (MS-MS) is employed, the unique daughter ions formed by fragmentation of the parent ion by collision induced dissociation (CID). The use of an electrospray ionization (ESI) source, which is commonly used for these types of analyses, generally gives a strong molecular ion signal, and hence, the population of daughter ions produced by CID is also high. This is ideal for quantitative methodologies, as it allows for lower limits of detection (LOD) and a more sensitive method. However, the use of MS-MS for trace analyses is generally limited to the use of triple quadrupole (QqQ) mass analyzer based instruments. As such, these are predominantly used in the quantification of surfactants.

Although ion trap (IT) MS mass analyzers are capable of MS-MS (in fact MS^n is possible), the nature of the instrument as an "MS-MS in time" technique results in lower analytical sensitivity when running the instrument in multiple (or selected) reaction monitoring (MRM or SRM) mode. Specifically, the duty cycle of the instrument, where selected precursor ions are isolated, fragmented and the population of daughter ions are scanned to produce the MS-MS spectrum, takes time. This time means that fewer measurements are taken across the peak response of a compound eluting from the HPLC system, and sensitivity is reduced as a result. Hence, quantitation using IT-MS is typically carried out by running the instrument in full scan MS^2 mode and using the extracted ion chromatogram (EIC) obtained from the total ion chromatogram trace (TIC). Identification of compounds is based upon retention time (t_r), molecular ion mass (M^+ or M^-) and concomitant observation of diagnostic, confirmatory fragment ions in the MS^2 spectrum.

Triple quadrupole instruments do not suffer from this limitation, due to their "MS-MS in space" functionality, and actually increase in sensitivity when run in MRM mode. Briefly, the first quadrupole (Q_1) acts a mass filter to select a set of chosen molecular ions and those of unwanted masses are discarded. In the second quadrupole (q_2), or collision cell, the chosen ions are fragmented to afford a population of daughter ions which are subsequently analyzed by Q_3. So, because each quadrupole is dedicated to a specific function of the MS-MS experiment, more scan cycles are applied per ion of a specific m/z per unit time. Because only a small selection of precursor ions and transitions to daughter ions are used, the instrument noise is greatly reduced, giving a lower LOD. Additionally, the fragmentation of precursors gives specific and reproducible populations of daughter ions, so the selectivity of the technique is also greatly enhanced.

1.2.4.1 Quantitative analysis by mass spectrometry

Like all quantitative chemical analyses, quantitation by mass spectrometry involves the comparison of the instrument response of a known quantity of analyte with the instrument response of an unknown quantity of analyte *[63]*. The comparison of instrument response is usually achieved by the use of a calibration curve that is constructed by running analytical standards of increasing concentration through the analytical method. This produces a plot that relates instrument response to analyte concentration. In order to correct for variations in instrument response, an internal standard is usually added at a constant concentration and the ratio of analyte to internal standard is used as the comparative measure (response factor or normalized response)*[44,60,63]*.

1.2.4.1.1 Internal standards

Ideally, the internal standard used for a quantitative MS assay is a stable isotope enriched version of the target analyte *[63]*. Hence, methods that have been developed to quantify DOSS have employed this type of internal standard, with ^{2}H-DOSS, DOSS-$^{13}C_4$ and DOSS-D_{34} being commonly used (Table **1-9**) *[24,25,27,28,31,35,69]*. The advantage of using an isotopically labelled internal

standard is that they behave nearly identically to the unlabelled target material so that losses during the sample work up can be easily accounted for. They also ionize similarly at the MS source, have similar LC retention times and can be resolved from each other by mass when using MS detection. However, isotopically labelled standards are often unavailable for uncommon compounds, are very expensive and in some cases need to be synthesized to order or in-house. Other isotopically labelled standards that have been used in quantitative MS methodologies for DOSS include ibuprofen-d3 and SDS-$^{2}D_{25}$ *[24,27,28]*. As synthesizing labelled compounds is a difficult synthetic task, other options include the use of a chemical isomer, homologue or analogue. In the case of DOSS, pyrene sulfonate (1-pyrene sulfonic acid sodium salt, 1-PSA) has been suggested as a possible option (Figure **1-9**) *[34]*. With the non-ionic components of C9500, quantification methodologies have used an external standard approach that employs the use of commercially available compounds of the same chemical composition as the target analyte *[25,72]*.

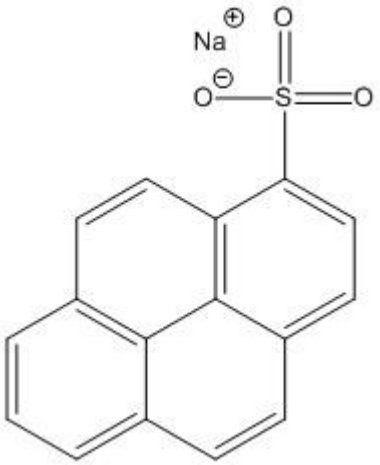

Figure 1-9: Structure of 1-pyrene sulfonic acid sodium salt.

Table 1-9: Standards and quantification methods used in C9500 analyses.

Analyte	Standard	Quantitative method	Reference
DOSS	$^{13}C_4$-DOSS, ibuprofen-D3	Internal standard	*[28]*
DOSS	$^{13}C_4$-DOSS, ^{2}H-DOSS	Internal standard	*[35]*
Span 80	Span 80	External standard	*[72]*
DOSS	DOSS-D34	Internal standard	*[31]*
DOSS, α/β EHSS	DOSS, α/β EHSS	External standard	*[26]*
DOSS	$^{13}C_4$-DOSS, SDS-$^{2}H_{25}$	Internal standard	*[24]*
DOSS	$^{13}C_4$-DOSS, ibuprofen-D3	Internal standard	*[27]*
DOSS, α/β EHSS, Span 80, Tween 80, Tween 85	$^{13}C_4$-DOSS, $^{13}C_4$-EHSS Span 80, Tween 80, Tween 85	Internal standard External standard	*[25]*
DOSS	$^{13}C_4$-DOSS, ^{2}H-DOSS	Internal standard	*[73]*
DOSS	SDS-D25, SDS-D1, SOS-D17	Internal standard	*[69]*

2 Development of the instrumental method

An LC-MS-MS method was developed for the detection and quantification of DOSS as a marker for the presence of C9500 at trace levels. This involved MS experiments to determine molecular ions, development of MS-MS transitions, optimization of the MS source and implementation of a suitable HPLC method.

2.1 Direct infusion mass spectrometry

Preliminary experiments involved direct infusion of C9500 (Nalco), DOSS, Tween 80® and Span 80® (Sigma-Aldrich) at appropriate dilutions to assess the initial mass spectrum and required source polarities. Initial scan width settings were guided by the published literature on the compounds present in C9500 and their respective molecular weights (Table **2-1**) *[31,34]*. The default MS parameter settings for voltage, dry gas and ion optics were used for these initial tests; capillary voltage 3.5 kV, end plate offset -500 V, dry gas flow rate 10 $L.min^{-1}$ and dry gas temperature 250^{o}C. Nitrogen was used as the drying and collision gas. Direct infusion mass spectrometry was carried out using a Bruker amaZon X ion trap mass spectrometer controlled by the Compass 3.2 trap control software (Bruker).

Table 2-1: Molecular weight of major C9500 components.

Compound	Molecular weight
Butoxypropylene glycol	190.28
α/β-EHSS	332.35
DOSS	444.56
Span 80	428.60
Tween 80	1310 (average)
Tween 85	1838 (average)

2.1.1 Direct infusion mass spectrometry of C9500

Direct infusion of C9500 was carried out by introducing a 125 $mg.L^{-1}$ solution (made to volume with 50% ACN and 5mM NH_4HCO_2) into the ESI source via the syringe pump at a flow rate of 10 $\mu L.min^{-1}$. From the literature *[25]*, this represents concentrations of approximately 5.5 $mg.L^{-1}$, 22.5 $mg.L^{-1}$ and 22.5 $mg.L^{-1}$ for Span 80®, Tween 80® and DOSS respectively. The initial scan range was m/z 50-2000 at 8100 $m/z.sec^{-1}$, tuned to m/z 400.

Negative ion mode gave a single, strong peak at m/z 421, which was indicative of the presence of the $[DOSS\text{-}Na]^-$ molecular ion. A small peak was also observed at m/z 865. This is likely due to the formation of the dimer $[DOSS_2Na]^-$, although the amount formed is negligible (Figure **2-1**, Table **2-2**).

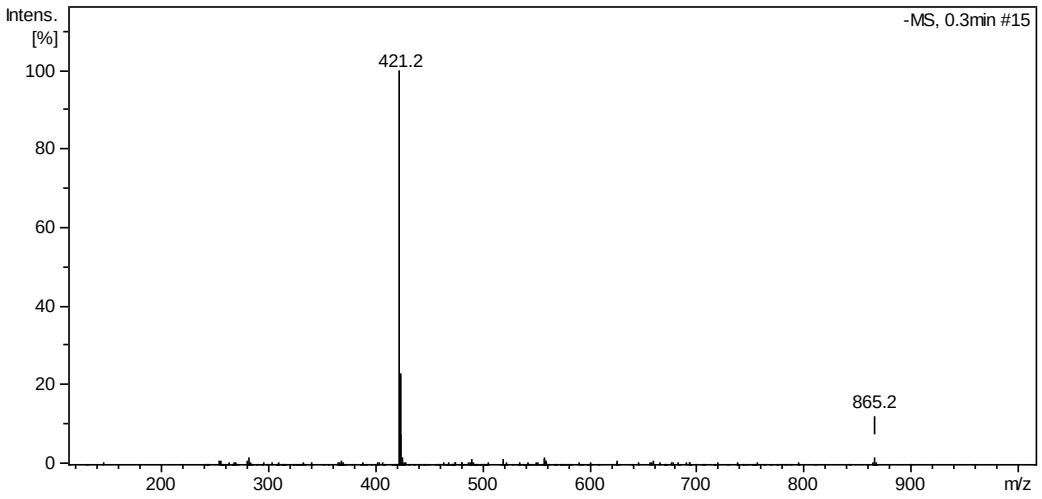

Figure 2-1: Negative mode direct injection ESI-MS spectrum of C9500.

The positive ion mass spectrum was rather more complicated, but was generally in accordance with what would be expected from the listed components (Figure **2-2**, Table **2-3**). At the low molecular weight end of the spectrum, the peak at m/z 213 was consistent with the formation of a butoxypropylene glycol sodium adduct, $[C_{10}H_{22}O_3+Na]^+$. The strong peak at m/z 440 can again be attributed to the presence of DOSS in the form of an H_2O adduct $[DOSSH+H_2O]^+$.

The multiply overlapped envelope of ions spread from m/z 300 – 2000 was characteristic of the non-ionic Tween 80 and Tween 85 surfactants (Figure **5-3**, Figure **5-4**, Figure **5-5** and Figure **5-6**). A notable feature of these sequences of

ions is the loss of 44 Da neutral fragments which equate to the mass of the polyoxyethylene repeating units (CH_2CH_2O). For example, the series of ions that peaks at m/z 652 could likely represent an isosorbide polyethoxylate sodium adduct with the loss of oleic acid, $[C_6H_8O_2(C_2H_4O)n(OH)_2+Na]^+$. Overlaid with this sequence is a series of less intense signals centered around m/z 628. This equates to a doubly charged ammonium adduct of sorbitan polyethoxylate, $[C_6H_8O.(C_2H_4O)_n+2NH_4]^{2+}$. The oleic acid fragment of these fragments was also observed at m/z 283 $(C_{17}H_{33}COOH + H)^+$.

Other clusters across the m/z range that are separated by m/z 44 can also be similarly rationalized by the formation of various ions and adducts of sorbitan polyethoxylate, sorbitan polyethoxylate monooleate, sorbitan polyethoxylate diooleate and their isosorbide equivalents *[33,40,74,75]*. The peak at m/z 341 may also be evidence of the presence of polysorbate based surfactants, being consistent with a sorbitan unit with four ethylene oxide units, $[C_6H_8O.(C_2H_4O)_4(OH)_4+H]^+$.

Due to the mass of the oleic acid moiety being equivalent to six ethylene oxide units, there was significant isobaric overlap of sequences that both contain and do not contain the oleate group *[40,75]*.

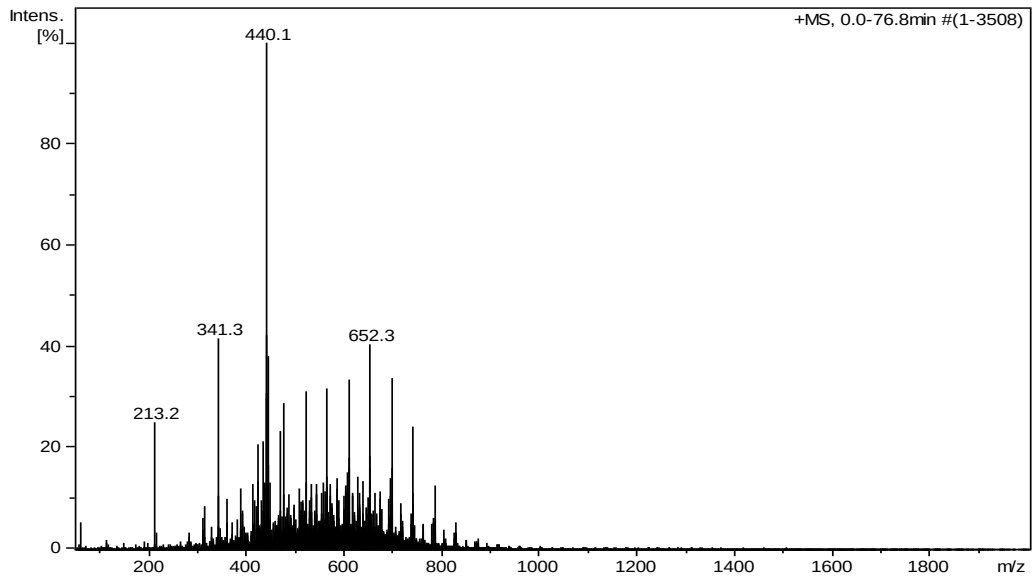

Figure 2-2: Positive mode direct injection ESI-MS spectrum of C9500.

2.1.2 Direct infusion mass spectrometry of surfactant standards

In order to assess the validity of the assignment of ions, direct injection ESI spectra were recorded of pure surfactant samples where available. Separate samples of DOSS, Tween 80® and Span 80® were injected at concentrations of approximately 125 $mg.L^{-1}$. Samples were prepared in 50% ACN solution with 5mM NH_4HCO_2. The direct injection system was flushed with blank 50% ACN, 5mM NH_4HCO_2 solution followed by a second flush with MeOH between the analyses of each surfactant to minimize cross contamination of the ESI source. Assignment of the observed ions are listed in Table **2-2** and Table **2-3**.

The negative mode spectra for DOSS (Figure **5-7**) showed a strong molecular ion signal at m/z 421, corresponding to $[DOSS\text{-}Na]^-$. A small peak at m/z 865 was indicative of the $[DOSS_2Na]^-$ adduct. The negative ion mode spectrum of pure DOSS resembles that of C9500 very closely and gave sufficient reason to conclude that the signal at m/z 421 in the C9500 sample was attributable to DOSS with a small population of DOSS molecules forming dimeric Na adducts (m/z 865). This was also in agreement with reports in the literature *[31,34]*.

The cluster of ions at m/z 297,311,325,339 present in the DOSS negative ion mode spectrum (Figure **5-8**) is a commonly used group of ions in the identification of LAS surfactants *[41]*. LAS surfactants are widely used in cleaning products and the presence of these ions likely reflect residual build-up of LAS on laboratory glassware and equipment due to cleaning with LAS based detergents.

In positive mode (Figure **5-9**), there were strong signals at m/z 440 and 445 which were likely due to $[HDOSS+H_2O]^+$ and $[HDOSS+Na]^+$ adducts respectively. These were also observed in the C9500 sample. Various dimeric ions appeared clustered around m/z 865 including $[2HDOSS+H+H_2O]^+$. The intensity of these dimeric cluster ions is very low in both positive and negative ion mode and unlikely to be apparent when working with low ($\mu g.L^{-1}$) concentration samples. No signals were observed that correlated to the presence of α/β-EHSS.

In the negative ionization mode, Span 80® ionizes poorly (Figure **5-10**). However, two strong peaks are observed at m/z 281 and 473. These were likely to be the deprotonated oleic acid fragment of the molecule ($[C_{18}H_{34}O_2]^-$) and the formate adduct of the molecular ion ($[C_{22}H_{44}O_6 + HCOO]^-$). The absence of these peaks in the C9500 spectra was possibly due to ionization suppression caused by the preferential ionization of DOSS present in the mixture and the lower concentration of Span 80® present in C9500 compared to DOSS *[25]* (Table 1-8). The cluster of ions at m/z 297,311,325,339 was again present, reflecting LAS background contamination. Span 80® ionizes more readily in positive ion mode (Figure **5-11**), with a cluster of peaks of good intensity at m/z 411, 429, 451 and 491. The peak at m/z 411 is of equivalent mass to the dehydrated molecular ion ($[C_{24}H_{44}O_6 - H_2O + H]^+$) while the other 3 are equivalent to the molecular ion, Na adduct and ACN + Na adducts respectively ($[C_{22}H_{44}O_6 + H]^+$, $[C_{22}H_{44}O_6 + Na]^+$, $[C_{22}H_{44}O_6 + ACN + Na]^+$). The peak at m/z 283 is consistent with the formation of oleic acid that has gained a proton ($[C_{17}H_{33}COOH + H]^+$).

As with Span 80®, Tween 80® is poorly ionized in negative ion mode, with the strongest peaks being those associated with LAS contamination (Figure **5-13**, Figure **5-14**). The most notable peak that is likely indicative of the presence of Tween 80 is that at m/z 281 formed by the oleic acid part of the molecule ($[C_{17}H_{33}COO]^-$).

The positive mode however gave good ionization, with the characteristic overlay of the various polymeric series present in these surfactant mixtures (Figure **5-15**, Figure **5-16**, Figure **5-17**, Figure **5-18** and Figure **5-19**). Much of the same series of ions are observed as seen in the C9500 spectrum discussed previously, although some extra details are noticed due to the lower degree of overlap and cluttering of the spectra from the other surfactants present in C9500 (particularly Tween 85 for which no standard was tested).

Table 2-2: Observed ions in negative ion mode direct injection ESI-MS for C9500, DOSS, Tween 80® and Span 80®.

Sample	Observed m/z	Assignment
C9500	421	$[DOSS]^-$
	865	$[DOSS_2 + Na]^-$
DOSS	421	$[DOSS]^-$
	865	$[DOSS_2 + Na]^-$
Tween 80	281	$[C_{17}H_{33}COO]^-$
Span 80	281	$[C_{17}H_{33}COO]^-$
	473	$[C_{22}H_{44}O_6 + HCOO]^-$

Table 2-3: Observed ions in positive ion mode direct injection ESI-MS for C9500, DOSS, Tween 80® and Span 80®.

Sample	Observed m/z	Assignment
C9500	213	$[C_{10}H_{22}O_3 + Na]^+$
	309	$[C_{17}H_{33}COOCH_2CH_2]^+$
	341	$[C_6H_8O(C_2H_4O)_4(OH)_4 + H]^+$
	440	$[HDOSS + H_2O]^+$
	445	$[HDOSS + Na]^+$
	628	$[C_6H_8O(C_2H_4O)_n(OH)_4+2NH_4]^{2+}$
	652	$[C_6H_8O_2(C_2H_4O)n(OH)_2+Na]^+$
	1133	$[C_6H_8O(C_2H_4O)_n(OH)_4+H]^+$
	1502	$[C_6H_8O(C_2H_4O)_n(OH)_4+NH_4]^+$
DOSS	440	$[HDOSS + H_2O]^+$
	445	$[HDOSS + Na]^+$
	865	$[2HDOSS + H + H_2O]^+$
Tween 80	149	$[C_6H_8O(C_2H_4O)_3(OH)_4 + 2H]^{2+}$
	283	$[C_{18}H_{33}COOH + H]^+$
	309	$[C_{18}H_{33}COOCH_2CH_2]^+$
	390	$[C_6H_8O_2(CH_2CH_2O)_n(OH)_2 + 3NH_4]^{3+}$
	487	$[C_6H_8O_2(CH_2CH_2O)_n(OH)_2 + 2NH_4]^{2+}$
	586	$[C_6H_8O_2(CH_2CH_2O)_n(OH)_2 + H]^+$
	804	$[C_6H_8O(CH_2CH_2O)_n(OH)_4 + 2NH_4]^{2+}$
	826	$[C_6H_8O(CH_2CH_2O)_n(OH)_4 + H]^+$
	1136	$[C_6H_8O_2(CH_2CH_2O)_n(OH)_2 + Na]^+$
	1176	$[C_6H_8O(CH_2CH_2O)_n(OH)_3C_{18}H_{33}COOH + H]^+$
	1414	$[C_6H_8O(CH_2CH_2O)_n(OH)_4 + NH_4]^+$
Span 80	283	$[C_1H_{33}COOH + H]^+$
	411	$[C_{24}H_{44}O_6 - H_2O + H]^+$
	429	$[C_{24}H_{44}O_6 + H]^+$
	451	$[C_{24}H_{44}O_6 + Na]^+$
	491	$[C_{24}H_{44}O_6 + ACN + Na]^+$

2.2 HPLC-MS

In order to separate the analyte components from themselves and other matrix components, an HPLC method was adapted from the literature. Due to the complicated nature of the mass spectra of non-ionic surfactants, the lack of available analytical standards and the variation in composition between commercially available Tween surfactants, DOSS was chosen as a suitable marker for detecting the presence of C9500. Although only one analyte was chosen for quantitation, a chromatographic method is still required to ensure each surfactant compound and matrix component is introduced to the MS source individually, as combinations can lead to ionization suppression (matrix effects). Also, quantification of the analyte is usually carried out using an internal standard approach, so a chromatographic method needs to be employed to separate the standard from the analyte. Ion trap MS (IT-MS) was chosen for detection. Although this type of instrument is not as suited to quantitative applications as QqQ instruments, the choice was limited by the available instrumentation.

2.2.1 HPLC

Evaluation of the literature showed that successful chromatography could be achieved from a relatively narrow set of chromatographic parameters (Table **1-8**). However, due to the use of an IT-MS, the methodology employed by Kujawinski *et al.* and developed further by Mathew *et al.* was initially trialled (Table **2-9**) *[31,35]*. During initial trials of HPLC methods, the MS was operated with default voltage, dry gas and ion optic parameters as stated previously. The HPLC method employed the use of HPLC grade ACN (Merck Millipore), deionized (DI) water at >17.8 Ω resistivity (Barnstead E-pure) and ammonium formate (NH_4HCO_2, 97%, Sigma-Aldrich).

2.2.1.1 Stability of MS signal response

During the initial trials of analytical and internal standards, it was noticed that the MS signal response would decrease with replicate injections of the same concentration. This was first noticed when running a series of calibration standards, during which standards of higher concentration were giving a lower instrument response to the point where no signal response was recorded at all. These initial chromatographic trials employed the use of a C18, 5µm, 100Å column (Phenomenex) and default mass spectrometer settings.

The problem was investigated more thoroughly by injecting 20 replicates of 100ug.L^{-1} DOSS and 1-PSA mixtures and plotting the peak response against the replicate number. The plot this produces clearly demonstrates the loss of MS signal response (Figure **2-3**).

Although the standards were prepared in a 50% ACN solution to reduce the partitioning of the surfactants at the glass/solvent interface *[31]*, it was thought this might still be occurring. In order to test the hypothesis, deactivated, silanized glass auto sampler vials were trialled (Agilent). Although the use of these vials significantly reduced the degree of signal attenuation, there was still a marked decrease over time (Figure **2-4**). This suggested that a secondary factor was influencing the instrument response.

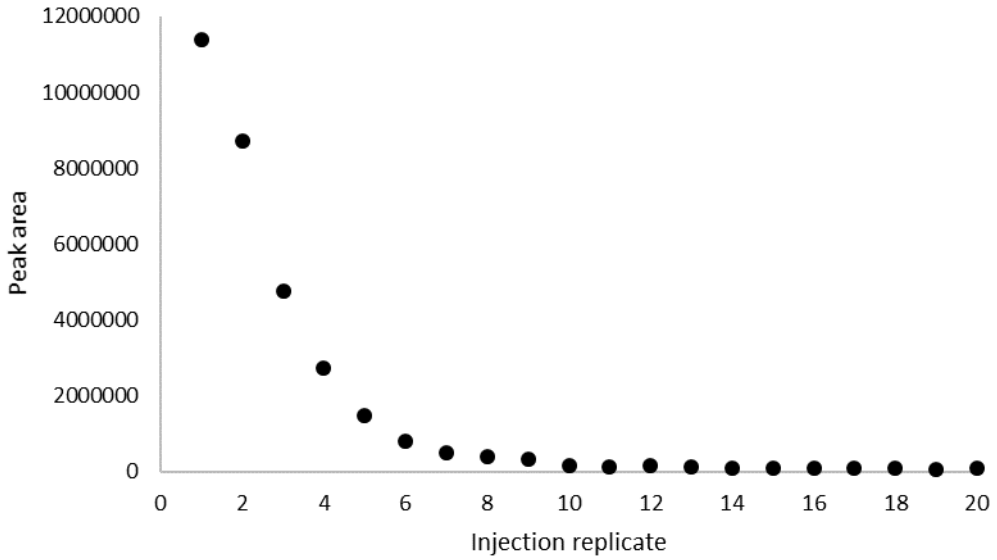

Figure 2-3: DOSS instrument response with respect to injection replicate.

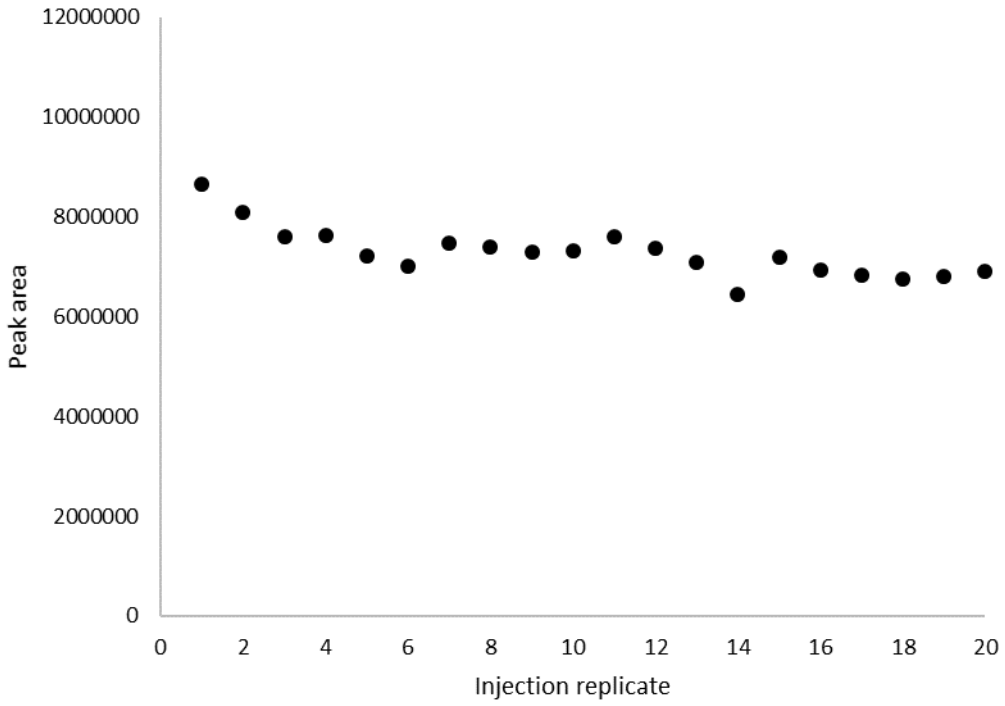

Figure 2-4: DOSS instrument response with respect to injection replicate using silanized glass vials.

Due to the tendency of surfactants to bind to many surfaces and their known ionization suppression tendencies, the accumulation of surfactant molecules at the MS source could possibly produce the observed phenomena. By inserting wash and blank injections between each standard injection, it was possible to produce a relatively stable signal response. However, this resulted in exceedingly long analytical run times and was wasteful of solvent.

Changes in chromatographic peak height can also be attributed to changes in column activity *[76]*. To assess whether this was indeed the problem, a different column was tested (octylsilane (C8), 5µm, 100Å; Phenomenex). This solved the problem and gave repeatable MS signal response (Figure **2-5**). Interestingly, the C8 column was shown to give longer retention times (t_r), although it was expected that the less hydrophobic stationary phase would shorten the retention time (Table **2-4**, Table **2-5**). A possible explanation for this is that the shorter chain lengths of the C8 column leave any silanol groups (Si-OH) groups of the silica support more exposed to the mobile phase. These groups can then interact with the anionic group of the surfactants in addition to the hydrophobic

interactions between the hydrophobic tails of the surfactants and the C8 chains of the stationary phase. This would lead to the observed increase in retention times.

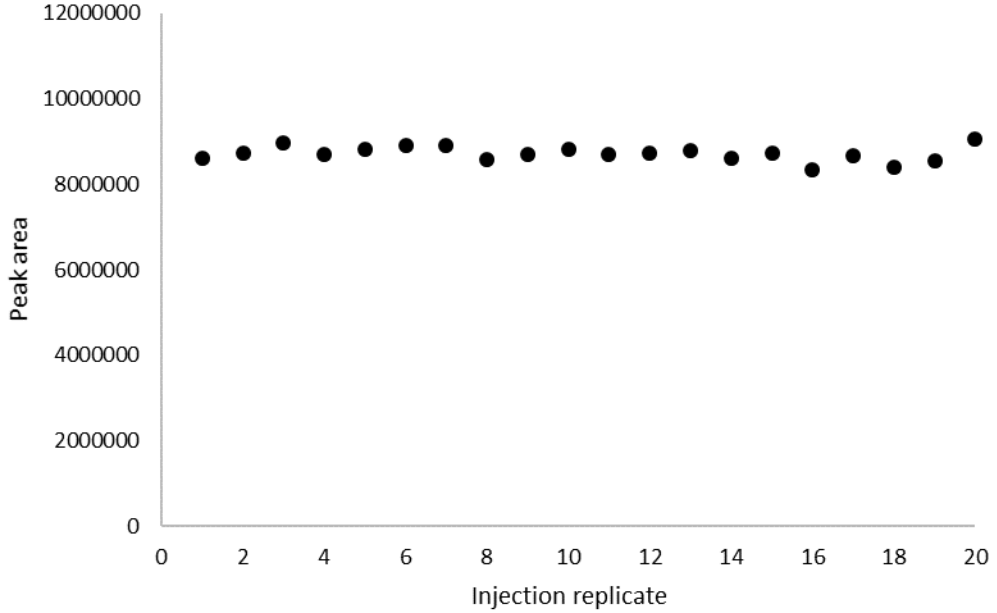

Figure 2-5: DOSS instrument response with respect to injection replicate using a C8 column and silanized glass vials.

2.2.1.2 Analytical standards

An analytical standard of DOSS (>97% purity, Sigma-Aldrich) was used as the calibrating standard and for initial tests of the LC-MS gradient and source settings. This was carried out to ensure DOSS could be adequately be detected and to determine the retention time of DOSS under the HPLC conditions used (Figure **5-22**, Figure **5-23**).

Table 2-4: Retention times for DOSS on C8 and C18 HPLC columns.

Column	Retention time (min)
C8 5µm 100 Å	7.1
C18 5µm 100 Å	6.9

2.2.1.3 Internal standards

Two internal standards were tested. These were both chemical analogues chosen for their availability and relative cost effectiveness compared with deuterated, isotopically labelled internal standards. Both sodium dodecyl sulfate (SDS, 97% purity, Sigma-Aldrich) and 1-pyrene sulfonic acid sodium salt (1-PSA, > 98% purity, Sigma-Aldrich) were trialled to assess their ionization characteristics and determine their retention times (Table **2-5**, Figure **5-22**, Figure **5-23** and Figure **5-24**). Of these compounds, 1-PSA was chosen for the remaining experiments due to persistent background contamination of laboratory water and environmental samples with SDS (see Section **3.2.4.1**).

Table 2-5: Retention times for 1-PSA and SDS on C8 and C18 HPLC columns

Column	1-PSA Retention time (min)	SDS Retention time (min)
C8 5µm 100 Å	5.7	6.7
C18 5µm 100 Å	5.4	6.3

2.2.1.4 Auto-sampler carryover

Preliminary tests of standards containing DOSS only, showed that sample carryover was occurring. In order to alleviate the problem, various auto-sampler needle wash solutions mentioned in the literature were trialled *[24,31,35]*, with a 2mL wash volume of 40% IPA and 60% ACN being found to be effective.

2.2.1.5 UV-DAD detection

UV detection was initially considered to give complementary data and detection power when coupled to the MS instrument. UV-vis experiments were carried out using a Varian Cary 100 UV-vis spectrophotometer for DOSS, SDS and 1-PSA to determine λ_{max} for each compound (Table **2-6**, Figure **5-25**, Figure **5-26** and Figure **5-27**). However, the use of UV-DAD detection proved not to be sensitive enough at the concentration ranges under study.

Table 2-6: λ_{max} values for DOSS, SDS and 1-PSA as determined by UV-vis spectroscopy.

Compound	λ_{max} (nm)
DOSS	222
SDS	224
1-PSA	242

2.2.2 ESI-IT-MS

Mass spectrometer experiments were carried out in order to optimize the ionization efficiency for DOSS.

2.2.2.1 Eluent modifiers

The use of MS detection precludes the use of many common organic modifiers used in HPLC eluents. As ESI-MS requires these modifiers to be volatile, buffers such at phosphates cannot be used. Additionally, ion pairing reagents such as trifluoroacetic acid (TFA) are not recommended due to the strong ionization suppression that they exhibit (problematic for quantitative trace analysis) and their tendency to persist as a background contaminant in LC-MS systems *[63]*.

In the case of surfactant analysis, formic acid (HCOOH) and ammonium formate (NH_4HCO_2) are most often used. These modifiers were both trialled to assess their effect on the ionization of DOSS. The use of NH_4HCO_2 gave good MS signal response. The use of HCOOH gave no signal response. It is possible that the addition of HCOOH results in DOSS in its protonated, neutral form (HDOSS) which would not be seen in the negative ESI-MS spectrum. Alternatively, HCOOH may significantly suppress the ionization of DOSS in negative ionization mode (Figure **5-28** and Figure **5-29**).

2.2.2.2 ESI source settings

ESI source settings were adjusted to afford the highest intensity signal for the DOSS molecular ion (m/z 421.2). In order to assess the optimum capillary voltage and dry gas temperatures, triplicate analyses of a constant concentration (100 $\mu g.L^{-1}$) DOSS standard were carried out at three drying gas temperature settings (250°C, 300°C and 350°C) while varying the spray capillary voltage for each temperature level (3.5 kV, 4.0 kV, 4.5 kV). Instrument response was assessed on a peak area and maximum ion count basis, with the maximum intensity being found with settings of 4.0 kV and 350°C (Table **2-7**, Figure **2-6**, Figure **2-7** and Table **5-1**).

Table 2-7: Mean DOSS peak area and ion count at three different capillary voltages and drying gas temperatures.

	Mean DOSS peak area			Mean DOSS ion count		
Voltage	250°C	300°C	350°C	250°C	300°C	350°C
3.5kV	7387882	8545591	9379765	352432	401258	463136
4.0kV	7759345	8689326	9810938	388345	412956	478586
4.5kV	8000585	8949784	9804510	409575	434526	458614

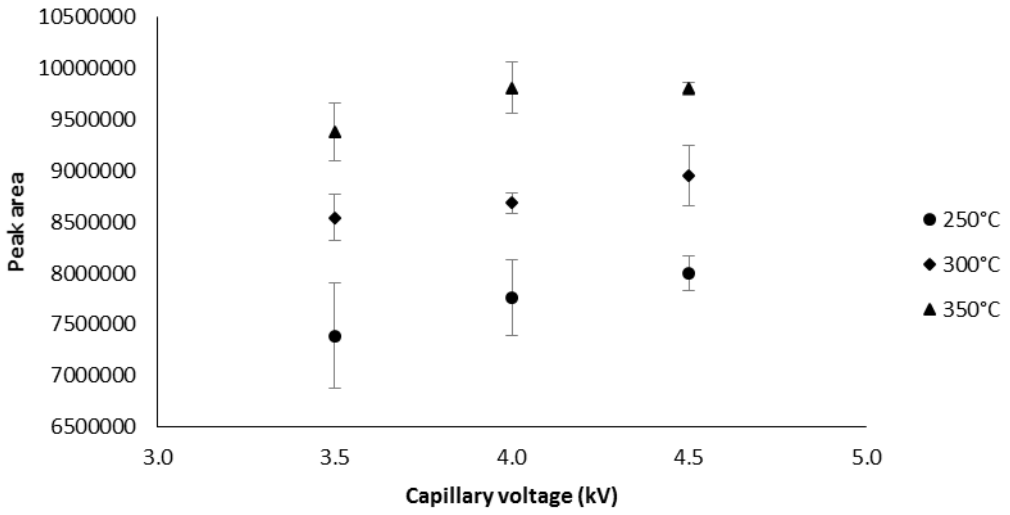

Figure 2-6: DOSS peak area at three different dry gas temperatures and capillary voltages.

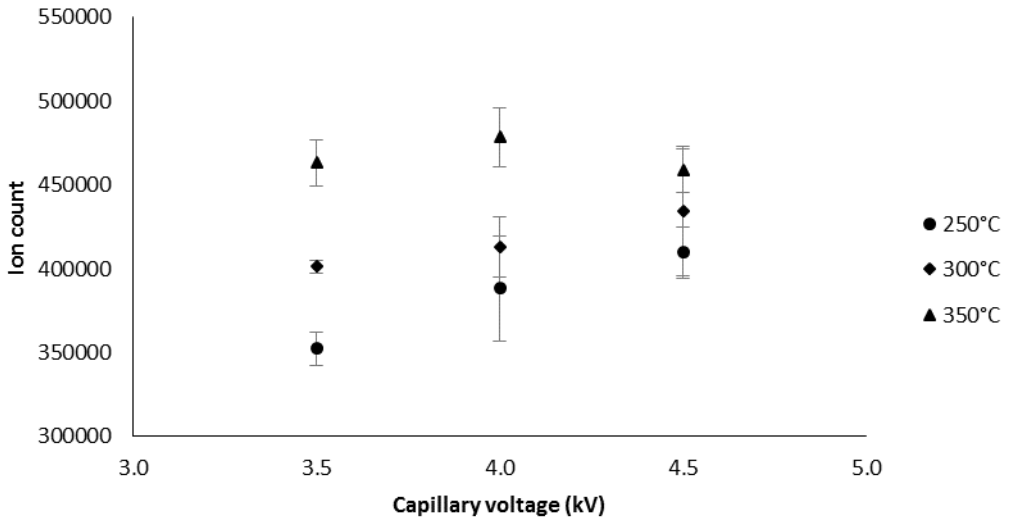

Figure 2-7: DOSS maximum ion count at three different dry gas temperatures and capillary voltages.

2.2.2.3 ESI-MS-MS transitions

MS-MS experiments were carried out for DOSS, SDS and 1-PSA. In order to best simulate the ionization conditions for each compound, the eluent composition and flow rate at the known retention times was simulated while the compounds were introduced individually to the ESI-MS source. This was achieved by introducing the sample via the syringe pump connected to a tee-connector while running the HPLC system at the same mobile phase composition as when the compound would normally elute (Figure **2-8**). From the retention times obtained for the analytical and internal standards, all were found to elute when the HPLC gradient composition was that of 100% eluent B (95% ACN, 5% H_2O, 5mM NH_4HCO_2). The flow rate of the syringe pump (10 µL.min^{-1}) and the HPLC system (290 µL.min^{-1}) were adjusted to give a total flow rate equal to the flow rate used for the LC-MS method (300 µL.min^{-1}). Sample concentrations of 100 µg.L^{-1} were used. The ESI source settings were those previously developed for DOSS (Section **2.2.2.2**).

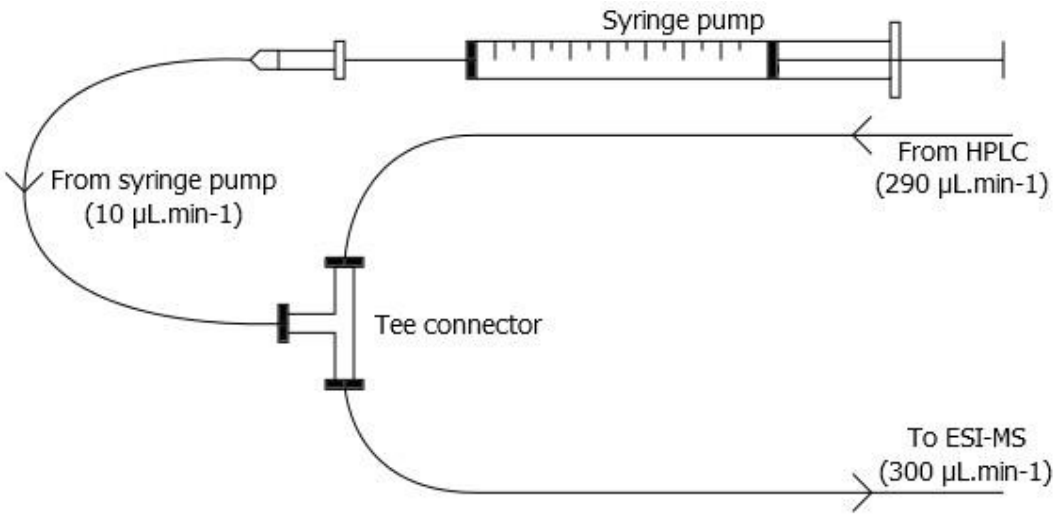

Figure 2-8: Schematic of direct infusion tee connection setup for the development of MS-MS transitions.

Isolation and fragmentation of the DOSS molecular ion (m/z = 421) affords three main fragment ions at m/z 81, 227 and 291 (Figure **5-30**). The base peak of this fragmentation pattern is m/z 81. This ion can be attributed to the cleaved sulfonate group which has picked up a proton (HSO_3^-; bisulfate ion). The ions at m/z 227 and 291 are of significantly lower intensity, but the presence of two extra fragmentation ions give added confirmatory information when using MS-MS detection as a quantification tool. That is, the detection of an ion at m/z 421 in a real world sample will not in all cases represent the detection of DOSS. However, the detection of m/z 421 with a fragmentation pattern that affords the ions associated with the MS-MS spectra of DOSS, gives added selectivity to the analytical method. The structures of m/z 227 and 291 can be tentatively assigned by hypothesizing the loss of various substituent groups and the shortening of alkyl chains. These result in the loss of radical or positively charged fragments with negatively charged radical or poly radical ions being formed (Figure **2-9**).

The MS-MS spectrum for the SDS (Figure **5-31**) molecular ion (m/z 265, Figure **5-20**) gave two major fragment ions (m/z 80 and 97). These ions were likely to be formed by cleavage of the sulfate group either between the sulfur and the oxygen bonded to the α carbon (m/z 80), or cleavage between oxygen and the α carbon with the addition of a proton (m/z 97) (Figure **2-10**).

The 1-PSA molecular ion (Figure **5-21**) gives very limited fragmentation, with only one noteworthy transition (m/z 281 > 217) being observed (Figure **5-32**). This is somewhat expected of a PAH based compound, which are inherently stable because of resonance stabilization and resist fragmentation (Figure **2-10**).

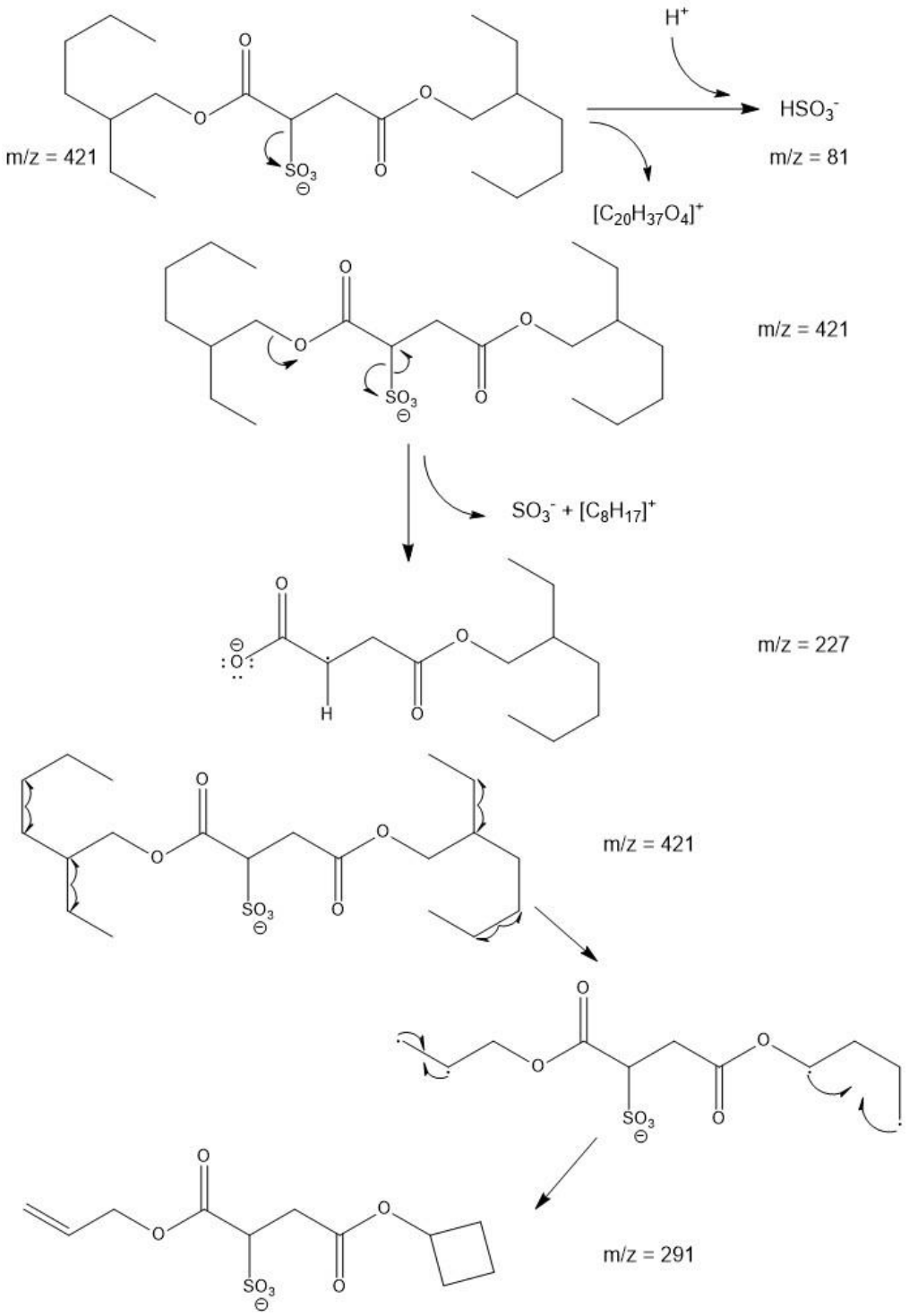

Figure 2-9: Possible MS-MS fragmentation of DOSS to give the observed MS-MS fragmentation ions.

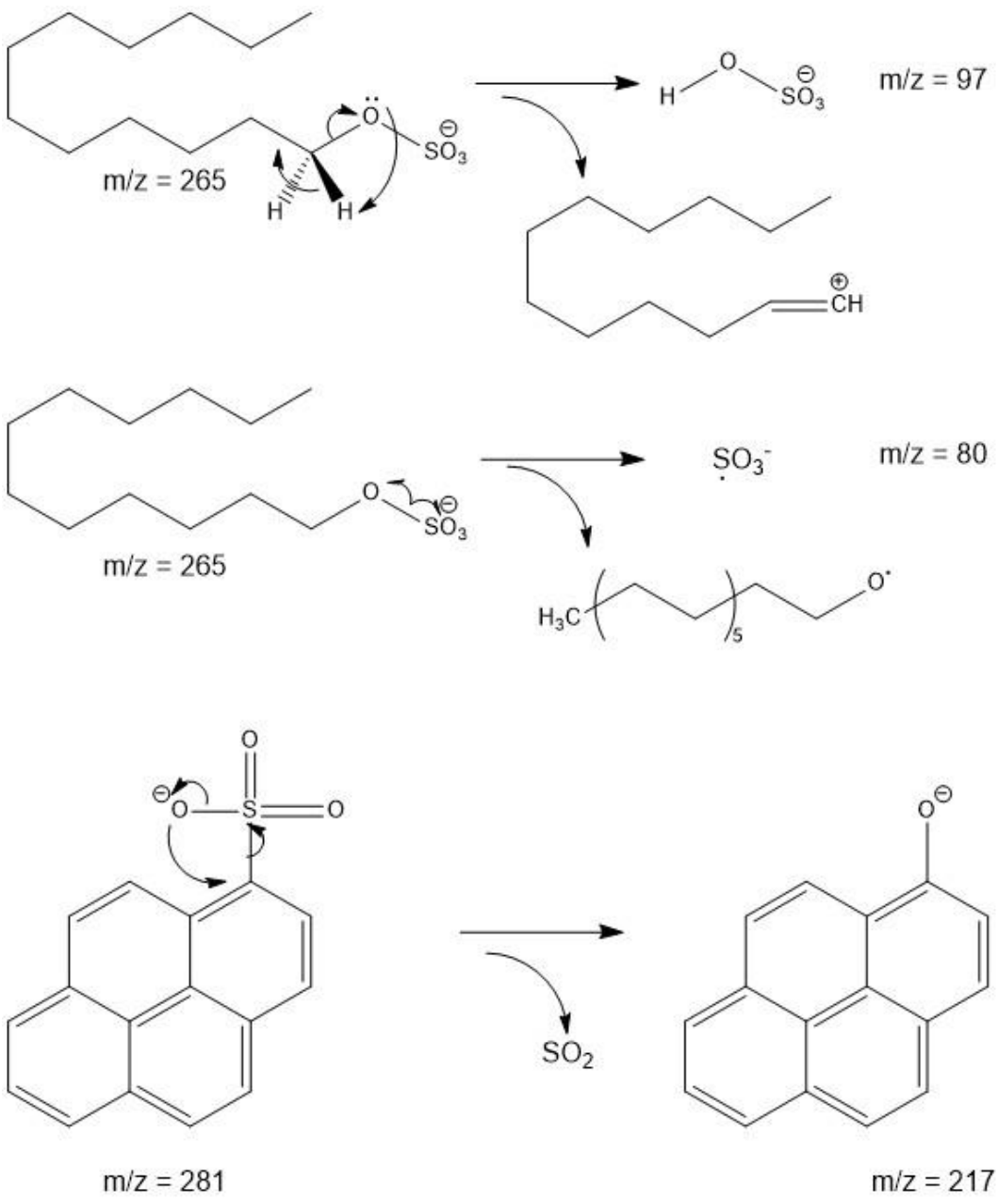

Figure 2-10: Possible MS-MS fragmentation pathways for SDS and 1-PSA.

2.2.2.4 Fragmentation amplitude

The MS-MS fragmentation amplitude was optimized by direct infusion of DOSS as described previously (Section **2.2.2.3**) and varying the fragmentation amplitude. MS-MS spectra for DOSS (m/z 421) were recorded for intervals of 1 minute at a range of fragmentation amplitudes (0.30 – 1.00 V; Δ0.5 V). The average of the mass spectrum was taken and the ion count for each major daughter ion was recorded for each fragmentation amplitude (Figure **2-11**). The maximum ion count for m/z 81, which is the major product ion observed in DOSS MS-MS experiments, was found to be attained at a fragmentation amplitude of 0.80 V. This coincides with the maximum ion count for m/z 227 and as such was chosen as the fragmentation amplitude used in future LC-MS-MS experiments. Variations in fragmentation amplitude had little effect on m/z 291, which is generally the weakest MS-MS transition observed for DOSS.

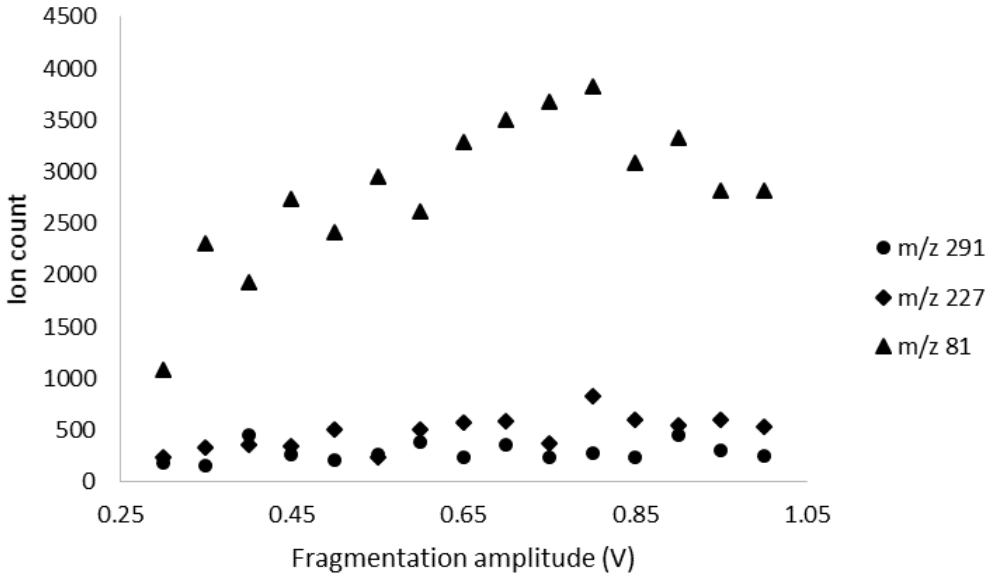

Figure 2-11: Ion count for DOSS MS-MS product ions at various fragmentation amplitudes.

2.2.2.5 LC-MS-MS instrument calibration

Instrument calibration was carried out using a five point set of calibration standards. Calibration standards of DOSS were prepared from a 4 $mg.L^{-1}$ intermediate stock solution of DOSS. Calibration standards were prepared for each analysis day at concentrations of 10, 20, 50, 100, and 200 $\mu g.L^{-1}$ with a blank injection being included as the response for 0 $\mu g.L^{-1}$ DOSS concentration. Each calibration standard was amended with 200 $\mu g.L^{-1}$ 1-PSA as internal standard. The calibration curve was constructed by plotting the ratio of peak area response (DOSS/1-PSA) against the ratio of concentration (DOSS/1-PSA) to give the relationship between peak area and concentration as shown in Equation **2-1**. The instrument response was found to be linear over this calibration range. All stock standards, intermediate standards and calibration standards were prepared in 50% ACN solutions with 5 mM NH_4HCO_2. A typical chromatogram and the corresponding full scan MS^2 spectra obtained for a calibration standard of DOSS and 1-PSA are shown in Figure **2-12**, Figure **2-13** and Figure **2-14**.

The stability of DOSS in solution has been reported elsewhere *[25,31]*. Recommended storage conditions and maximum recommended shelf life was adhered to for all experimental work with respect to stock and intermediate stock solutions (4°C, 3 months).

$$\frac{(Peak\ Area)_{DOSS}}{(Peak\ Area)_{1-PSA}} = m\frac{(Concentration)_{DOSS}}{(Concentration)_{1-PSA}} \qquad \textbf{(2-1)}$$

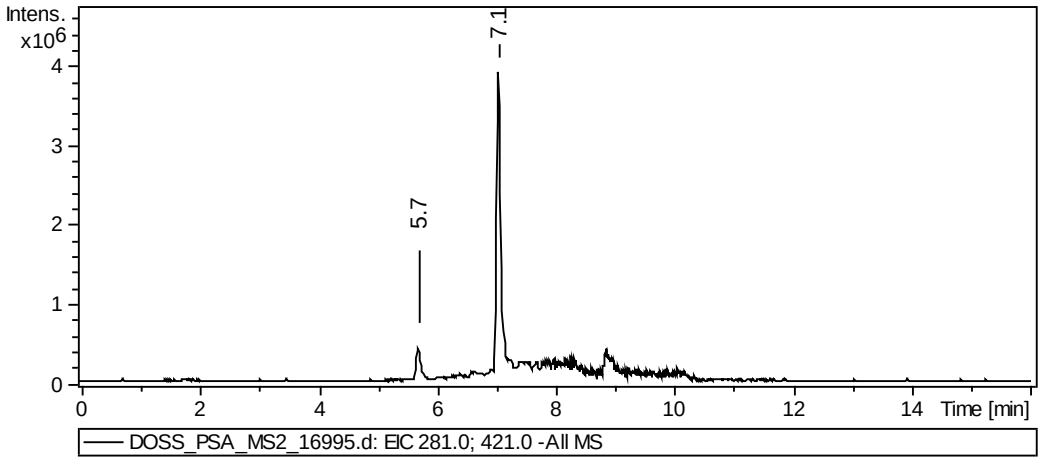

Figure 2-12: Typical full scan MS^2 chromatogram (EIC) of 1 - PSA (t_r = 5.7, m/z = 281) and DOSS (t_r = 7.1, m/z = 421) calibration standard.

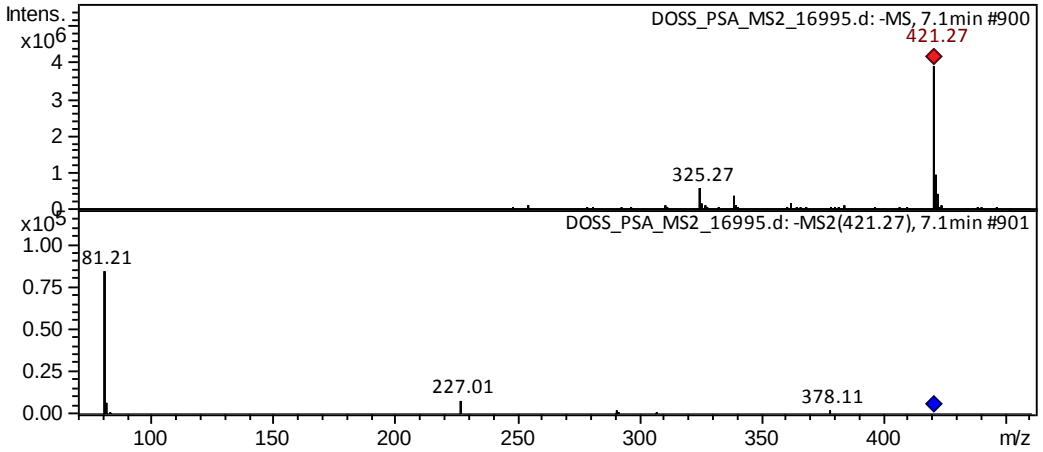

Figure 2-13: Typical MS^2 spectrum obtained for DOSS (t_r = 7.1, m/z = 421 > 81; 227; (291)).

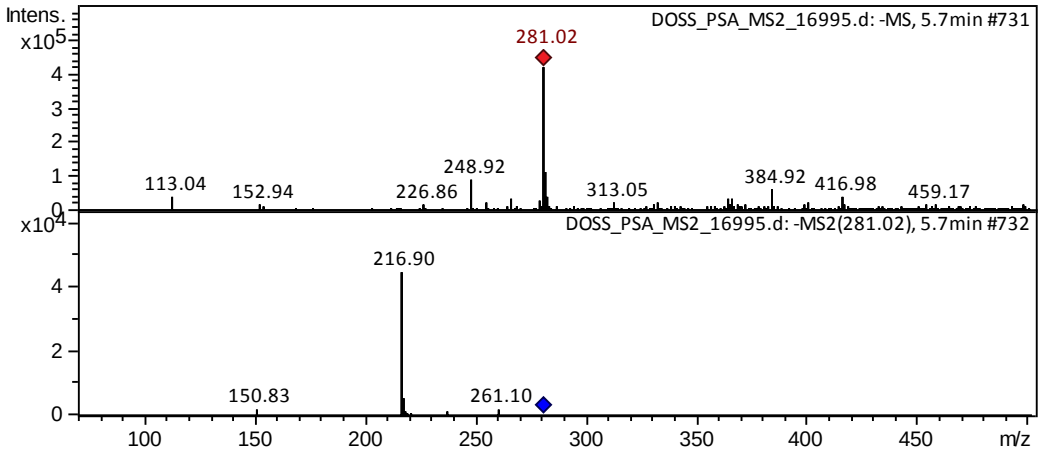

Figure 2-14: Typical MS^2 spectrum obtained for 1-PSA (t_r = 5.7, m/z = 281 > 217).

2.2.3 Validation

Intra-day validation was carried out on four separate days using a calibration curve for DOSS (0 – 200 $\mu g.L^{-1}$) and 3 replicate quality control (QC) standards spiked with DOSS (100 $\mu g.L^{-1}$) each day. Calibration curves were found to be give good linearity ($R^2 > 0.998$). QC standards were injected at regular intervals during each analysis day alongside analyses of regular samples. Summarized intra and inter-day validation data are displayed in Table **2-8**. The validation results showed good precision, with percent coefficient of variation (%CV) values lower than 5%. Accuracy was also found to be acceptable, with an inter-day accuracy of greater than 90%. Full validation data is displayed in Section **5.6** and summarized LC-MS-MS operating parameters are listed in Section **2.3.**

Table 2-8: Summarized validation data for DOSS LC-MS-MS method.

Intra-day results					
Date	R^2	Mean conc.	SD	%CV	Accuracy
28/02/2015	0.9998	89.5	1.2	1.4	89.5%
01/03/2015	0.9999	93.3	1.8	1.9	93.3%
12/03/2015	0.9989	98.4	2.8	2.9	98.4%
21/03/2015	0.9993	95.4	2.6	2.7	95.4%
Inter-day results					
		Mean conc.	SD	%CV	Accuracy
		94.2	4.5	4.8	94.2%

2.3 Final LC-MS-MS instrument parameters

Table 2-9: Gradient programme for HPLC method.

Time (min)	Column temperature (°C)	Auto sampler temperature (°C)	Flow rate ($\mu L.min^{-1}$)	Mobile phase composition‡ %A	%B
0.0	35	15	300	100	0
2.0	35	15	300	100	0
5.0	35	15	300	0	100
8.0	35	15	300	0	100
8.3	35	15	300	100	0
16.0	35	15	300	100	0

‡ Mobile phase A = 95% water, 5% ACN, 5mM NH_4HCO_2
Mobile phase B = 95% ACN, 5% water, 5mM NH_4HCO_2

Table 2-10: Operating conditions for the Bruker amazon X ion trap mass spectrometer.

Operating mode	Scan range (m/z)	Scan speed ($m/z.sec^{-1}$)	Capillary voltage (kV)	Dry gas (N_2) temp (°C)	End plate offset (V)
Full scan MS^2	70-500	32, 500	4.0	350	-500

Table 2-11: Full scan MS^2 settings.

Compound	Retention time (min)	Time tolerance (min)	Precursor ion (m/z)
1-PSA	5.7	± 0.5	281
DOSS	7.1	± 0.5	421
Compound	**Mass tolerance(m/z)**	**Fragmentation amplitude (V)**	**MS^2 fragments (m/z)**
1-PSA	± 0.4	0.80	217
DOSS	± 0.4	0.80	81, 227, 291

Table 2-12: Instrument limit of detection and lower limit of quantitation for the DOSS LC-MS-MS method.

LOD ($ng.L^{-1}$)	LLOQ ($ng.L^{-1}$)
174	528

3 Application of the instrumental method to real and simulated samples

The previously described LC-MS-MS method was applied to beach sand and tar-ball samples collected from the BOP region following the grounding of the MV Rena as part of the Rena Environmental Recovery Monitoring Programme in 2011. Sand and tar-ball samples were stored under refrigeration (4^{o}C) in sealed glass containers from the time of collection.

The analysis by LC-MS-MS requires the sample to be in a form suitable for injection into the HPLC system. This is achieved by employing an appropriate extraction methodology.

A range of extraction methods were tested with the aim of extracting DOSS from a specified sample matrix followed by an appropriate sample clean up regime. The choice of extraction protocol is dictated largely by the nature of the sample matrix. The types of sample matrices investigated included ocean sediment (sand), weathered HFO tar-balls and oiled beach sand.

In order to develop an extraction method, a blank sample (procedural blank) matrix is required of the same or similar composition to that of the real samples to be analyzed. This blank matrix can then be spiked with known amounts of analyte and subject to the extraction procedure in order to assess the suitability of the method.

3.1 Preparation of procedural blank sample matrices

3.1.1 Beach sand procedural blank

Extraction recovery efficiency of DOSS from sand matrices was carried out using a procedural blank sand matrix (Waikato Organics, Hamilton, New Zealand). The spiked procedural blank sand matrix was prepared by the following procedure.

A solution (50 mL) of surfactants (DOSS, Tween 80® and Span 80®; Sigma-Aldrich) at three concentration levels (10, 20 and 40 $\mu g.L^{-1}$) in DI water containing mercury (II) chloride (0.1% $HgCl_2$) were added to beach sand (100 g) in a glass beaker (400 mL) with HFO (HFO380CST, Z Energy Ltd, New Zealand) being added at a ratio of 20:1 (200, 400 and 800 $\mu g.L^{-1}$). This ratio was chosen based upon the Maritime New Zealand recommendation regarding the application of oil dispersants to oil slicks *[77]*. To the control group, un-spiked DI water (50 mL, 0.1% $HgCl_2$) was added. Each mixture was thoroughly mixed and allowed to stand at room temperature (24 h). These were then frozen and freeze dried to give sand samples containing surfactants at concentrations of 5, 10 and 20 $\mu g.kg^{-1}$. The un-spiked sand was used as a control group.

Sub-samples (10 g) of the spiked procedural blank sample matrix were then subjected to extraction methods for DOSS from beach sand (Section **3.2**).

3.1.2 HFO tar-ball procedural blank

A procedural blank tar-ball matrix was prepared by allowing HFO380CST (Z Energy Ltd, New Zealand) to evaporate under atmospheric conditions for 1 week. This blank matrix was used in spiking experiments to assess the extraction efficiency of DOSS from an HFO tar-ball sample matrix. Spiked procedural blanks were prepared by the following procedure.

A procedural blank HFO tar-ball sample (5 g) was spiked with DOSS, Tween 80® and Span 80® at three concentration levels in triplicate (10, 20 and 40 $\mu g.L^{-1}$) by adding the appropriate volume of stock solution (2 $mg.L^{-1}$) of surfactants (25, 50 and 100 µL). This was mixed well with a small volume (5 mL) of *n*-heptane and allowed to evaporate overnight. Un-spiked control blanks were also prepared.

Each spiked procedural blank was then subjected to extraction methods for DOSS from HFO tar-balls (Section **3.3**).

3.1.3 Oiled sand procedural blank

A procedural blank oiled sand matrix was prepared by allowing a 50% w/w mixture of beach sand (Waikato Organics, Hamilton, New Zealand) and HFO380CST (Z Energy Ltd, New Zealand) to evaporate at 50^{o}C for 3 days. This blank matrix was used in spiking experiments to assess the extraction efficiency of DOSS from oiled sand matrices. Spiked procedural blanks were prepared by the following procedure.

Procedural blanks (30 g) of oiled sand matrix were spiked with surfactant mixtures in *n*-heptane at three concentration levels (5, 10 and 20 µg.kg^{-1}). Each procedural blank was dissolved and mixed well with toluene (20 mL) to disperse the surfactants throughout the mixture and allowed to evaporate (1 day) to remove the toluene. Un-spiked control blanks were also prepared.

Each spiked procedural blank was then subjected to the extraction method for DOSS from oiled sands (Sections **3.3**).

3.2 Extraction from beach sand

The extraction of surfactants from ocean sediments is often carried out by means of Soxhlet or sonication assisted extraction with an appropriate solvent. For anionic surfactants, the extraction solvent is usually methanol or methanol and water mixtures *[66,67,73]*.

3.2.1 Soxhlet extraction

Sand samples (10 g) were transferred into cellulose extraction thimbles and extracted by Soxhlet extraction (7 h) using MeOH as the extraction solvent. The extract was then evaporated to dryness by rotary evaporation before being re-dissolved in DI water (10 mL). The reconstituted extract was then purified by SPE (section **3.2.3**).

3.2.2 Sonication assisted extraction

Sonication extraction was carried out by transferring sand samples (10 g) into two separate centrifuge tubes (5 g per tube) to which 50% MeOH (10 mL) was added. Each tube was then sonicated (30 min). The sonicated samples were then centrifuged (30 min, 4000 rpm) with the supernatant of the two tubes being collected and combined. The sand was then re-extracted by the same procedure with the supernatant from the second extraction being combined with that from the first extraction. The combined extracts were then evaporated to dryness and re-dissolved in 10 mL of DI water before processing by SPE (section **3.2.3**).

3.2.3 Sample clean-up: Solid phase extraction

All extracts were further purified using SPE in a method similar to that employed by Lara-Martin *et al. [66]*. SPE was performed using Strata C18-T, 55 µm, 140 Å SPE cartridges (1000 mg, 6 mL, Phenomenex). Each cartridge was conditioned with MeOH (10 mL) followed by DI water (5 mL). The sample was passed through the cartridge followed by DI water (5 mL) with the eluent being discarded. The cartridge was eluted with MeOH (10 mL) which was collected and evaporated to dryness under a stream of N_2 in a heating block (50^{o}C). The dried extract was dissolved in 50% ACN, 5 mM NH_4HCO_2 solution (1 mL) containing the internal standard (1-PSA, 200 µg.L^{-1}) and analyzed by LC-MS-MS.

3.2.4 Results

3.2.4.1 Sources of contamination

Initial recovery experiments which employed SDS as the internal standard showed considerable background contamination of SDS in both blank and spiked sand extracts which made response normalization of DOSS impossible. In order to determine the source of the contamination, LC-MS-MS experiments of blank Soxhlet extractions of beach sand with HPLC and extraction grade MeOH were

compared to LC-MS-MS data for both grades of MeOH (Table **3-1**, Figure **5-33**, Figure **5-34**, Figure **5-35** and Figure **5-36**). This showed that the SDS contamination was being introduced during the extraction process due to its strong background presence in the procedural blank sample matrix. SDS was subsequently rejected for use as an internal standard. As the blank extractions showed no presence of 1-PSA, this was used to replace SDS as internal standard for all subsequent experiments.

Table 3-1: SDS peak area data for 50% ACN blanks, unextracted MeOH and un-spiked sand samples extracted with extraction grade and HPLC grade MeOH.

Sample	Retention time (min)	Molecular ion (m/z)	Daughter ions (m/z)	Peak area
MeOH (extraction grade)	6.7	265	97	101683
MeOH (HPLC grade)	6.7	265	97	52869
50% ACN, 5mM NH_4HCO_2 Blank	6.7	265	97	409077
Soxhlet (extraction grade MeOH)	6.7	265	97	17580404
Soxhlet (HPLC grade MeOH)	6.7	265	97	16954274

3.2.4.2 Solid phase extraction

Extraction efficiency of the SPE method was carried out in order to assess whether the method was performing as intended.

Replicate 10 mL solutions (10 mL) containing DOSS (20 $\mu g.L^{-1}$) were prepared in DI water and DI water containing 5mM NH_4HCO_2. Each solution was then processed by SPE and analyzed by LC-MS-MS to determine the extraction efficiency.

It was found that a very good percentage of DOSS was recovered by the SPE method, both from DI water and 5mM NH_4HCO_2 (Table **3-2**). Due to this, it was

deemed appropriate to reconstitute the raw extracts for all samples in DI water prior to processing by SPE.

The rather large confidence intervals (95% CI) for these tests reflects the small sample size (n=2). However, extraction recovery tests from spike sample matrices which employed larger sample sets showed much lower variation (Section **3.2.4.3**). This suggests that the extraction efficiency of the SPE method is in fact much less variable. This is indicated by the low standard deviation (SD) and %CV for the SPE method (Table **3-2**, Section **5.5.2**).

Table 3-2: Summarized SPE recovery values for DOSS dissolved in 5mM NH_4HCO_2 and DI water.

	5mM NH_4HCO_2	DI water
% Recovery	86.0	89.2
SD (n=2)	1.1	3.2
%CV	1.3	3.6
95% CI	10.2	29.1

3.2.4.3 Extraction recovery efficiency

Extraction efficiency was calculated by measuring the concentration of extracted samples which were spiked prior to extraction and those obtained for blank samples spiked post extraction based on the calibration curve obtained from the calibration standards. The recovery percentage for each extraction method was calculated using Equation **3-1**. Post extraction blanks are used so that any ionization suppression introduced from the sample matrix is reflected in the recovery efficiency calculation as the calibration standards are prepared in a matrix free solvent and presumably free from matrix effects. Recoveries for each successful extraction technique are shown in Table **3-3**. Based on the overall extraction efficiencies for both methods, sonication assisted extraction was shown to give a consistently higher recovery with lower variability (Table **3-4**, Section **5.5.3**).

$$\% \, Recovery = \left(\frac{Concentration \, of \, spiked \, samples}{Concentration \, of \, blank \, samples}\right) \times 100 \qquad \textbf{(3-1)}$$

Table 3-3: Extraction efficiencies for DOSS from sand matrices at different concentration levels.

	Sand (Soxhlet)			Sand (sonication)		
Spike level ($\mu g.kg^{-1}$)	5	10	20	5	10	20
Measured concentration ($\mu g.kg^{-1}$)	3.83	7.26	12.09	3.52	7.99	14.45
SD (n=3)	0.40	0.21	0.99	0.03	0.06	0.83
% CV	10.37	2.88	8.16	0.87	0.78	5.78
% Recovery (± 95% CI)	77 ± 20	73 ± 6	60 ± 13	70 ± 2	73 ± 1	72 ± 13

Table 3-4: Overall extraction efficiencies for Soxhlet and sonication assisted extraction for all replicates and concentration levels.

	Soxhlet (% recovery)	Sonication (% recovery)
Mean	69.9	71.9
SD (n=9)	8.2	2.3
%CV	11.8	3.1
95% CI	6.3	1.7

3.2.4.4 Limit of detection and lower limit of quantitation

Method limits of detection (LOD) and lower limits of quantitation (LLOQ) were calculated by procedures described by the ICH harmonized tripartite guideline *[78]*. Specifically, the method LOD and LLOQ were estimated from the standard deviation of the lowest concentration spiked samples run through the method by equations **3-2** and **3-3**, where σ is the standard deviation of the response and S is the slope of the calibration curve. This value is then divided by 10 to account for the ten-fold concentration factor incorporated into the sample work-up. Based

on this, sonication assisted extraction of DOSS from sand matrices provides the most sensitive analysis (Table **3-5**).

$$LOD = \left(\frac{3.3 \times \sigma}{S}\right) \quad \textbf{(3-2)}$$

$$LLOQ = \left(\frac{10 \times \sigma}{S}\right) \quad \textbf{(3-3)}$$

Table 3-5: Method limits of detection and lower limits of quantification for DOSS extraction from sand matrices.

	Sand (Soxhlet)	Sand (sonication)
LOD ($ng.kg^{-1}$)	603	134
LLOQ ($ng.kg^{-1}$)	1830	406

3.2.4.5 Method application to environmental samples

The described method was applied to samples collected from the BOP region following the grounding of the MV Rena in 2011. Of the available samples, only two were of beach sand that could be analyzed by the method developed for the extraction and quantitation of DOSS.

Samples collected from Taylor Reserve (25/10/2011) and Papamoa beach (07/11/2011) in the BOP region were analyzed in triplicate using sonication assisted extraction followed by SPE and analysis by LC-MS-MS. The results of these analysis showed no traces of DOSS in excess of the method LOD in either sample.

3.3 Extraction from tar-balls and oiled sands

3.3.1 Liquid-liquid extraction of HFO tar-balls

The most appropriate and exhaustive extraction method for this type of sample matrix was thought to be LLE. Due to the highly viscous, liquid nature of HFO tar-balls, Soxhlet extraction was deemed inappropriate due to the difficulty in exposing a high surface area of the tar-ball to the extracting solvent.

3.3.1.1 LLE with MeOH from tar-balls in *n*-heptane

HFO tar-ball samples (5 g) were dissolved in *n*-heptane (40 mL) and extracted with MeOH using a continuous LLE apparatus (18 h). The MeOH phase was evaporated to dryness, reconstituted in DI water, further purified by SPE (Section **3.2.3**) and analyzed by LC-MS-MS.

3.3.1.1.1 Results

This choice of solvent system suffered from two major problems which rendered the LLE apparatus inoperable and gave extracts that were insoluble in aqueous solvents. The first of these problems was caused by the use of *n*-heptane. The use of aliphatic hydrocarbon solvents to dissolve HFO results in precipitation of the asphaltene and fraction of HFO *[79]*. This precipitate eventually sinks to the bottom of the LLE apparatus and is transferred to the MeOH distillation pot, fouling it with asphaltene residue and other HFO components it carries with it. The second problem arises from the use of methanol as the extracting solvent. As MeOH is able to extract HFO components that are insoluble in water, problems are encountered with the solubility of the extracts during sample clean-up procedures and introduction to the LC-MS system.

3.3.1.2 LLE with water from tar-balls in toluene

A 5 g procedural blank sample HFO was spiked with DOSS, Tween 80 and Span 80 (10, 20 and 40 $\mu g.L^{-1}$) by adding the appropriate volume of stock solution (2 $mg.L^{-}$

[1]) of surfactants (25, 50 and 100 µL) and mixed well with a small volume (5 mL) of *n*-heptane and allowed to evaporate overnight. Each 5 g subsample of spiked HFO was then dissolved in toluene (40 mL) and extracted with DI water using a continuous LLE apparatus (18 h). The aqueous phase was reduced in volume by rotary evaporation (≈ 10 mL) and further purified by SPE as previously described (section **3.2.3**) and analyzed by LC-MS-MS.

3.3.1.2.1 Results

In order to overcome the problems associated with the use of *n*-heptane and MeOH, the solvent system was changed to something more suited to dissolving asphaltene and high molecular weight PAH's. As asphaltenes are classified as the aliphatic hydrocarbon insoluble, toluene soluble fraction of HFO *[79]*, toluene was substituted for *n*-heptane. Other solvents that may be suitable include benzene, xylene and DCM. Due to LLE requiring two immiscible solvent phases, the extracting solvent was limited to the use of water due to toluene being miscible with a wide range of organic solvents. Although the LLE apparatus operated as intended with this choice of solvent system, analysis of the aqueous extract by LC-MS-MS showed that DOSS had not been extracted at detectable levels.

3.3.1.3 Extraction from tar-balls and oiled sand using a separating funnel

Samples of HFO tar-balls or oiled sand (5 g) were dissolved in *n*-heptane (40 mL) and filtered into a separating funnel containing DI water (40 mL). The mixture was agitated and allowed to separate. The aqueous phase was then recovered and the organic phase was re-extracted with DI water (40 mL). The aqueous extracts were then combined, evaporated to dryness, reconstituted with DI water (10 mL) before processing by SPE (Section **3.2.3**) and analysis by LC-MS-MS

3.3.1.3.1 Results

The initial combination of the aqueous and organic phases produced good phase separation. However, the vigorous agitation of the separating funnel resulted in the formation of an emulsion between the two phases that would not re-partition with time. As a result, the aqueous phase could not be recovered for analysis.

3.3.2 Sonication assisted extraction

Sonication assisted extraction methodologies were applied in an attempt to extract DOSS from both HFO tar-balls and oiled sand matrices.

3.3.2.1 Extraction from HFO tar-balls in toluene with water

Samples of HFO tar-balls (5 g) were dissolved in toluene (5 mL). DI water (5 mL) was added and mixed with a vortex mixer (1 min) before being sonicated (30 min). The water layer was then recovered and the toluene phase was re-extracted with water. The two extracts were combined and purified by SPE (Section **3.2.3**) and analyzed by LC-MS-MS.

3.3.2.2 Extraction from HFO tar-balls with other solvent systems

HFO tar-ball samples (5 g) were added to a centrifuge tube (50 mL). Extracting solvent (50% ACN, 50% MeOH or MeOH) was then added (10 mL) and mixed thoroughly using a vortex mixer then sonicated (15 min). The extracting solvent was recovered and the HFO phase was extracted again with solvent (10 mL). The extracting solvent from each extraction was combined and centrifuged (15 min, 4000 rpm) with the collected supernatant being evaporated to dryness before being reconstituted in DI water (10 mL) and processed by SPE (section **3.2.3**).

3.3.2.3 Extraction from oiled sands

Oiled sand samples (5g) were transferred to centrifuge tubes (50 mL) to which 50% ACN (10 mL) was added. Each sample was vortex mixed, sonicated (15 min)

and centrifuged (10 min, 3500 rpm) with the supernatant being collected. The samples were then re-extracted by the same procedure with the supernatants being combined, evaporated to dryness and reconstituted in DI water (10 mL) for processing by SPE (section **3.2.3**) before analysis by LC-MS-MS.

3.3.2.3.1 Results

Sonication assisted extraction with DI water failed after vortex mixing, as the high viscosity of the organic layer prevented adequate re-partitioning of the organic and aqueous layers. This gave frothy emulsion which could not be separated easily in any practical sense.

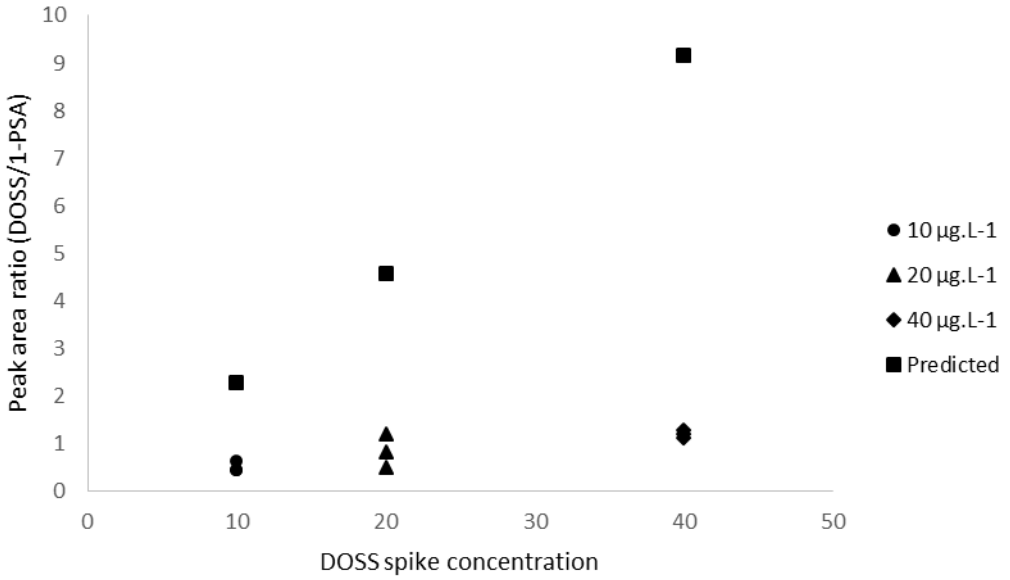

Figure 3-1: Measured peak area ratios for sonication assisted extraction of DOSS from HFO tar-balls at three spike concentration levels compared with the predicted peak area ratio.

This method was slightly modified by trying three different extraction solvent systems; MeOH, 50% MeOH and 50% ACN. Of these solvent systems trialled, 50 % ACN was found to give the highest recovery in preliminary experiments so was employed as the solvent system of choice for subsequent extraction recovery efficiency experiments. Recovery experiments gave recovery values that were very low, not reproducible and unrelated to the spike concentration (Figure **3-1**).

The method was therefore deemed unsuitable for a quantitative assay. This was also found to be the case with the application of this method to oiled sand sample matrices.

3.3.3 Anion exchange extraction

3.3.3.1 Aqueous phase anion exchange

An anionic exchange resin (1 g, AG 1-X8, 50 – 100 mesh, Chloride form, Bio-Rad) was packed into a glass bench column (10 mm i.d.) and conditioned with NaOH (10 bed volumes, 1 M). HFO tar-ball or oiled sand samples (5 g) in toluene (20 mL) were then passed through the column and washed with toluene (10 bed volumes). The column was then washed with water (5 bed volumes) and then eluted with NaCl (10 bed volumes, 1 M). The eluent was then evaporated to dryness, processed by SPE and analyzed by LC-MS.

3.3.3.2 Organic phase anion exchange

A dried (100^{o}C, 24 h) anionic exchange resin (1 g, AG 1-X8, 50 – 100 mesh, Chloride form, Bio-Rad) was packed into a glass bench column (10 mm i.d.) and conditioned with toluene (10 bed volumes, 1 M). HFO tar-ball or oiled sand samples (5 g) in toluene (20 mL) were then passed through the column and washed with toluene (10 bed volumes) followed by MeOH (10 bed volumes). The column was then washed with DI water (5 bed volumes) and then eluted with NaCl (10 bed volumes, 1 M). The eluent was then evaporated to dryness, processed by SPE and analyzed by LC-MS.

3.3.3.2.1 Results

Due to the anionic nature of DOSS, it was thought that the use of an anion exchange (AEX) resin may allow for the separation of DOSS from HFO. Analysis of the AEX extract by LC-MS showed that DOSS had not been extracted. It is likely that the conditioning of the resin with an aqueous solvent prevents the organic phase from contacting and penetrating the resin sufficiently in order for ion

exchange to take place. To overcome this, an attempt was made to extract DOSS directly from the organic phase onto a dried AEX resin. This was in an effort to exclude water from the resin so that the organic phase could sufficiently penetrate the resin and allow ion exchange to occur. However, LC-MS-MS analysis showed that no DOSS had been recovered at levels above the instrument LOD. This suggested that DOSS has a higher affinity for the organic/HFO phase than the AEX solid phase, or conversely, the anions present on the AEX resin have a very low affinity for the organic phase compared with DOSS, which prevents exchange occurring.

3.3.4 Further comments

The quantitative extraction of DOSS from tar-ball and oiled sand sample matrices proved to be problematic and unsuccessful overall. At present, it seems that the extraction of DOSS from these sample matrices has not been reported in the literature, with most published studies focusing on the WAF of DOSS in the presence of the WAF of HFO. The basis of the problem stems from the need to transfer the DOSS from an organic phase into an aqueous or aqueous miscible phase suitable for processing by SPE and LC-MS-MS. The main aim of this is to remove the vast majority of the HFO components (PAH's, asphaltenes, hydrocarbons etc.) from the sample matrix to give a purified, concentrated extract that is compatible with the HPLC mobile phase. However, it seems clear from the extraction experiments discussed herein, that the affinity of DOSS for organic solvents and HFO is very high compared with its affinity for water and other polar solvents (MeOH, ACN). This is particularly apparent with the use of LLE, which is regarded as a benchmark and exhaustive extraction technique. One explanation for this may be that is that the partition coefficient ($P_{organic/water}$) of DOSS is very high such that it greatly prefers the organic phase over water which means that only very small quantities of DOSS are transferred into the aqueous phase during extraction. Another possibility is that DOSS is in fact being transferred into the aqueous phase during the extraction procedure, but is also

transferring tightly bound HFO components with it as a solubilizing agent. It could well be that the binding of DOSS to HFO components in aqueous systems is strong enough that they pass through the HPLC system as DOSS/HFO aggregates and as such would not elute at the specified retention time due to markedly different physicochemical behaviour and the expected MS^2 molecular and fragmentation ions would not be observed.

Either way, the high affinity of DOSS for non-polar solvents has implications with respect to environmental monitoring and the health of marine ecosystems. This chemical behaviour in the context of the application of C9500 to surface oil slicks may mean that the weathered oil could act as a sequestrant for DOSS with subsequent monitoring of water systems giving results underestimating or misrepresenting the distribution of DOSS in the environment. Or, if the solubilized DOSS/HFO aggregates are prevalent as postulated, then estimates of the WAF of DOSS are limited to the estimate of free DOSS. The possibility that HFO could act as a sequestrant for DOSS may also impact the biodegradation of DOSS by inhibiting the mechanism by which bacteria metabolize HFO. Additionally, the high affinity of DOSS for non-polar phases could lead to its bioaccumulation in marine organisms by directly permeating cell membranes and may be implicated in studies that have investigated the toxicity of DOSS.

4 Conclusions and recommendations

4.1 LC-MS-MS analysis of DOSS

The LC-MS-MS method developed here proved to be reproducible, accurate selective and sensitive. Improvements to the method could be made by the use of a QqQ mass spectrometer operating in MRM mode to give better sensitivity by means of lowering the LOD and LLOQ. Additionally, the use of a deuterated internal standard would allow for compensation for any matrix effects that may be present due to incomplete sample clean-up. This too would increase the sensitivity of the method and also increase the accuracy. Further development of the method could extend to the inclusion of quantitative analysis of non-ionic surfactants present in Corexit®, which would require altered HPLC and MS^2 experimental parameters.

4.2 Extraction of DOSS from ocean sediment

Application of the instrumental method to ocean sediment samples was shown to give the best results by the use of sonication assisted extraction followed by purification and concentration by SPE. The SPE method could be developed further by trialling a variety of column types, particularly AEX columns for anionic surfactants. Extension of the method to non-ionic surfactants would require the development of other extraction and sample clean-up procedures.

Application of the method to environmental samples showed no presence of DOSS. This could either reflect the relatively small quantities of Corexit® applied to the spill resulting in DOSS concentrations too low to measure or that the majority of the DOSS is bound up with the HFO that was deposited on the shoreline around the BOP. The small amount of beach sand samples available from the time of the spill means that no conclusions can be made about the relative distribution of DOSS in beach sand in the areas affected by the incident.

However, the method could be applied to newly collected sand samples to assess whether DOSS remains persistent in the area, or to provide background levels of DOSS in other areas around New Zealand in case of similar incidents in the future. It could also be applied to monitoring the runoff of DOSS from agricultural spraying or domestic pharmaceutical use into waterways.

4.3 Extraction of DOSS from HFO samples

The extraction of DOSS from samples consisting of HFO such as tar-balls or oiled sand proved problematic and largely unsuccessful for all of the extraction methods investigated. The implications this has for environmental monitoring programmes highlights the need for further work into the behaviour of DOSS in the environment. Investigations into the partitioning of DOSS between organic and aqueous phases could be undertaken in order to ascertain where DOSS is likely to accumulate when it is applied in an environmental setting. If the preference is for organic phases, the possibility exists that much of the DOSS applied in such situations ends up bound to HFO components that are persistent in the environment. As such, current methods for the quantitation of DOSS in water samples may be limited to the free, water accommodated fraction of DOSS and therefore provide an underestimate of the levels of DOSS present in the environment. The development of a quantitative GC-MS method for the direct injection of organic phase sample extracts may provide a way to circumvent this issue by exploiting the affinity of DOSS for organic solvents and increasing the extraction efficiency.

5 Appendix

5.1 Direct infusion mass spectra

5.1.1 Corexit® 9500

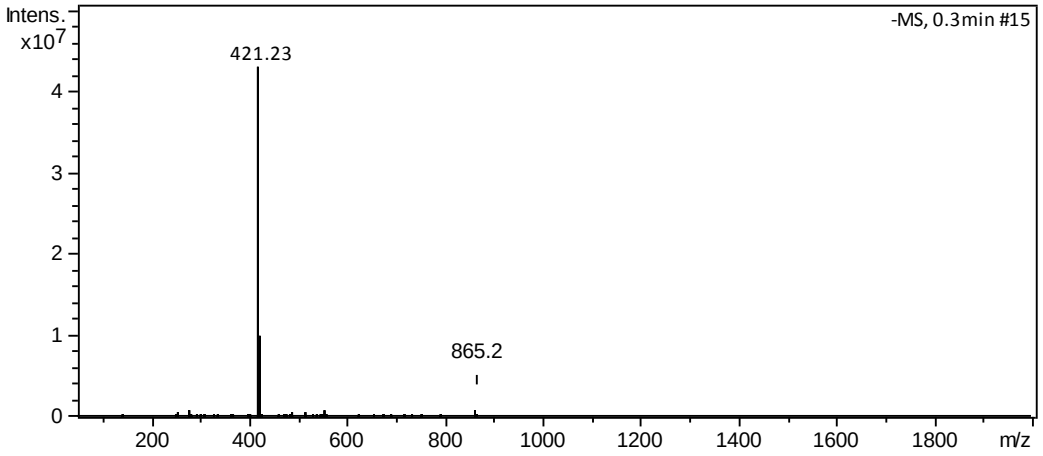

Figure 5-1: Negative ion mode, direct injection ESI-MS spectrum for C9500.

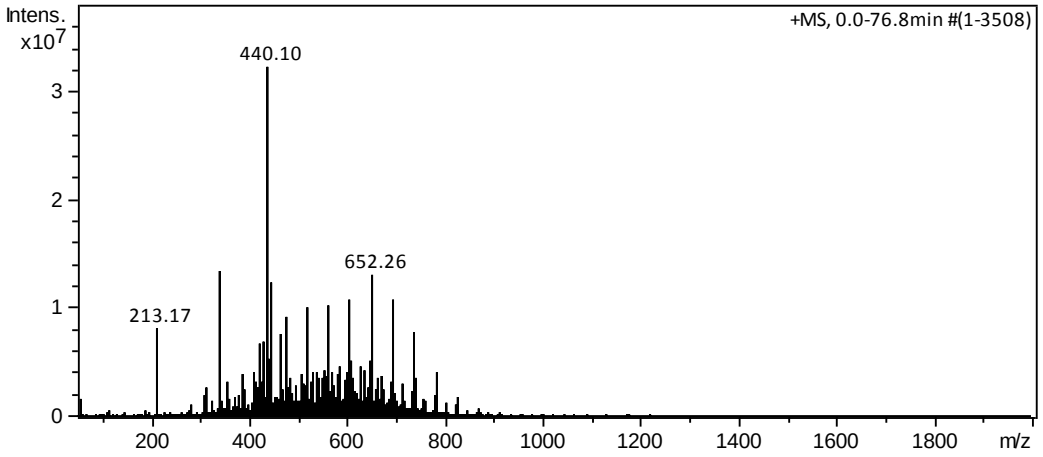

Figure 5-2: Positive ion mode, direct injection ESI-MS spectrum for C9500.

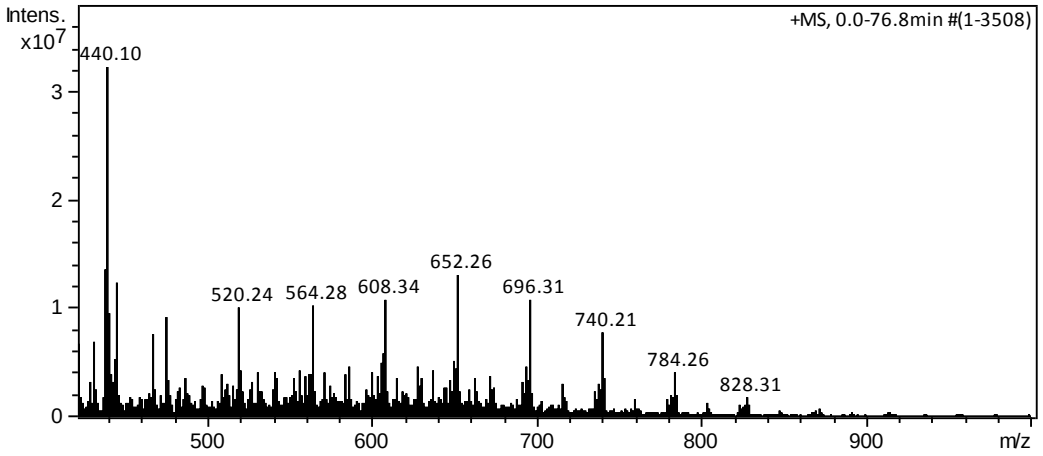

Figure 5-3: Positive ion mode, direct injection ESI-MS spectrum for C9500 (zoom).

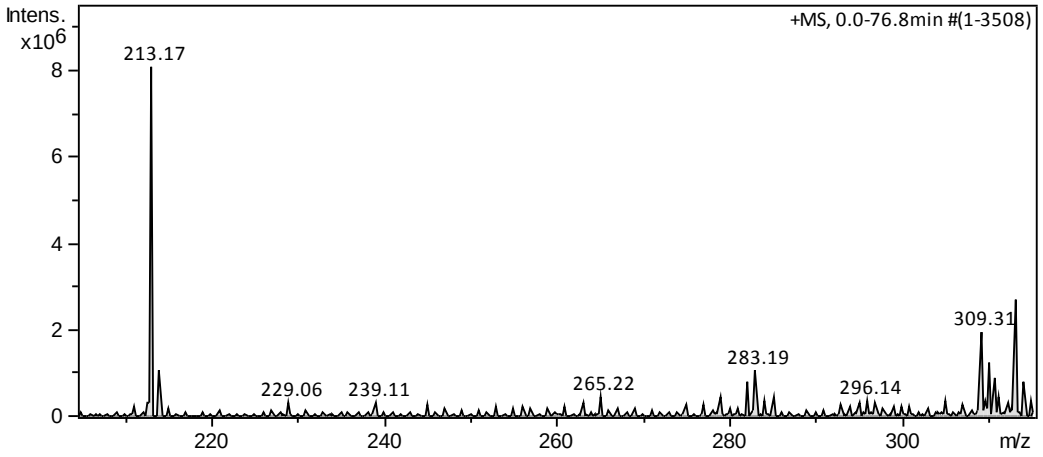

Figure 5-4: Positive ion mode, direct injection ESI-MS spectrum for C9500 (zoom).

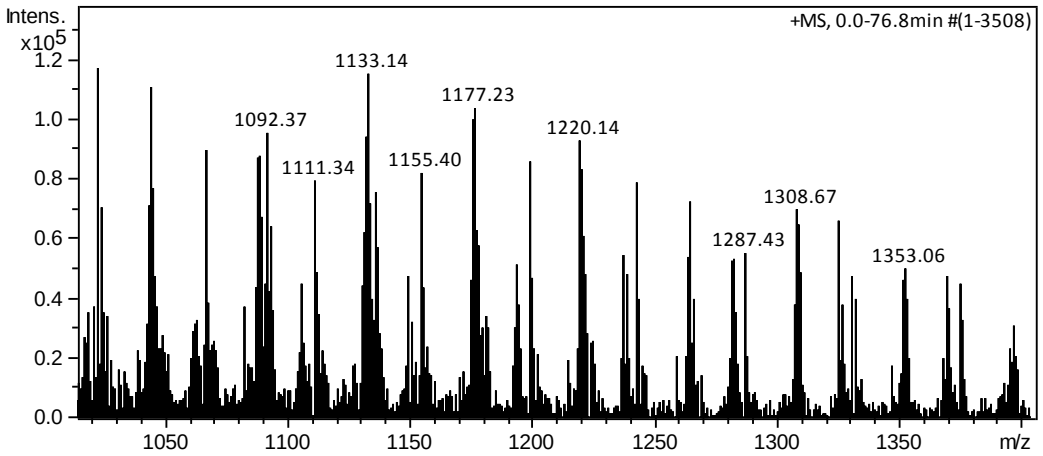

Figure 5-5: Positive ion mode, direct injection ESI-MS spectrum for C9500 (zoom).

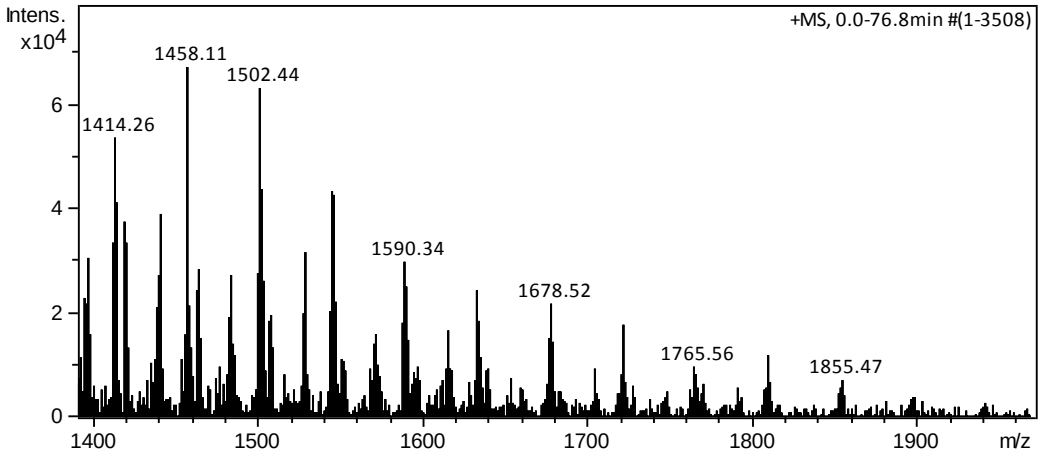

Figure 5-6: Positive ion mode, direct injection ESI-MS spectrum for C9500 (zoom).

5.1.2 Dioctyl sodium sulfosuccinate

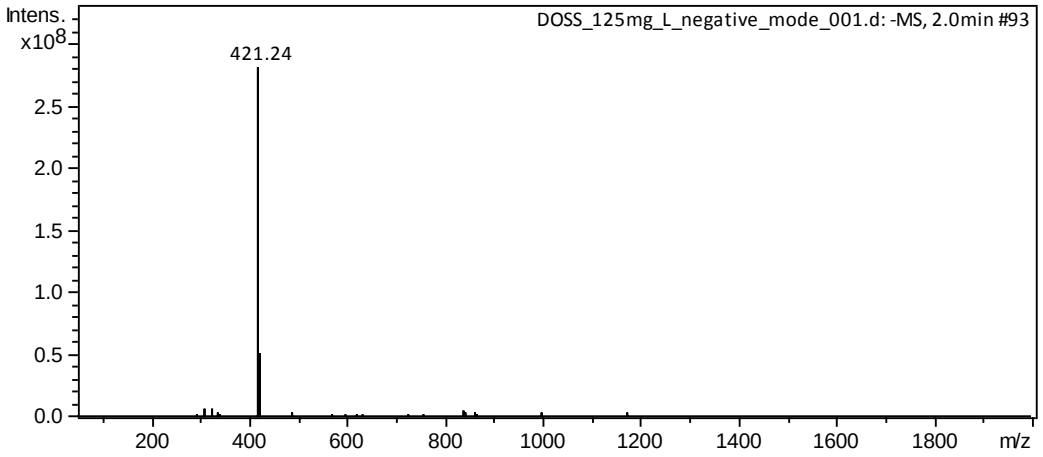

Figure 5-7: Negative ion mode, direct injection ESI-MS spectrum for DOSS.

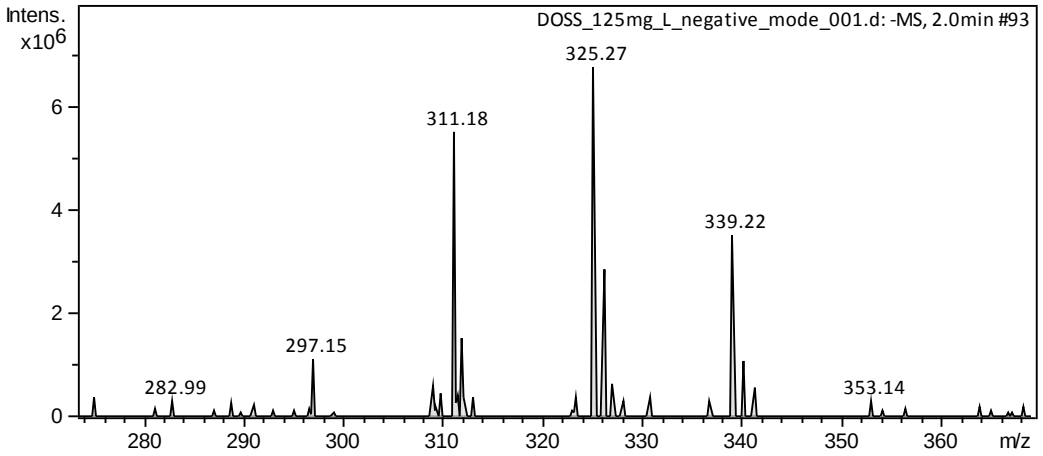

Figure 5-8: Ion cluster characteristic of LAS background contamination (m/z = 297, 311, 325, 339).

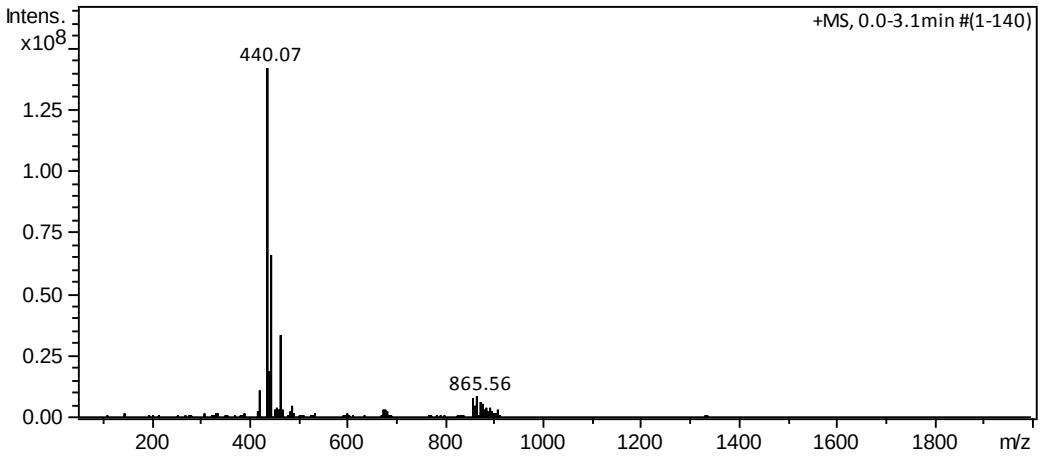

Figure 5-9: Positive ion mode, direct injection ESI-MS spectrum for DOSS.

5.1.3 Span® 80

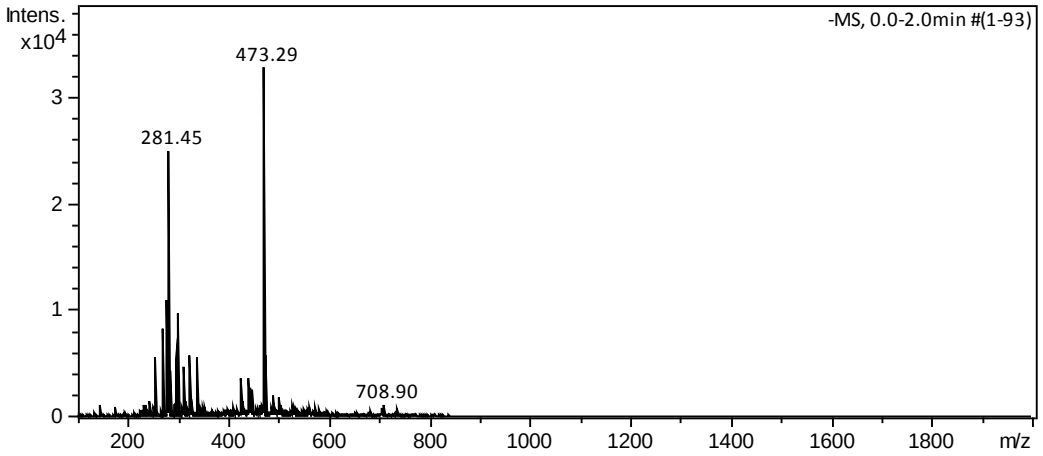

Figure 5-10: Negative ion mode, direct injection ESI-MS spectrum for Span® 80.

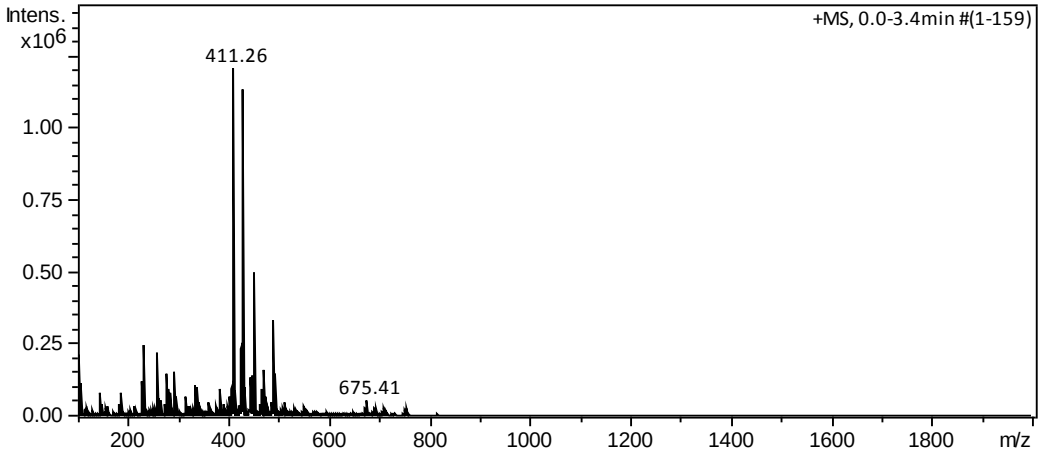

Figure 5-11: Positive ion mode, direct injection ESI-MS spectrum for Span® 80.

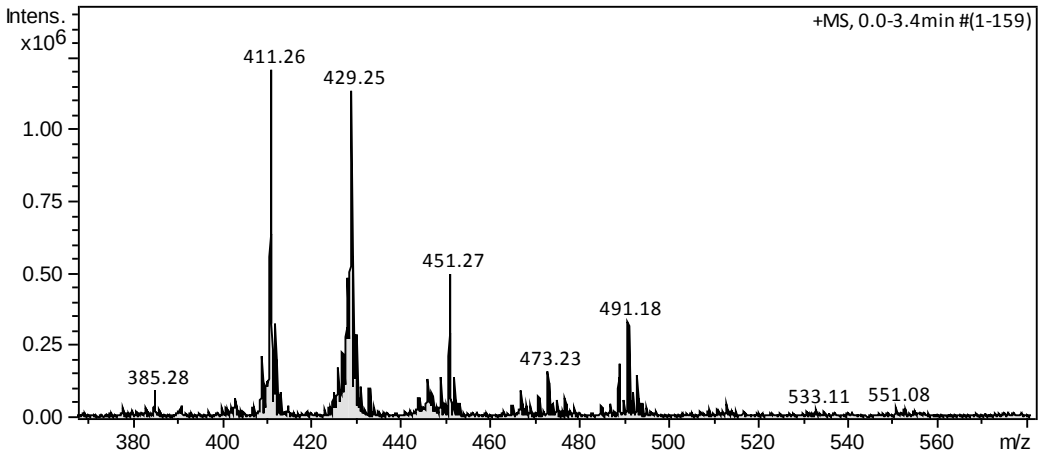

Figure 5-12: Positive ion mode, direct injection ESI-MS spectrum for Span® 80 (zoom).

5.1.4 Tween® 80

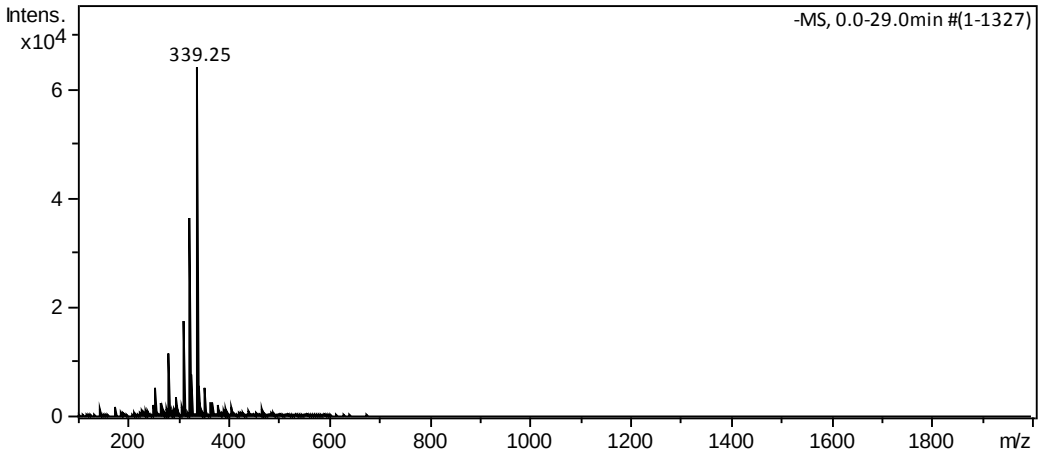

Figure 5-13: Negative ion mode, direct injection ESI-MS spectrum for Tween® 80.

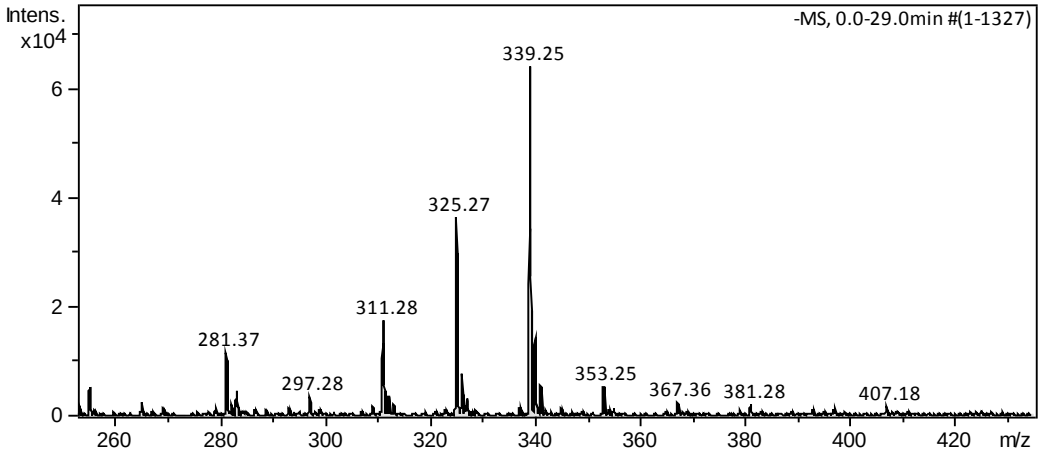

Figure 5-14: Negative ion mode, direct injection ESI-MS spectrum for Tween® 80 (zoom) showing the oleic acid moiety (m/z = 281) and LAS background contamination (m/z = 297, 311, 325, 339).

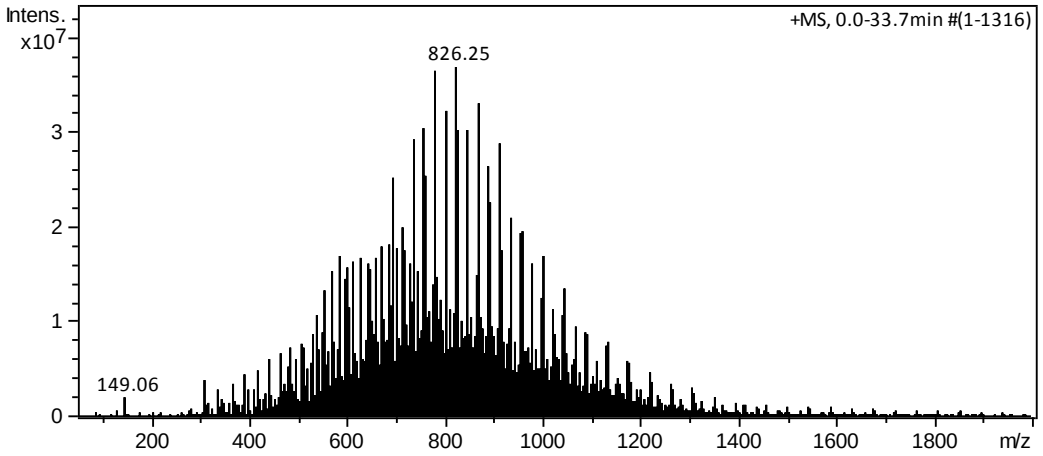

Figure 5-15: Positive ion mode, direct injection ESI-MS spectrum for Tween® 80.

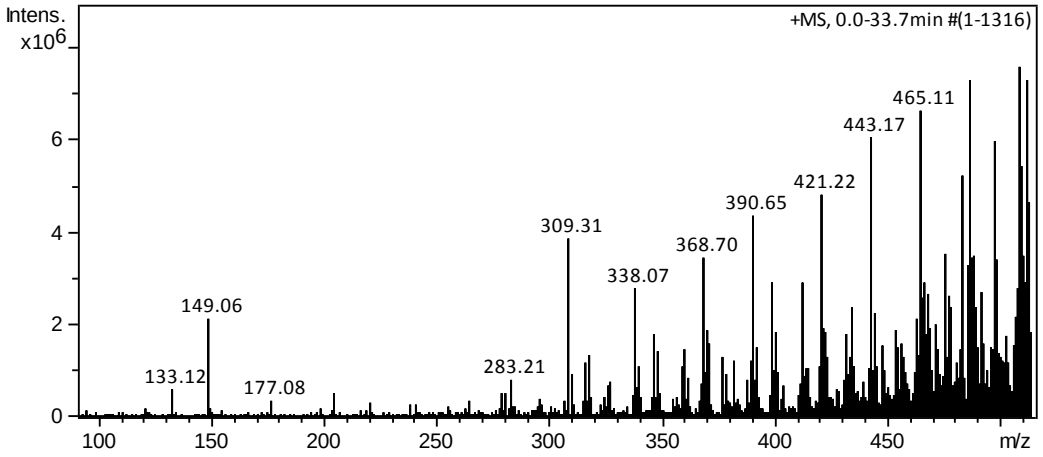

Figure 5-16: Positive ion mode, direct injection ESI-MS spectrum for Tween® 80 (zoom).

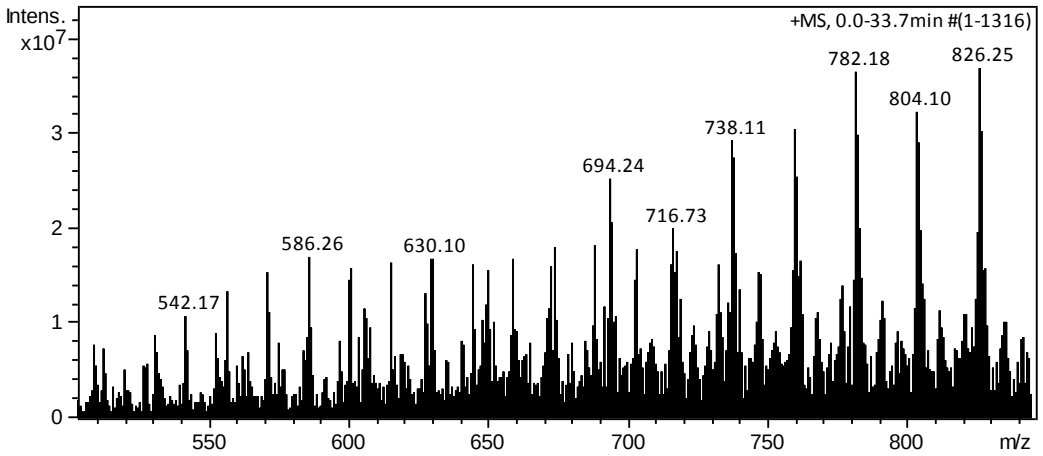

Figure 5-17: Positive ion mode, direct injection ESI-MS spectrum for Tween® 80 (zoom).

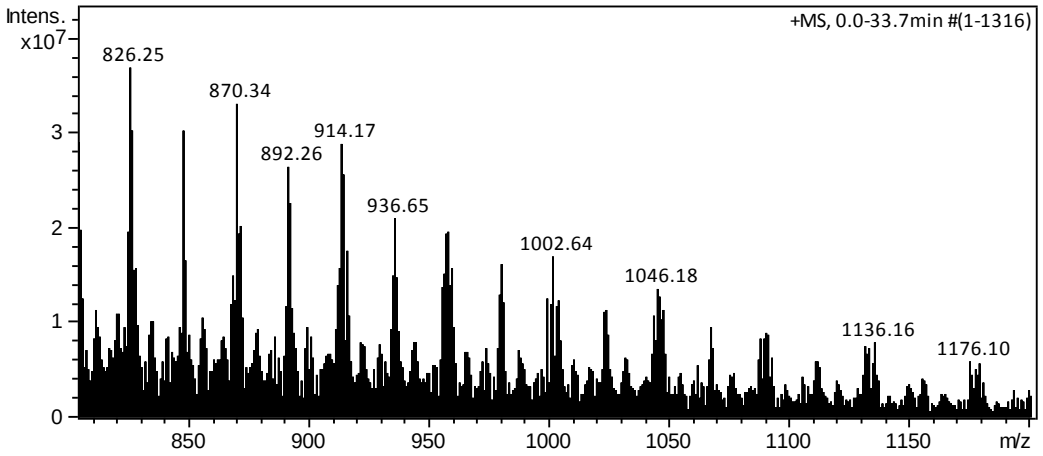

Figure 5-18: Positive ion mode, direct injection ESI-MS spectrum for Tween® 80 (zoom).

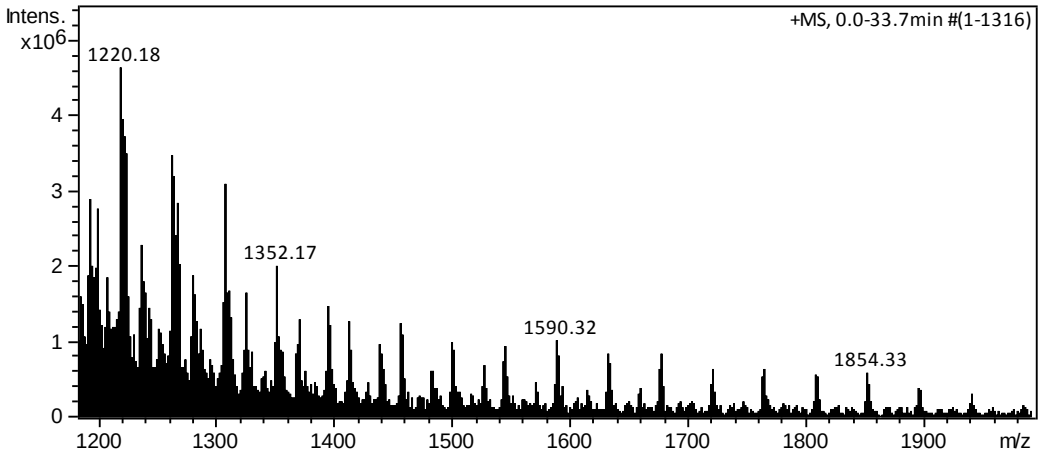

Figure 5-19: Positive ion mode, direct injection ESI-MS spectrum for Tween® 80 (zoom).

5.1.5 Sodium dodecyl sulfate

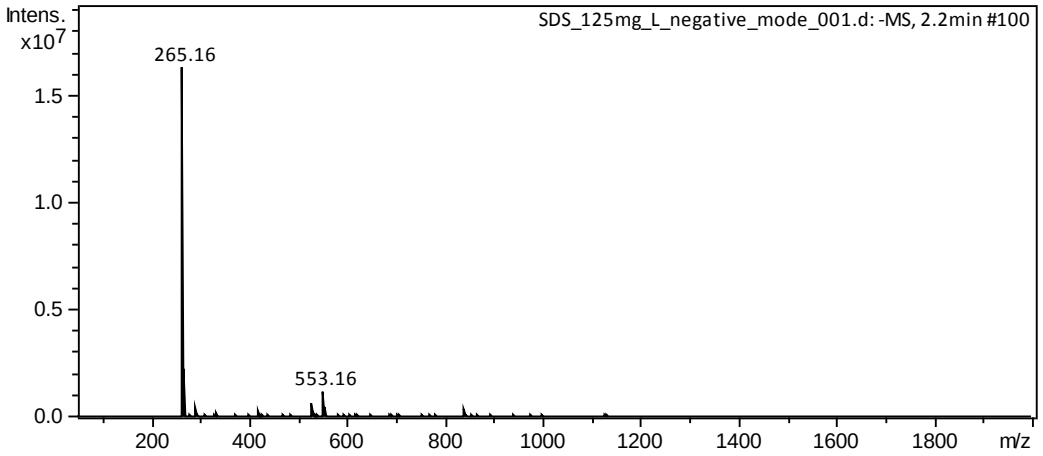

Figure 5-20: Negative ion mode, direct injection ESI-MS spectrum for SDS.

5.1.6 1-pyrene sulfonic acid sodium salt

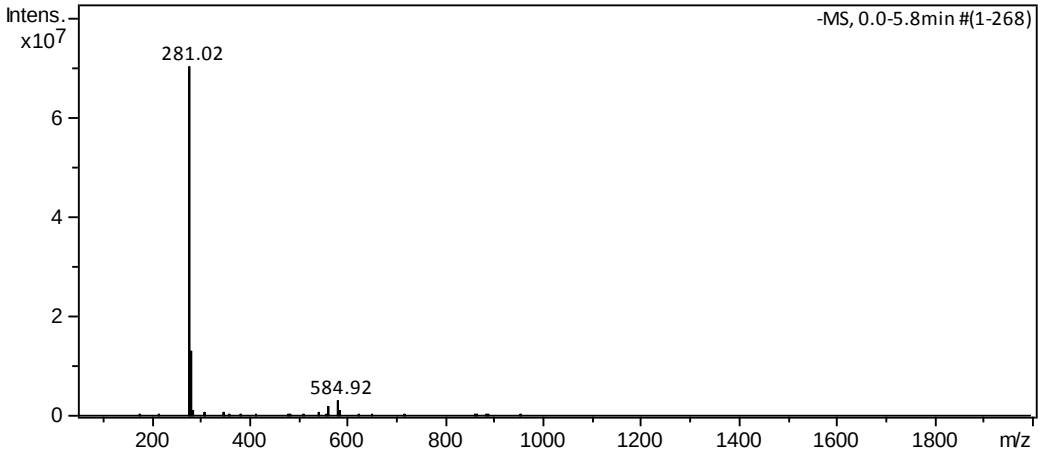

Figure 5-21: Negative ion mode, direct injection ESI-MS spectrum for 1-PSA.

5.2 HPLC of analytical and internal standards

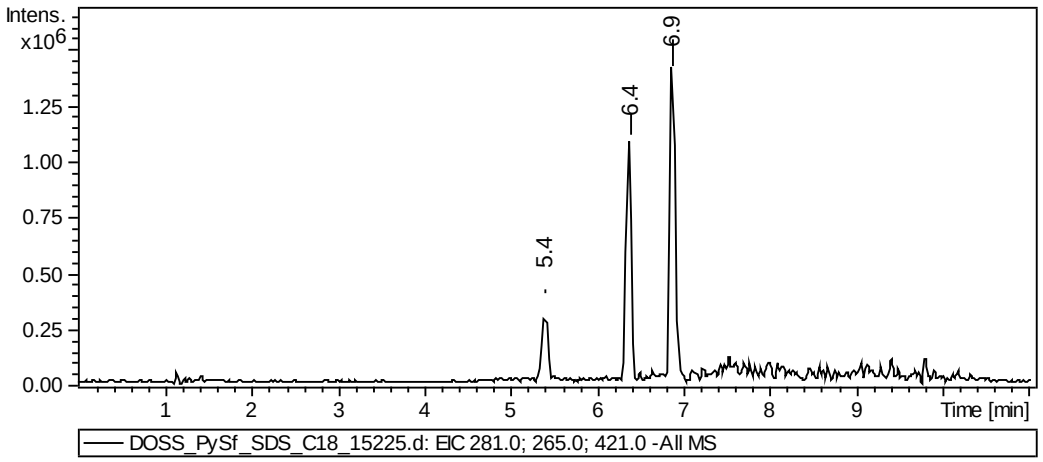

Figure 5-22: Typical chromatogram (EIC) of 1 - PSA (t_r = 5.4 min), SDS (t_r = 6.4 min) and DOSS (t_r = 6.9) on a C18 column.

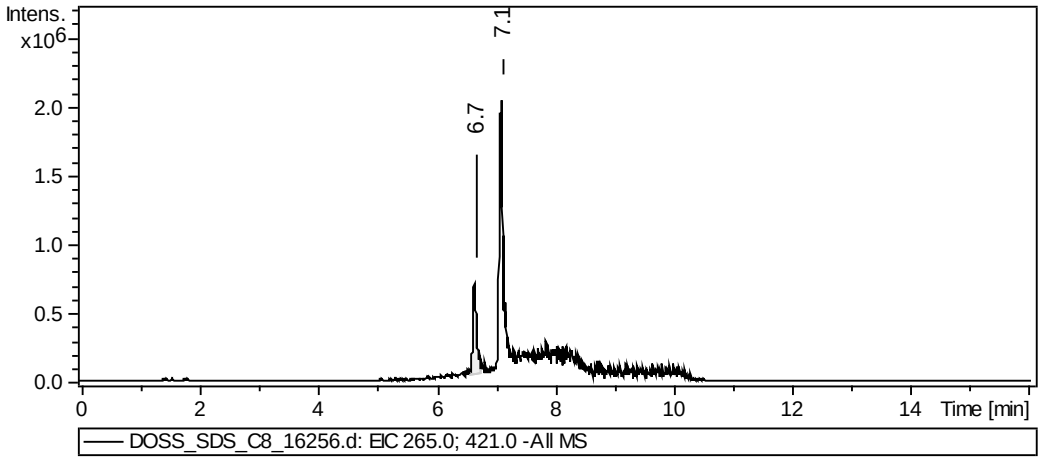

Figure 5-23: Typical chromatogram (EIC) of SDS (t_r = 6.7 min), DOSS (t_r = 7.1 min) on a C8 column.

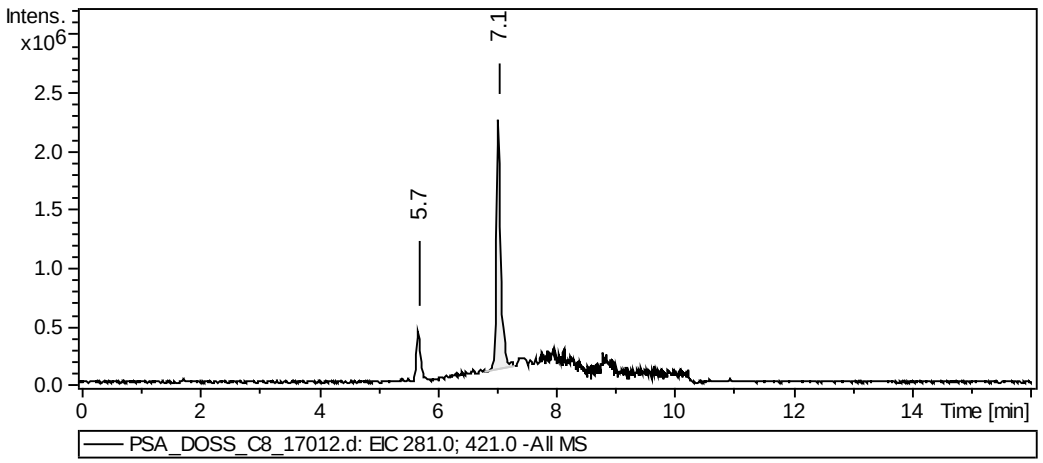

Figure 5-24: Typical chromatogram (EIC) of 1-PSA (tr = 5.7 min), DOSS (tr = 7.1 min) on a C8 column.

5.2.1 UV spectra

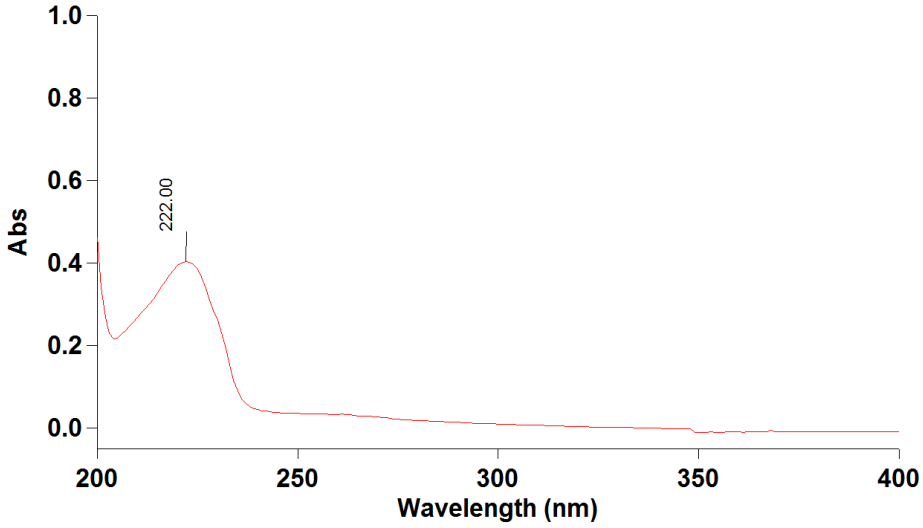

Figure 5-25: UV spectrum for DOSS.

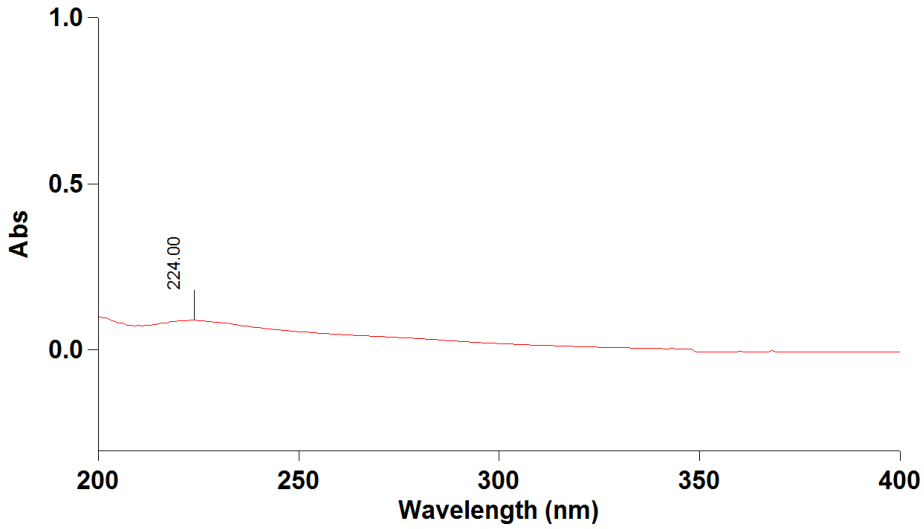

Figure 5-26: UV spectra for SDS.

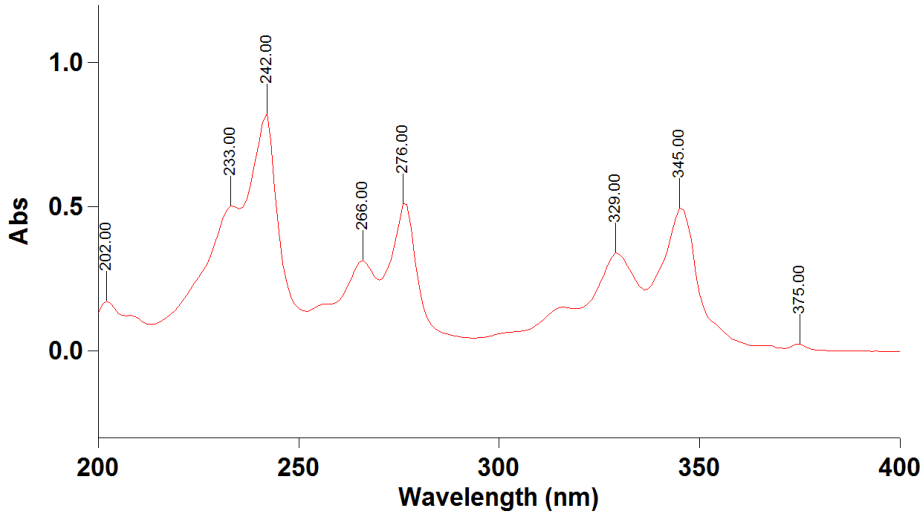

Figure 5-27: UV spectrum for 1-PSA.

5.2.2 Eluent modifiers

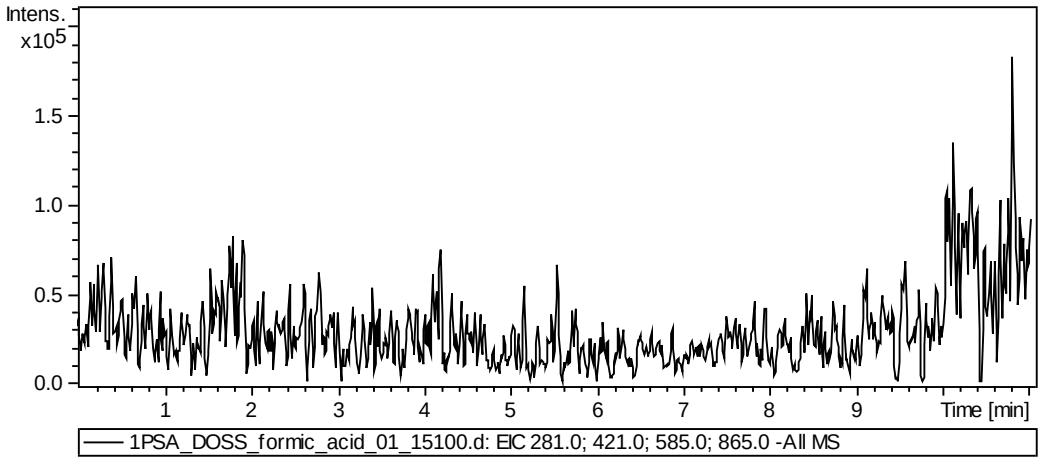

Figure 5-28: Typical chromatogram (EIC) obtained for 1-PSA and DOSS using formic acid as mobile phase modifier (C18 column).

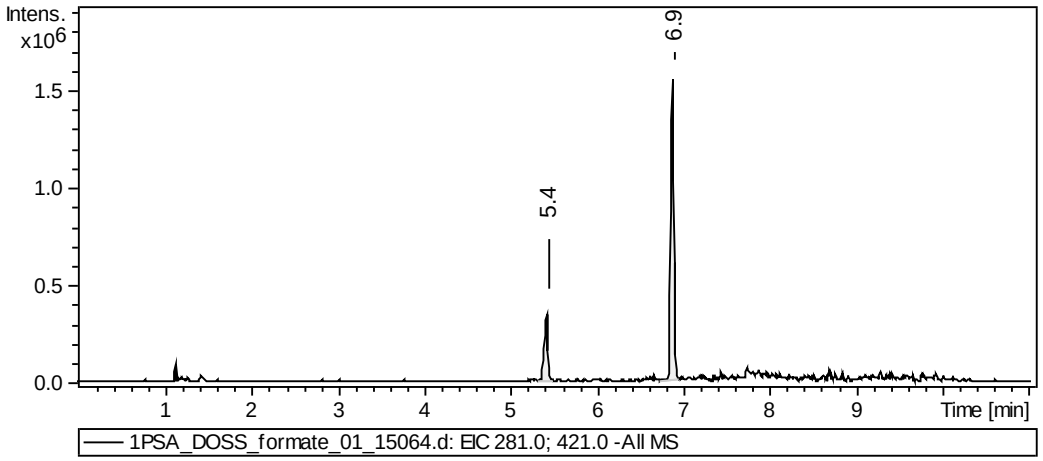

Figure 5-29: Typical chromatogram (EIC) obtained for 1-PSA and DOSS using ammonium formate as mobile phase modifier (C18 column).

5.3 ESI-MS-MS transitions

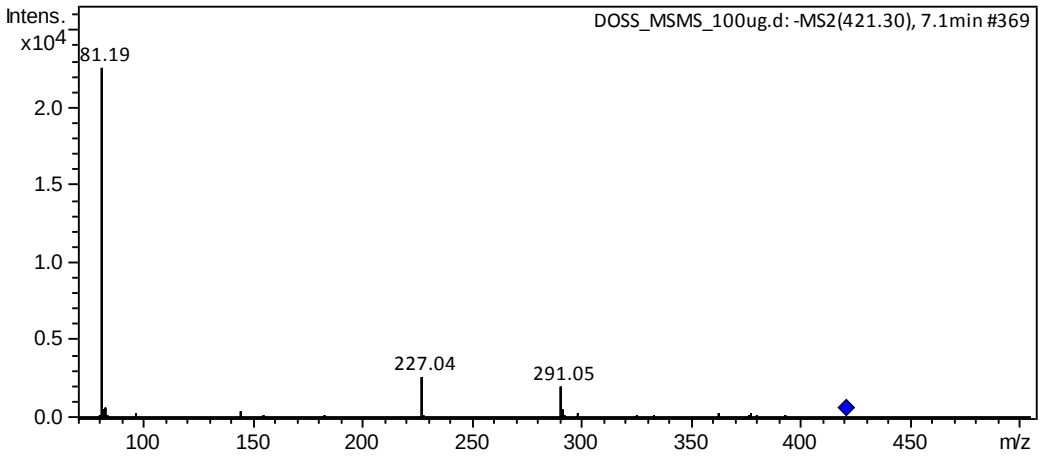

Figure 5-30: MS-MS spectrum for DOSS.

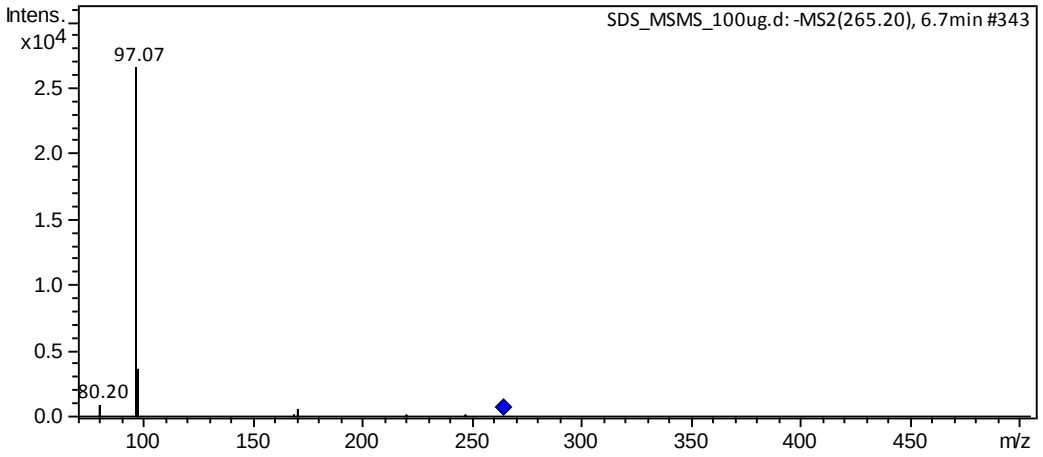

Figure 5-31: MS-MS spectrum for SDS.

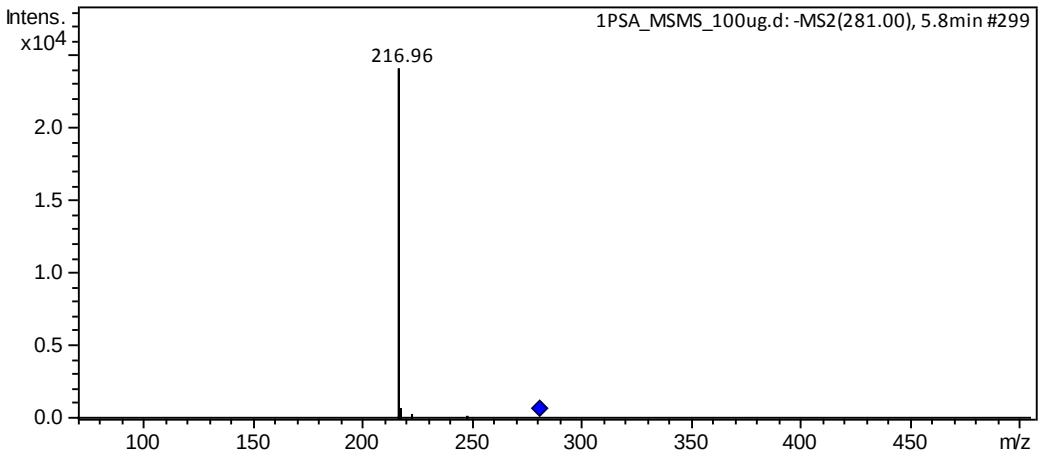

Figure 5-32: MS-MS spectrum for 1-PSA.

5.4 ESI-MS source settings

Table 5-1: Raw data for peak area and peak ion count for DOSS at various drying gas temperatures and capillary voltages.

		Peak area			Peak ion count		
Temperature		250°C			250°C		
Voltage		3.5kV	4.0kV	4.5kV	3.5kV	4.0kV	4.5kV
	1	7955037	8189163	8195991	363931	413916	425781
	2	7256611	7566526	7946541	345230	353438	407884
	3	6951997	7522345	7859223	348134	397681	395059
Mean		7387882	7759345	8000585	352432	388345	409575
SD		514243.4	372888.5	174767.7	10064.0	31301.2	15430.6
%CV		7.0	4.8	2.2	2.9	8.1	3.8
95% CI		1277451	926306	434147	25000	77757	38332
Temperature		300°C			300°C		
Voltage		3.5kV	4.0kV	4.5kV	3.5kV	4.0kV	4.5kV
	1	8317308	8701890	8646128	398517	424586	406034
	2	8768448	8783560	9236368	399796	421945	478835
	3	8551017	8582527	8966855	405461	392338	418709
Mean		8545591	8689326	8949784	401258	412956	434526
SD		225618.9	101103.7	295490.1	3695.7	17904.8	38892.5
%CV		2.6	1.2	3.3	0.9	4.3	9.0
95% CI		560469	251156	734038	9181	44478	96614
Temperature		350°C			350°C		
Voltage		3.5kV	4.0kV	4.5kV	3.5kV	4.0kV	4.5kV
	1	9675475	9886791	9810213	452767	488800	464201
	2	9348368	9529874	9867877	457894	458277	468202
	3	9115452	10016150	9735440	478748	488680	443438
Mean		9379765	9810938	9804510	463136	478586	458614
SD		281328.6	251855.7	66402.4	13761.0	17587.9	13293.9
%CV		3.0	2.6	0.7	3.0	3.7	2.9
95% CI		698859	625644	164953	34184	43691	33024

5.5 Extraction method development data

5.5.1 SDS contamination

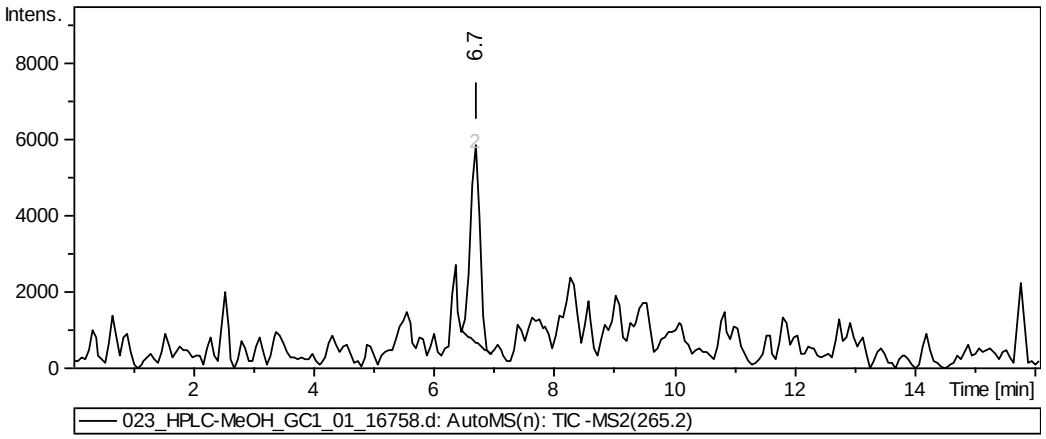

Figure 5-33: MS^2 chromatogram of HPLC grade MeOH showing background SDS contamination (t_r = 6.7 min, m/z = 265).

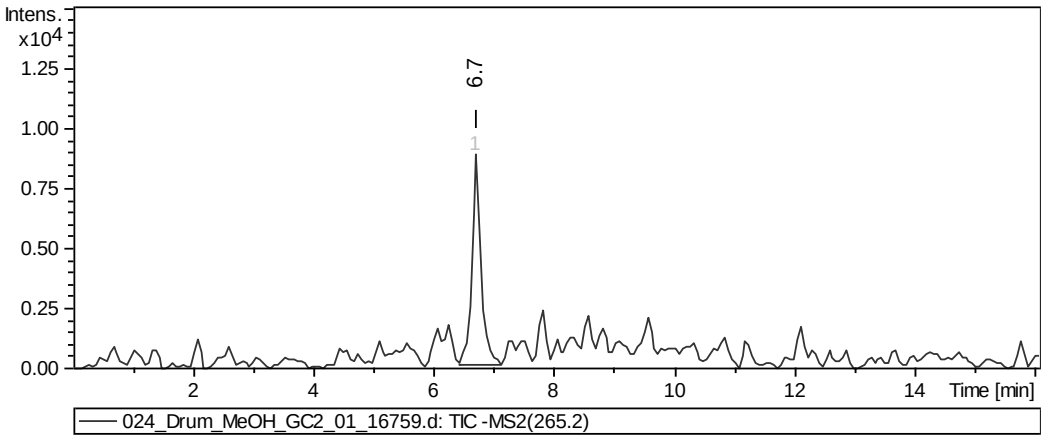

Figure 5-34: MS^2 chromatogram of extraction grade MeOH showing background SDS contamination (t_r = 6.7 min, m/z = 265).

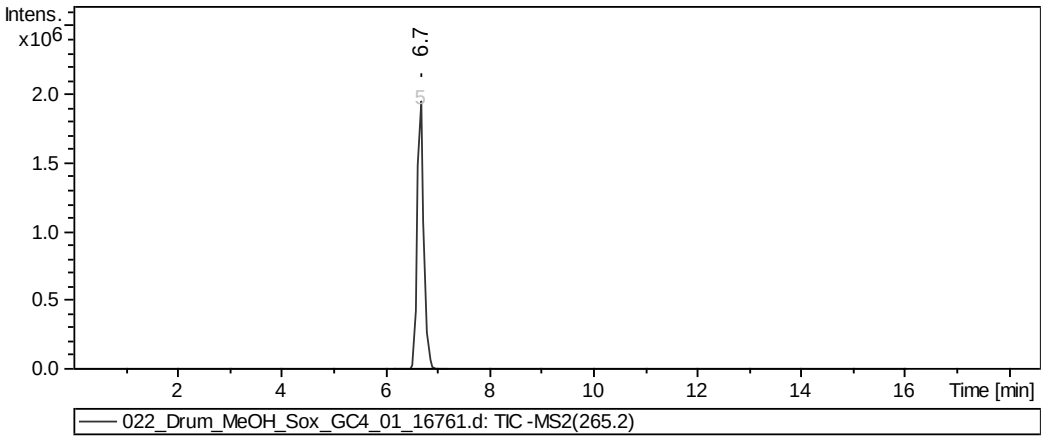

Figure 5-35: MS^2 chromatogram of Soxhlet extracted sand using HPLC grade MeOH showing background SDS contamination (t_r = 6.7 min, m/z = 265).

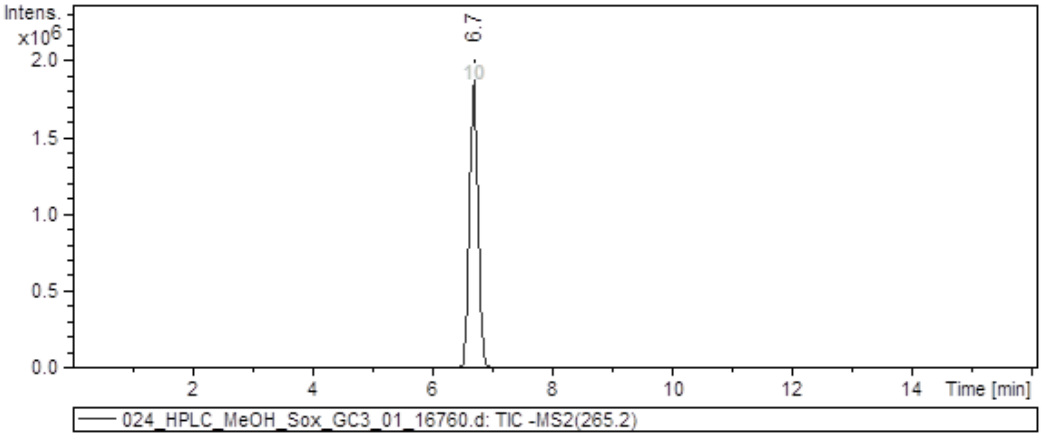

Figure 5-36: MS2 chromatogram of Soxhlet extracted sand using extraction grade MeOH showing background SDS contamination (tr = 6.7 min, m/z = 265).

5.5.2 Solid phase extraction validation data

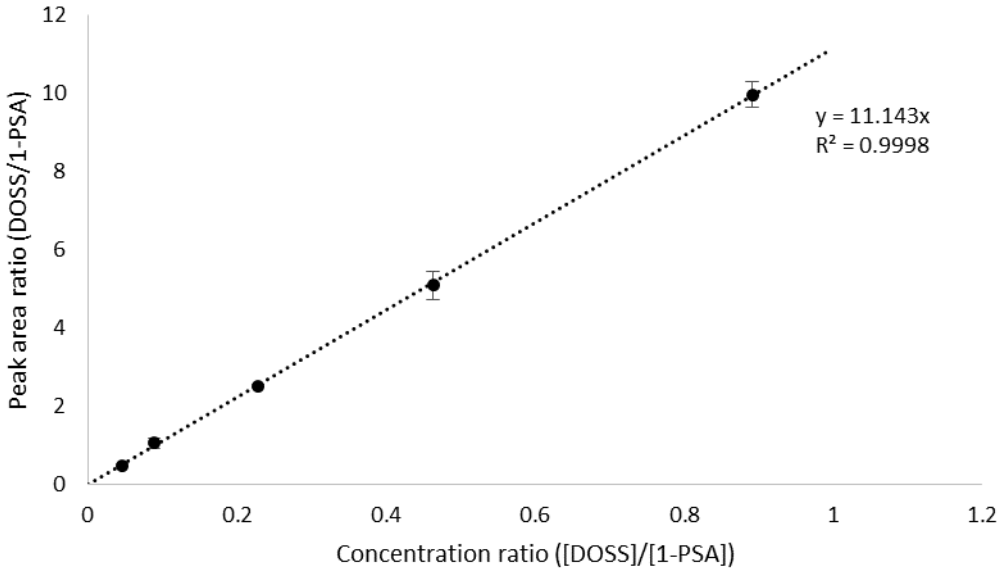

Figure 5-37: Calibration curve used for validation of SPE of DOSS from spiked DI water.

Table 5-2: Concentration data for SPE extraction validation calibration standards (n=3)

Conc(DOSS)*	error(abs)*	Conc Ratio (DOSS/1-PSA)**	Ratio upper	Ratio lower
10.1	0.2	0.04601441	0.0472369	0.0460144
19.5	0.3	0.08924007	0.0908049	0.0892401
49.9	0.8	0.22821287	0.2325155	0.2282129
101.4	1.7	0.46339763	0.4728273	0.4633977
195.0	3.2	0.89147107	0.9089658	0.8914711

* concentrations in µg.L^{-1}

** 1-PSA concentration = 216.6 ± 1.45 µg.L^{-1}

Example calculation for error in concentration:

$$\%\ error\ [DOSS]_{stock} = \%\ error\ (balance) + \%\ error\ (100\ mL\ flask)$$

$$m(DOSS) = 0.09939\ g\ \times 0.98(\%\ purity) = 0.09740\ \pm 0.00001\ g$$

$$\%\ error\ (balance) = \frac{0.00001\ g}{0.09939\ g} \times 100 = 0.01\%$$

$$\%\ error\ (100\ mL\ flask) = \frac{0.1\ mL}{100\ mL} \times 100 = 0.1\ \%$$

$$\%\ error\ [DOSS]_{stock} = 0.1\% + 0.01\% = 0.11\%$$

$$\%\ error\ [DOSS]_{intermediate} = \%\ error\ ([DOSS]_{stock}) + \%\ error\ (pipette) + \%\ error\ (50\ mL\ flask)$$

$$= 0.11\% + 0.2\% + 0.12\% = 0.43\%$$

$$\%\ error\ [DOSS]_{calibration} = \%\ error\ ([DOSS]_{intermediate}) + \%\ error\ (pipette) + \%\ error\ (5\ mL\ flask)$$

$$= 0.43\% + 0.2\% + 1\% = 1.63\%$$

$$absolute\ error\ [DOSS]_{calibration} = [DOSS]_{calibration} \times \frac{\%\ error\ [DOSS]_{calibration}}{100}$$

For example, 49.9 ug.L^{-1} DOSS calibration standard;

$$absolute\ error\ [DOSS]_{49.9\ \mu g.L^{-1}} = 49.9\ \mu g.L^{-1} \times \frac{1.63\ \%}{100} = \pm 0.8\ \mu g.L^{-1}$$

Errors for all calibration standards were calculated similarly, including the 1-PSA spiking solution.

Calculation of concentration ratio:

$$Concentration_{Ratio} = \frac{[DOSS]}{[1 - PSA]}$$

$$Concentration_{Upper\ Ratio} = \frac{[DOSS] + abs\ error\ [DOSS]}{[1 - PSA] + abs\ error\ [1 - PSA]}$$

$$Concentration_{Lower\ Ratio} = \frac{[DOSS] - abs\ error\ [DOSS]}{[1 - PSA] - abs\ error\ [1 - PSA]}$$

The calibration plot was constructed by plotting the average peak area ratio against the concentration ratio. Errors were included for concentration as previously described. Errors in peak area were based on 95% confidence intervals for 3 replicates of each concentration level.

Table 5-3: Peak area data for calibration standards of DOSS and 1-PSA used in SPE validation experiments.

Concentration		10.1 µg.L^{-1}			19.5 µg.L^{-1}		
Replicate		1-PSA	DOSS	Ratio	1-PSA	DOSS	Ratio
	1	2221428	1107217	0.50	2279760	2434099	1.07
	2	2221907	1040740	0.47	2209016	2193271	0.99
	3	2222978	1064243	0.48	2248217	2449372	1.09
Mean		2222104	1070733	0.48	2245664	2358914	1.05
SD		794	33710	0.02	35441	143654	0.05
%CV		0.04	3.15	3.17	1.58	6.09	4.83
95% CI		1971	83741	0.04	88040	356857	0.13
Upper CI		2224076	1154475	0.52	2333705	2715771	1.18
Lower CI		2220133	986992	0.44	2157624	2002057	0.92
Concentration		49.9 µg.L^{-1}			101.4 µg.L^{-1}		
Replicate		1-PSA	DOSS	Ratio	1-PSA	DOSS	Ratio
	1	2205335	5590530	2.54	2237875	11016652	4.92
	2	2231866	5601208	2.51	2219457	11501383	5.18
	3	2235061	5628849	2.52	2214976	11461100	5.17
Mean		2224087	5606862	2.52	2224103	11326378	5.09
SD		16318	19775	0.01	12136	268986	0.15
%CV		0.73	0.35	0.51	0.55	2.37	2.90
95% CI		40537	49125	0.03	30147	668198	0.37
Upper CI		2264624	5655987	2.55	2254250	11994577	5.46
Lower CI		2183550	5557738	2.49	2193956	10658180	4.73
Concentration		195 µg.L^{-1}					
Replicate		1-PSA	DOSS	Ratio			
	1	2230741	21942797	9.84			
	2	2262748	22852242	10.10			
	3	2240785	22364956	9.98			
Mean		2244758	22386665	9.97			
SD		16369	455111	0.13			
%CV		0.73	2.03	1.32			
95% CI		40663	1130558	0.33			
Upper CI		2285421	23517223	10.30			
Lower CI		2204095	21256107	9.65			

Table 5-4: Peak area data for SPE of DOSS in DI water and 5mM NH_4HCO_2.

		5mM NH_4HCO_2			DI water		
Replicate		1-PSA	DOSS	Ratio	1-PSA	DOSS	Ratio
	1	2565743	21938664	8.55	2512947	21921948	8.72
	2	2519988	21955037	8.71	2356899	21642369	9.18
Mean		2542866	21946851	8.63	2434923	21782159	8.95
SD		22878	8187	0.08	78024	139790	0.23
%CV		0.90	0.04	0.94	3.20	0.64	2.56
95% CI		205546	73553	0.73	701018	1255959	2.06
Upper CI		2748412	22020403	9.36	3135941	23038117	11.01
Lower CI		2337319	21873298	7.90	1733905	20526200	6.89

Table 5-5: Measured concentrations and extraction recovery efficiencies of DOSS by SPE in DI water and 5mM NH_4HCO_2

	Concentration ($\mu g.L^{-1}$)			% Recovery	
Replicate	5mM NH_4HCO_2	DI water	Replicate	5mM NH_4HCO_2	DI water
1	166.2	169.6	1	85.2	87.0
2	169.4	178.5	2	86.8	91.5
Mean	167.8	174.0	% Recovery	86.0	89.2
SD (n=2)	2.2	6.3	SD (n=2)	1.1	3.2
%CV	1.3	3.6	%CV	1.3	3.6
95% CI	20.0	56.7	95% CI	10.2	29.1

5.5.3 Extraction from beach sand

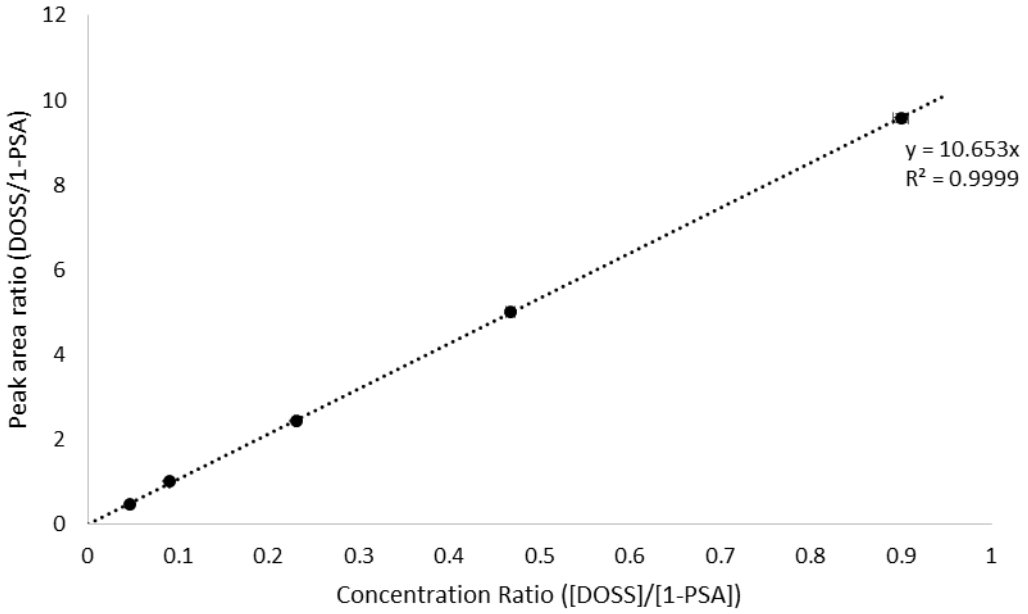

Figure 5-38: Calibration plot for DOSS used for extraction recovery efficiency experiments from beach sand.

Table 5-6: Concentration data for beach sand extraction calibration standards (n=3)

Conc(DOSS)*	error(abs)*	Conc Ratio (DOSS/1-PSA)**	Ratio upper	Ratio lower
10.1	0.2	0.04662973	0.0472369	0.0460144
19.5	0.3	0.09002770	0.0908049	0.0892401
49.9	0.8	0.23037858	0.2325155	0.2282129
101.4	1.7	0.46814404	0.4728273	0.4633977
195.0	3.2	0.90027701	0.9089658	0.8914711

* concentrations in $\mu g.L^{-1}$

** 1-PSA concentration = 216.6 ± 1.5 $\mu g.L^{-1}$

Table 5-7: Peak area data for calibration standards of DOSS and 1-PSA used in extraction recovery experiments from beach sand.

Concentration		10.1 µg.L^{-1}			19.5 µg.L^{-1}		
Replicate		1-PSA	DOSS	Ratio	1-PSA	DOSS	Ratio
	1	2331404	1106037	0.47	2317804	2280453	0.98
	2	2306248	1104687	0.48	2282803	2357610	1.03
	3	2318563	1101946	0.48	2329737	2328418	1.00
Mean		2318738	1104223	0.48	2310115	2322160	1.01
SD		12579	2085	0.00	24394	38957	0.02
%CV		0.54	0.19	0.51	1.06	1.68	2.48
95% CI		5930	983	0.00	11499	18365	0.01
Upper CI		2324668	1105206	0.48	2321614	2340525	1.02
Lower CI		2312809	1103241	0.48	2298615	2303796	0.99
Concentration		49.9 µg.L^{-1}			101.4 µg.L^{-1}		
Replicate		1-PSA	DOSS	Ratio	1-PSA	DOSS	Ratio
	1	2326848	5679252	2.44	2302914	11593963	5.03
	2	2270440	5615476	2.47	2315600	11306369	4.88
	3	2299835	5539400	2.41	2300842	11710538	5.09
Mean		2299041	5611376	2.44	2306452	11536957	5.00
SD		28212	70016	0.03	7990	208027	0.11
%CV		1.23	1.25	1.33	0.35	1.80	2.14
95% CI		13299	33006	0.02	3766	98065	0.05
Upper CI		2312340	5644382	2.46	2310218	11635022	5.05
Lower CI		2285742	5578370	2.43	2302686	11438892	4.95
Concentration		195 µg.L^{-1}					
Replicate		1-PSA	DOSS	Ratio			
	1	2331151	21795126	9.35			
	2	2306732	22488582	9.75			
	3	2278606	21985163	9.65			
Mean		2305496	22089624	9.58			
SD		26294	358335	0.21			
%CV		1.14	1.62	2.17			
95% CI		12395	168921	0.10			
Upper CI		2317892	22258545	9.68			
Lower CI		2293101	21920703	9.48			

.

Table 5-8: Peak area data for extraction recovery experiments of DOSS from beach sand by Soxhlet extraction.

Spike level	5 µg.L^{-1}			10 µg.L^{-1}			20 µg.L^{-1}		
Replicate	1-PSA	DOSS	Ratio	1-PSA	DOSS	Ratio	1-PSA	DOSS	Ratio
1	2341273	4869518	2.08	2349451	8366046	3.56	2307018	15995051	6.93
2	2310521	4419138	1.91	2226762	8502476	3.82	2306355	14321991	6.21
3	2310065	4482051	1.94	2309491	8566903	3.71	2287375	14879977	6.51
Mean	2320620	4590236	1.98	2295235	8478475	3.70	2300249	15065673	6.55
SD	17888	243903	0.09	62575	102557	0.13	11154	851848	0.36
%CV	0.77	5.31	4.53	2.73	1.21	3.50	0.48	5.65	5.55
95% CI	44436	605888	0.22	155444	254765	0.32	27709	2116107	0.90
Upper CI	2365055	5196123	2.20	2450679	8733240	4.02	2327958	17181780	7.45
Lower CI	2276184	3984348	1.75	2139791	8223710	3.38	2272540	12949566	5.65

Table 5-9: Extraction recovery efficiency data for DOSS extraction from beach sand by Soxhlet extraction.

Spike level	5 µg.L^{-1}			10 µg.L^{-1}			20 µg.L^{-1}		
Replicate	Conc (µg.L^{-1})	Mass sand (g)	Conc (µg.kg^{-1})	Conc (µg.L^{-1})	Mass sand (g)	Conc (µg.kg^{-1})	Conc (µg.L^{-1})	Mass sand (g)	Conc (µg.kg^{-1})
1	42.1	10.0337	4.2	72.2	10.0337	7.2	131.1	10.7517	13.1
2	34.2	11.3662	3.4	70.8	10.9646	7.1	111.4	11.3310	11.1
3	38.5	10.2423	3.9	74.9	10.0675	7.5	120.1	11.0117	12.0
Mean	38.3	10.5474	3.8	72.6	10.3553	7.3	120.9	11.0315	12.1
SD	4.0	0.7	0.4	2.1	0.5	0.2	9.9	0.3	1.0
%CV	10.37	6.80	10.37	2.88	5.10	2.88	8.16	2.63	8.16
95% CI	9.9	1.8	1.0	5.2	1.3	0.5	24.5	0.7	2.5
Upper CI	48.7	17.3	4.8	77.8	15.5	7.8	145.4	13.7	14.5
Lower CI	28.4	8.8	2.8	67.4	9.0	6.7	96.4	10.3	9.6
Mean %	77		77	73		73	60		60
Upper %	97		96	78		78	73		73
Lower %	57		57	67		67	48		48

Table 5-10: Peak area data for extraction recovery experiments of DOSS from beach sand by sonication assisted extraction.

Spike level		5 µg.L^{-1}			10 µg.L^{-1}			20 µg.L^{-1}		
Replicate		1-PSA	DOSS	Ratio	1-PSA	DOSS	Ratio	1-PSA	DOSS	Ratio
	1	2319970	4111400	1.77	2293195	8083597	3.53	2389677	17059373	7.14
	2	2304119	4115866	1.79	2342780	8213436	3.51	2342951	17198860	7.34
	3	2324091	4047005	1.74	2311732	8277363	3.58	2342971	17691591	7.55
Mean		2316060	4091424	1.77	2315902	8191465	3.54	2358533	17316608	7.34
SD		10544	38532	0.02	25054	98734	0.04	26971	332150	0.21
%CV		0.46	0.94	1.30	1.08	1.21	1.10	1.14	1.92	2.81
95% CI		26194	95720	0.06	62238	245268	0.10	67001	825105	0.51
Upper CI		2342254	4187144	1.82	2378140	8436734	3.63	2425534	18141713	7.86
Lower CI		2289866	3995704	1.71	2253664	7946197	3.44	2291532	16491503	6.83

Table 5-11: Extraction recovery efficiency data for DOSS extraction from beach sand by sonication assisted extraction.

Spike level		5 µg.L^{-1}			10 µg.L^{-1}			20 µg.L^{-1}		
Replicate		Conc (µg.L^{-1})	Mass sand (g)	Conc (µg.kg^{-1})	Conc (µg.L^{-1})	Mass sand (g)	Conc (µg.kg^{-1})	Conc (µg.L^{-1})	Mass sand (g)	Conc (µg.kg^{-1})
	1	35.3	9.8644	3.5	72.7	10.5625	7.3	137.4	9.4900	13.7
	2	35.5	9.8279	3.6	72.5	10.4791	7.3	142.4	10.4990	14.2
	3	34.9	9.8944	3.5	73.6	9.9876	7.4	153.7	9.8484	15.4
Mean		35.2	9.8622	3.5	72.9	10.3431	7.3	144.5	9.9458	14.5
SD		0.3	0.0	0.0	0.6	0.3	0.1	8.3	0.5	0.8
%CV		0.90	0.34	0.90	0.78	3.00	0.78	5.78	5.14	5.78
95% CI		0.8	0.1	0.1	1.4	0.8	0.1	20.7	1.3	2.1
Upper CI		36.0	9.9	3.6	74.3	11.1	7.4	165.3	11.2	16.5
Lower CI		34.4	9.8	3.4	71.5	9.6	7.2	123.8	8.7	12.4
Mean %		70		70	73		73	72		72
Upper %		72		72	74		74	83		83
Lower %		69		69	72		72	62		62

5.6 Validation data

Table 5-12: Validation data for DOSS LC-MS-MS method.

12/03/2015							
		Peak area			Concentration		
Replicate		1PSA	DOSS	Ratio	Conc.	Actual conc.	Accuracy
	1	2304506	10217191	4.433571	95.2	100.0	95.2
	2	2272700	10579646	4.6551	99.9	100.0	99.9
	3	2300002	10734946	4.667364	100.2	100.0	100.2
Mean		2292403	10510594	4.6	98.4	100.0	98.4
SD		17211	265695	0.1	2.8	0	2.8
%CV		0.8	2.5	2.9	2.9	0	2.9
01/03/2015							
		Peak area			Concentration		
Replicate		1PSA	DOSS	Ratio	Conc.	Actual conc.	Accuracy
	1	2278534	10519680	4.616863	93.9	100.0	93.9
	2	2248446	10483322	4.662474	94.8	100.0	94.8
	3	2339878	10509877	4.491635	91.3	100.0	91.3
Mean		2288953	10504293	4.590324	93.3	100.0	93.3
SD		46598	18811	0.1	1.8	0	1.8
%CV		2.0	0.2	1.9	1.9	0	1.9
28/2/2015							
		Peak area			Concentration		
Replicate		1PSA	DOSS	Ratio	Conc.	Actual conc.	Accuracy
	1	2281685	10269705	4.50093	88.4	100.0	88.4
	2	2273321	10511189	4.623715	90.8	100.0	90.8
	3	2284041	10375552	4.542629	89.2	100.0	89.2
Mean		2279682	10385482	4.6	89.5	100.0	89.5
SD		5634	121048	0.1	1.2	0	1.2
%CV		0.2	1.2	1.4	1.4	0.0	1.4

References

1. Wang, Z.; Stout, S. *Oil Spill Environmental Forensics : Fingerprinting and Source Identification*; Academic Press: Burlington, MA, USA, 2006.

2. Fingas, F. F.; Duval, W. S.; Stevenson, G. B. *The Basics of Oil Spill Cleanup with Particular Reference to Southern Canada*; Environment Canada: Canada, 1979.

3. Doerffer, J. W. *Oil Spill Response in the Marine Environment*; Pergamon Press: Oxford ; New York, 1992.

4. International Maritime Organization. *Field Guide for Oil Spill Response in Tropical Waters*, 1st ed.; International Maritime Organization: London, 1997.

5. Environmental Protection Agency. EPA Response to BP Spill in the Gulf of Mexico. http://www.epa.gov/bpspill/dispersants-qanda.html#chemicals (accessed 2 September 2014)

6. Hemmer, M. J.; Barron, M. G.; Greene, R. M. Comparative toxicity of eight oil dispersants, Louisiana sweet crude oil (LSC), and chemically dispersed LSC to two aquatic test species. *Environ. Toxicol. Chem.* **2011**, *30*, 2244-2252.

7. Kuhl, A. J.; Nyman, J. A.; Kaller, M. D.; Green, C. C. Dispersant and salinity effects on weathering and acute toxicity of South Louisiana crude oil. *Environ. Toxicol. Chem.* **2013**, *32*, 2611-2620.

8. Rico-Martinez, R.; Snell, T. W.; Shearer, T. L. Synergistic toxicity of Macondo crude oil and dispersant Corexit 9500A to the *Brachionus plicatilis* species complex (Rotifera). *Environ. Pollut. (Oxford, U. K.)* **2013**, *173*, 5-10.

9. Oil Spill Commision Action. The use of surface and subsea dispersants during the bp deepwater horizon oil spill. http://cybercemetery.unt.edu/archive/oilspill/20121210200502/http://www.oilspillcommission.gov/resources#staff-working-papers (accessed 23 November 2014)

10. Te Mauri Moana “Rena Environmental Recovery Monitoring Programme: Executive Summary,” University of Waikato, 2013.

11. Bay of Plenty Regional Council. Corexit Information Sheet. http://www.boprc.govt.nz/media/303418/4124-corexit-information-sheet-web-only-.pdf (accessed 4 September 2014)

12. Ling, N. Ecotoxicology of Rena oil, oispersant and cryolite on crayfish, snapper and wrasses. In *Report of the Rena Environmental Recovery Monitoring Programme*; University of Waikato: New Zealand, 2013.

13. Muncaster, S. Ecotoxicology of Rena heavy fuel oil and dispersant on early life stages of kingfish, *seriola lalandi*. In *Report of the Rena Environmental Recovery Monitoring Programme*; University of Waikato: New Zealand, 2013.

14. Garcia, M. T.; Campos, E.; Marsal, A.; Ribosa, I. Biodegradability and toxicity of sulphonate-based surfactants in aerobic and anaerobic aquatic environments. *Water. Res.* **2009**, *43*, 295-302.

15. Major, D.; Zhang, Q.; Wang, G.; Wang, H. Oil-dispersant mixtures: understanding chemical composition and its relation to human toxicity. *Toxicol. Environ. Chem.* **2012**, *94*, 1832-1845.

16. Singer, M. M.; George, S.; Jacobson, S.; Lee, I.; Weetman, L. L.; Tjeerdema, R. S.; Sowby, M. L. Comparison of acute aquatic effects of the oil dispersant Corexit 9500 with those of other Corexit series dispersants. *Ecotoxicol. Environ. Saf.* **1996**, *35*, 183-189.

17. Rosen, M. J. *Surfactants and Interfacial Phenomena*, 3 ed.; John Wiley & Sons Hoboken, NJ, USA 2004.

18. Thiele, B. Surfactants. *Chromatogr. Sci. Ser.* **2006**, *93*, 1173-1198.

19. Rouse, J. D.; Sabatini, D. A.; Suflita, J. M.; Harwell, J. H. Influence of surfactants on microbial-degradation of organic-compounds. *Crit. Rev. Env. Sci. Tech.* **1994**, *24*, 325-370.

20. Myers, D. *Surfactant Science and Technology* 3ed.; J. Wiley: Hoboken, N.J., 2006.

21. O'Lenick, A. J. *Surfactants : Strategic Personal Care Ingredients*; Allured Business Media: Carol Stream, IL, USA, 2005; 327.

22. Goodwin, J. W. *Colloids and Interfaces with Surfactants and Polymers: an Introduction*; J. Wiley: Chichester, England ; Hoboken, NJ, 2004.

23. Nalco. COREXIT® Oil Spill Dispersants. http://www.nalco.com/eu/applications/corexit-oil-spill-dispersants.htm (accessed 4 September 2014)

24. Ramirez, C. E.; Batchu, S. R.; Gardinali, P. R. High sensitivity liquid chromatography tandem mass spectrometric methods for the analysis of dioctyl sulfosuccinate in different stages of an oil spill response monitoring effort. *Anal. Bioanal. Chem.* **2013**, *405*, 4167-4175.

25. Place, B. J.; Perkins, M. J.; Sinclair, E.; Barsamian, A. L.; Blakemore, P. R.; Field, J. A. Trace analysis of surfactants in Corexit oil dispersant formulations and seawater. *Deep Sea Res., Part II* **2014**, Ahead of Print.

26. Glaubitz, J.; Schmidt, T. C. LC-MS quantification of a sulfosuccinate surfactant in agrochemical formulations. *Chromatographia* **2013**, *76*, 1729-1737.

27. Gray, J. L.; Kanagy, L. K.; Furlong, E. T.; Kanagy, C. J.; McCoy, J. W.; Mason, A.; Lauenstein, G. Presence of the Corexit component dioctyl sodium sulfosuccinate in Gulf of Mexico waters after the 2010 Deepwater Horizon oil spill. *Chemosphere* **2014**, *95*, 124-130.

28. Gray, J. L.; Kanagy, L. K.; Furlong, E. T.; McCoy, J. W.; Kanagy, C. J. "Determination of the anionic surfactant di(ethylhexyl) sodium sulfosuccinate in water samples collected from Gulf of Mexico coastal waters before and after landfall of oil from the Deepwater Horizon oil spill, May to October, 2010," U.S Geological Survey, 2010.

29. Hayworth, J. S.; Prabakhar Clement, T. Provenance of Corexit-related chemical constituents found in nearshore and inland Gulf Coast waters. *Mar. Pollut. Bull.* **2012**, *64*, 2005-2014.

30. Roslan, R. N.; Hanif, N. M.; Othman, M. R.; Azmi, W. N. F. W.; Yan, X. X.; Ali, M. M.; Mohamed, C. A. R.; Latif, M. T. Surfactants in the sea-surface microlayer and their contribution to atmospheric aerosols around coastal areas of the Malaysian peninsula. *Mar. Pollut. Bull.* **2010**, *60*, 1584-1590.

31. Mathew, J.; Schroeder, D. L.; Zintek, L. B.; Schupp, C. R.; Kosempa, M. G.; Zachary, A. M.; Schupp, G. C.; Wesolowski, D. J. Dioctyl sulfosuccinate analysis in near-shore Gulf of Mexico water by direct-injection liquid chromatography-tandem mass spectrometry. *J. Chromatogr. A* **2012**, *1231*, 46-51.

32. Cserhati, T.; Forgacs, E.; Oros, G. Biological activity and environmental impact of anionic surfactants. *Environ. Int.* **2002**, *28*, 337-348.

33. Zhang, R.; Wang, Y.; Tan, L.; Zhang, H. Y.; Yang, M. Analysis of polysorbate 80 and its related compounds by RP-HPLC with ELSD and MS detection. *J. Chromatogr. Sci.* **2012**, *50*, 598-607.

34. Place, B.; Anderson, B.; Mekebri, A.; Furlong, E. T.; Gray, J. L.; Tjeerdema, R.; Field, J. A role for analytical chemistry in advancing our understanding of the occurrence, fate, and effects of corexit oil dispersants. *Environ. Sci. Technol.* **2010**, *44*, 6016-6018.

35. Kujawinski, E. B.; Kido Soule, M. C.; Valentine, D. L.; Boysen, A. K.; Longnecker, K.; Redmond, M. C. Fate of dispersants associated with the deepwater horizon oil spill. *Environ. Sci. Technol.* **2011**, *45*, 1298-1306.

36. Campo, P.; Venosa, A. D.; Suidan, M. T. Biodegradability of Corexit 9500 and Dispersed South Louisiana Crude Oil at 5 and 25°C. *Environ. Sci. Technol.* **2013**, *47*, 1960-1967.

37. DOW. DOW Surfactants - Dioctyl Sulfosuccinates. http://www.dow.com/surfactants/products/dioctyl.htm (accessed 30 October 2014)

38. Patel, M.; Schimpf, M. O.; O'Sullivan, D. M.; LaSala, C. A. The use of senna with docusate for postoperative constipation after pelvic reconstructive surgery: a randomized, double-blind, placebo-controlled trial. *Am. J. Obstet. Gynecol.* **2010**, *202*, 479.e471-479.e475.

39. Hill, K.; LeHen-Ferrenbach, C. Sugar-based surfactants for consumer products and technical applications. *Surfactant Sci. Ser.* **2009**, *143*, 1-20.

40. Snelling, J. R.; Scarff, C. A.; Scrivens, J. H. Characterization of complex polysorbate formulations by means of shape-selective mass spectrometry. *Anal. Chem.* **2012**, *84*, 6521-6529.

41. Knepper, T. P.; Barceló, D.; De Voogt, P. *Analysis and Fate of Surfactants in the Aquatic Environment*; Elsevier: Amsterdam ; Boston, 2003.

42. Wang, Z.; Fingas, M. Analysis of sorbitan ester surfactants. Part I: High performance liquid chromatography. *J. High Resolut. Chromatogr.* **1994**, *17*, 15-19.

43. Oliver-Rodríguez, B.; Zafra-Gómez, A.; Camino-Sánchez, F. J.; Conde-González, J. E.; Pérez-Trujillo, J. P.; Vílchez, J. L. Multi-residue method for the analysis of commonly used commercial surfactants, homologues and ethoxymers, in marine sediments by liquid chromatography-electrospray mass spectrometry. *Microchem. J.* **2013**, *110*, 158-168.

44. Lebedev, A. T. Ed. *Comprehensive Environmental Mass Spectrometry.* ILM Publications: Glendale, Ariz., 2012.

45. Duarte, R. M.; Honda, R. T.; Val, A. L. Acute effects of chemically dispersed crude oil on gill ion regulation, plasma ion levels and haematological parameters in tambaqui (*Colossoma macropomum*). *Aquat. Toxicol.* **2010**, *97*, 134-141.

46. Gardiner, W. W.; Word, J. Q.; Word, J. D.; Perkins, R. A.; McFarlin, K. M.; Hester, B. W.; Word, L. S.; Ray, C. M. The acute toxicity of chemically and physically dispersed crude oil to key Arctic species under arctic conditions during the open water season. *Environ. Toxicol. Chem.* **2013**, *32*, 2284-2300.

47. Nalco. Corexit® EC9500A Safety Data Sheet. http://www.nalcoesllc.com/nes/employees/1617.htm (accessed 29 August 2014)

48. Hales, S. G. Biodegradation of the anionic surfactant dialkyl sulfosuccinate. *Environ. Toxicol. Chem.* **1993**, *12*, 1821-1828.

49. Manahan, F. J. *Environmental Chemistry*, 7th ed.; CRC Press: Boca Raton, Fl, 2000.

50. Garret, R. H.; Grisham, C. M. *Biochemistry*; Saunders College Publishing: USA, 1995.

51.Swisher, R. D. Surfactants and the environment: biodegradation aspects. Presented at Solution Behav. Surfactants: Theor. Appl. Aspects, [Proc. Int. Symp.], 1982.

52. El-Kabbani, O.; Darmanin, C.; Chung, R. P. T. Sorbitol dehydrogenase: structure, function and ligand design. *Curr. Med. Chem.* **2004**, *11*, 465-476.

53. Jeffery, J.; Joernvall, H. Sorbitol dehydrogenase. *Adv. Enzymol. Relat. Areas Mol. Biol.* **1988**, *61*, 47-106.

54. Gu, J.-D. Microbiological deterioration and degradation of synthetic polymeric materials: recent research advances. *Int. Biodeterior. Biodegradation* **2003**, *52*, 69-91.

55. Bernhard, M.; Eubeler, J. P.; Zok, S.; Knepper, T. P. Aerobic biodegradation of polyethylene glycols of different molecular weights in wastewater and seawater. *Water. Res.* **2008**, *42*, 4791-4801.

56. Kawai, F. The biochemistry of degradation of polyethers. *Crit. Rev. Biotechnol.* **1987**, *6*, 273-307.

57. Bruheim, P.; Bredholt, H.; Eimhjellen, K. Bacterial degradation of emulsified crude oil and the effect of various surfactants. *Can. J. Microbiol.* **1997**, *43*, 17-22.

58. Bruheim, P.; Eimhjellen, K. Chemically emulsified crude oil as substrate for bacterial oxidation: differences in species response. *Can. J. Microbiol.* **1998**, *44*, 195-199.

59. Scelfo, G. M.; Tjeerdema, R. S. A simple method for determination of Corexit 9527 in natural waters. *Mar. Environ. Res.* **1991**, *31*, 69-78.

60. Keller, R.; Mermet, J.-M.; Otto, M.; Valcarel, M.; Widmer, H. M. *Analytical Chemistry*, 2nd ed.; Wiley-VCH GmbH & Co. KGaA: Weinheim, 2004.

61. Kratochvil, B.; Wallace, D.; Taylor, J. K. Sampling for chemical analysis. *Anal. Chem.* **1984**, *56*, 113R-129R.

62. Barceló, D. *Environmental Analysis: Techniques, Applications, and Quality Assurance*; Elsevier: Amsterdam ; New York, 1993.

63. Boyd, R. K.; Basic, C.; A., B. R. *Trace Quantitative Analysis by Mass Spectrometry*; John Wiley & Sons: Hoboken, N.J., 2008.

64. Edwards, B. R.; Reddy, C. M.; Camilli, R.; Carmichael, C. A.; Longnecker, K.; Van Mooy, B. A. S. Rapid microbial respiration of oil from the Deepwater Horizon spill in offshore surface waters of the Gulf of Mexico. *Environ. Res. Lett.* **2011**, *6*, 035301/035301-035301/035309.

65. Lara-Martin, P. A.; Gomez-Parra, A.; Gonzalez-Mazo, E. Development of a method for the simultaneous analysis of anionic and non-ionic surfactants and their carboxylated metabolites in environmental samples by mixed-mode liquid chromatography-mass spectrometry. *J. Chromatogr. A* **2006**, *1137*, 188-197.

66. Lara-Martin, P. A.; Gomez-Parra, A.; Gonzalez-Mazo, E. Simultaneous extraction and determination of anionic surfactants in waters and sediments. *J. Chromatogr. A* **2006**, *1114*, 205-210.

67. Lara-Martin, P. A.; Petrovic, M.; Gomez-Parra, A.; Barcelo, D.; Gonzalez-Mazo, E. Presence of surfactants and their degradation intermediates in sediment cores and grabs from the Cadiz Bay area. *Environ. Pollut. (Amsterdam, Neth.)* **2006**, *144*, 483-491.

68. Lara-Martin, P. A.; Gonzalez-Mazo, E.; Brownawell, B. J. Multi-residue method for the analysis of synthetic surfactants and their degradation metabolites in aquatic systems by liquid chromatography-time-of-flight-mass spectrometry. *J. Chromatogr. A* **2011**, *1218*, 4799-4807.

69. Yeudakimau, A. V.; Perkins, C. R.; Guerrera, G. M.; Stuart, J. D.; Provatas, A. A. QuEChERS sample preparation followed by ultra-performance liquid chromatography - tandem mass spectrometry for rapid screening of dioctyl sulfosuccinate sodium salt in avian egg tissue. *Int. J. Environ. Anal. Chem.* **2014**, Ahead of Print.

70. Ali-Kanber, S.; Langdon, A. G.; Wilkins, A. L. Speciation and stability of particle-bound pulp and paper mill sourced resin acids in sodium azide preserved recipient water. *Bull. Environ. Contam. Toxicol.* **2005**, *75*, 135-142.

71. Traverso-Soto, J. M.; González-Mazo, E.; Lara-Martín, P. A. Analysis of surfactants in environmental samples by chromatographic techniques. In *Chromatography - The Most Versatile Method of Chemical Analysis*, 2012.

72. Cotte, J.-F.; Sonnery, S.; Martial, F.; Dubayle, J.; Dalencon, F.; Haensler, J.; Adam, O. Characterization of surfactants in an oil-in-water emulsion-based vaccine adjuvant using MS and HPLC-MS: Structural analysis and quantification. *Int. J. Pharm.* **2012**, *436*, 233-239.

73. White, H. K.; Lyons, S. L.; Harrison, S. J.; Findley, D. M.; Liu, Y.; Kujawinski, E. B. Long-term persistence of dispersants following the Deepwater Horizon oil spill. *Environ. Sci. Technol. Lett.* **2014**, *1*, 295-299.

74. Hewitt, D.; Alvarez, M.; Robinson, K.; Ji, J.; Wang, Y. J.; Kao, Y.-H.; Zhang, T. Mixed-mode and reversed-phase liquid chromatography–tandem mass spectrometry methodologies to study composition and base hydrolysis of polysorbate 20 and 80. *J. Chromatogr. A* **2011**, *1218*, 2138-2145.

75. Hvattum, E.; Yip, W. L.; Grace, D.; Dyrstad, K. Characterization of polysorbate 80 with liquid chromatography mass spectrometry and nuclear magnetic resonance spectroscopy: Specific determination of oxidation products of thermally oxidized polysorbate 80. *J. Pharm. Biomed. Anal.* **2012**, *62*, 7-16.

76. Sigma-Aldrich. HPLC Troubleshooting Guide: How to identify, isolate, and correct the most common HPLC problems. https://www.sigmaaldrich.com/content/dam/sigma-aldrich/docs/Supelco/Bulletin/4497.pdf (accessed 15 December 2014)

77. Stevens, L. M. “Guidelines for the use of Oil Spill Dispersants, Prepared for Maritime New Zealand,” Cawthron Institute, 2006.

78. ICH Expert Working Group ICH Harmonised Tripartite Guideline - Validation of Analytical Procedures: Text and Methodology Q2(R1) In *International Conference On Harmonisation Of Technical Requirements For Registration Of Pharmaceuticals For Human Use (ICH).* , 2005.

79. Mitchell, D. L.; Speight, J. G. Solubility of asphaltenes in hydrocarbon solvents. *Fuel* **1973**, *52*, 149-152.